2022-12-01

Influence Evaluation On Near-Road Concentrations Of Pm2.5 During Covid-19 Pandemic

Marcos Alan Banda Morales
University of Texas at El Paso

INFLUENCE EVALUATION ON NEAR-ROAD CONCENTRATIONS OF PM2.5 DURING COVID-19 PANDEMIC

MARCOS ALAN BANDA MORALES

Master's Program in Environmental Engineering

APPROVED:

Wen-Whai Li, Ph.D., P.E., Chair

Mayra Consuelo Chavez, Ph.D.

Soyoung Jeon, Ph.D.

Stephen L. Crites, Jr., Ph.D.
Dean of the Graduate School

Dedication

This thesis work is dedicated to my beloved wife, who has been my source of support and encouragement. I am thankful for all you do. This work is also dedicated to my parents, who are a living example that arduous work pays off.

A special thanks to Dr. Wen-Whai Li and Dr. Chavez for allowing me to collaborate with them and experience all that consists of being part of a research project team. Though our relationship seemed limited to academic work, I would not have been able to complete this project without you.

INFLUENCE EVALUATION ON NEAR-ROAD CONCENTRATIONS OF PM2.5 DURING COVID-19 PANDEMIC

by

MARCOS ALAN BANDA MORALES, BS

THESIS

Presented to the Faculty of the Graduate School of

The University of Texas at El Paso

in Partial Fulfillment

of the Requirements

for the Degree of

MASTER OF SCIENCE

Department of Civil Engineering

THE UNIVERSITY OF TEXAS AT EL PASO

December 2022

Acknowledgments

Primarily, I want to thank my research supervisors, Dr. Wen-Whai Li, and Dr. Chavez. Without their assistance and dedicated involvement in every step throughout the process, this paper would have never been accomplished. A special thanks to Dr. Wen-Whai Li for his guidance and his thriving passion for teaching.

This project was partially supported by a grant from the Texas Department of Transportation and a grant from the U.S. Department of Transportation through the Center for Advancing Research in Transportation Emissions, Energy, and Health (CARTEEH). The contents of this thesis are solely the responsibility of the author and do not represent the official views of the Texas Department of Transportation or the U.S. Department of Transportation.

Abstract

SARS-CoV-2, also known as COVID-19, was discovered in Wuhan, China in late 2019 and spread rapidly worldwide in 2020. The COVID-19 pandemic and its quarantine periods influenced the number of people using their vehicles and the number of miles traveled, which correspondingly influenced the air quality of urban areas. The influence of the restrictions caused by the quarantine period on air quality differs from location to location. Previous research accounted for countries, but no research was done at the state level individually. This research attempts to evaluate the transportation-related air quality during the COVID-19 pandemic period using data from the Texas Air Monitoring Information System from four cities in Texas (Austin, San Antonio, Houston, and Dallas-Fort Worth) from 2015 to 2021 for $PM_{2.5}$ concentrations and area meteorology. The concentrations were evaluated using time series, boxplots, and Welch's unpaired t-test for near-road stations and urban stations. $PM_{2.5}$ concentrations were found to increase in 2020 for Houston's near-road station CAMS 1052, but no significant differences were found for all other near-road stations in the other three cities. However, there was a significant increase in $PM_{2.5}$ in all of the urban stations in all four cities overall. This suggests that the COVID-19 quarantine period did affect the concentration of $PM_{2.5}$ in the four major cities in Texas.

Table of Contents

List of Tables

List of Figures

Chapter 1: Introduction

The SARS-CoV-2 (also known as COVID-19) pandemic started in 2019 and was the start of an unprecedented year-long event that set a worldwide footprint leaving millions of fatalities across the globe. The pandemic is traced to have originated from Wuhan in the Providence of Hubei in China, where patient zero was first observed. This virus caused major respiratory complications proving particularly fatal in immunocompromised people; during the pandemic, state, and local governments imposed restrictions on travel to diminish the spread of the contagious disease as death tolls kept increasing. The United States government recommended and imposed quarantine and other restrictions starting in March 2020. The COVID-19 pandemic and its quarantine altered people's daily life, particularly in vehicle usage and the number of miles traveled, which correspondingly changed the air quality of urban areas. The quarantine served to decrease viral infections as well as the number of people in public spaces. The change in vehicle usage during the quarantine period caused the air quality to shift concentrations such as $PM_{2.5}$. The difference in $PM_{2.5}$ concentrations produced during the quarantine period highlights the ideal conditions for their evaluation as traffic conditions differ from previous years. Transportation generates a significant amount of pollution that aggravates the problems related to air quality. The assumption that the more cars on the road, the more pollutants there are, have been agreed upon, and because of this, it is essential to examine the effects of transportation on air quality. Although technology has decreased the amount of pollution generated by motor vehicles, the amount of vehicle usage has been on a constant rise, creating more and prolonged traffic. Today, air pollution continues to be a problem and has been the leading environmental cause of death in recent years.

1.1 Problem Statement

This research attempts to find a relationship between ambient air concentrations and mobile emissions before, during, and after the COVID-19 pandemic and analyze the influence of this event on $PM_{2.5}$ concentrations in Texas' four major cities using Welch's unpaired one-tail t-test from 2015 to 2021.

1.2 Objective

The proposed research study aims to further understand the scope of transportation and its impact on Texas's regional and near-road air quality. The near-road research will focus on the cities of Austin, San Antonio, Houston, and Dallas-Fort Worth, considering $PM_{2.5}$ for urban and near-road stations. The research study will take advantage of the unique opportunity that the quarantine period provided to study the influence of a reduction of civilian vehicles in urban areas and their impact on air quality in the state of Texas, specifically $PM_{2.5}$ concentrations.

The tasks of this research include:

1. Selecting urban and near-road stations in the state of Texas
2. Downloading and analyzing $PM_{2.5}$ hourly data and daily averages as time series and boxplots to find any underlying trend or systematic pattern over time
3. Created wind roses for stations in 2020 to help identify local sources that contributed to $PM_{2.5}$ pollution in the study area
4. Develop polar annulus plots and concentration plots for years 2019 to 2021 to further clarify meteorological trends
5. Perform Welch t-test for urban stations and near-road stations from 2015 to 2021

The Welch t-test will show if the concentration of a year is significantly greater than another year, or if they are equal. This evaluation will determine the mean population of the studied year and determine if there was an increase in concentration in comparison to the other years evaluated even if there is no observable trend between each year.

Chapter 2 Background Knowledge

2.1 Importance of Air Quality

It has been seventy-four years since the Donora disaster in Pennsylvania. In 1948, a smog cloud took the lives of forty people, and hundreds more experienced heart and cardiovascular complications due to high concentrations of toxic chemicals in the air. Twenty-two years later, the United States federal government enacted the Clean Air Act of 1970, with it the Environmental Protection Agency (npr.org). Implementing the Clean Air Act of 1970 was a countermeasure to the adverse effects of pollution generated by industry and transportation. The Clean Air Act of 1970 mandated that federal and state governments regulate emissions from stationary and mobile sources.

Baby boomers had the highest population growth in the United States. As baby boomers approached adulthood, the U.S. experienced a rise in demand for supplies and cars during the seventies. During this time, the U.S. government decided to evaluate and research pollutants to prevent another environmental disaster generated by the population's consumption; the main concern was pollution in the form of acid rain. This law established the National Ambient Air Quality Standards, also known as NAAQS. The NAAQS considers ozone (O_3), atmospheric particulate matter (which includes $PM_{2.5}$ and PM_{10}), lead, carbon monoxide (CO), sulfur oxides (SO_x), and nitrogen oxides (NO_x) as the six major pollutants that are liable for extensive health problems. Therefore, the primary focus of limiting the concentration of such contaminants is to protect the population's health and, secondly, to protect the environment.

2.2 PARTICULATE MATTER & BACKGROUND CONCENTRATION

The Environmental Protection Agency defines particulate matter as a complex mixture usually in the form of smoke or haze of extremely small particles and liquid droplets. Particulate matter of 2.5 microns or $PM_{2.5}$ refers to a category of a particulate pollutant that is 2.5 microns or smaller in aerodynamic diameter. $PM_{2.5}$ can be characterized as any fine particle smaller than 2.5 microns including organic chemicals and metals. $PM_{2.5}$ is the primary pollutant of concern because it is mainly produced by burning fossil fuels by motor vehicles. Consequently, multiple studies have suggested that exposure to $PM_{2.5}$ can result in the aggravation of respiratory and cardiovascular diseases and potentially in their causation (Weber et al., 2016; Wei et al., 2017). The EPA considers $PM_{2.5}$ extremely detrimental to human health. Figure 1 shows the categorization of particles depending on size.

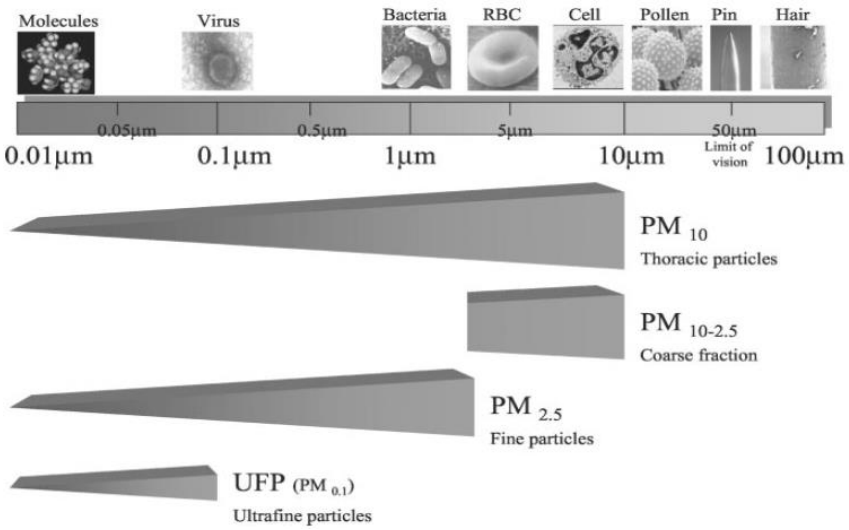

Figure 1 Particulate Matter Size Distribution (Source: Brook et al., 2004)

Since it is widely believed that a high number of vehicles corresponds to high pollution levels, there has been a remarkable decision to maintain air quality monitoring stations. The stations demonstrate and assess if the increment in traffic emissions will not comply with the

standards placed under the National Ambient Air Quality Standards (NAAQS) making sure changes are made to improve the air quality of an area. The 24-hour standard for $PM_{2.5}$ is 35 micrograms per cubic meter of air ($\mu g/m^3$). Near-road monitoring stations have detected $PM_{2.5}$ concentrations exceeding NAAQS (DeWinter et al., 2018). Concentrations of $PM_{2.5}$ decrease with distance from the source (Cortez-Lugo et al., 2013; Wang et al., 2021); this is due to varying factors of meteorology (wind speed and wind direction), type of vehicle, vehicular fleet, and other criteria. Variation of $PM_{2.5}$ correlates with the changes in meteorology between seasons. Several studies found that during the winter season higher concentrations of $PM_{2.5}$ are found due to the burning and combustion of fuel and biomass and lower concentrations of $PM_{2.5}$ in the summer because of the rain season as precipitation lowers the time particles are suspended in the air (Jain et al., 2020; Xie et al., 2019). This highlights the variability of PM and how seasons impact concentrations.

Not only is the meteorology of an area important to the levels of $PM_{2.5}$ concentrations, but the distance a receptor/population is away from the source is also a factor to consider as particles disperse. Background concentration is referred to pollutant concentrations that are already affecting an area. The comparison between near-road and urban background concentrations will display any fluctuation in concentration between both. At adjacent near-road air quality stations, the concentrations of $PM_{2.5}$ are higher than in stations in urban areas (Brown et al., 2019). After 150 meters from the source, the impacts of $PM_{2.5}$ are unnoticeable (Ginzburg, 2015). Furthermore, all stations not located near-road are background concentration receptors.

2.3 Near-road Air Pollution Hazards

Our natural respiratory system provides mechanisms to keep particulate matter that is larger than 2.5 microns from entering the deepest portion of the lung. However, particulate

matter smaller than 2.5 microns, $PM_{2.5}$, can reach deep into the lungs reaching the alveoli and diffusing into the bloodstream, which has serious health repercussions on the exposed individual(s) (EPA 2022). The aggravation of health-related problems with exposure to $PM_{2.5}$ increases as the source of $PM_{2.5}$ is near a population. The World Health Organization (WHO) stated that in 2019, 99% of the world's population lived in areas where the WHO's air quality guidelines were not complied with. Furthermore, the WHO also concluded that in 2016, ambient air pollution in urban and rural areas caused 4.2 million premature deaths worldwide. Unsurprisingly, air pollution is one of human health's most significant environmental risks. There is a correlation between $PM_{2.5}$ and the contraction of pneumonia, the aggravation of asthma, lung function reduction, and other problems that take a toll, especially in immunocompromised people and children (Oyana et al., 2021; Hua et al., 2014).

According to the World Health Organization, the most common chronic respiratory diseases are asthma and chronic obstructive pulmonary disease (COPD). *Asthma* is a condition in which an individual's airways become inflamed, narrowed, swollen, and produce extra mucus, making it difficult for the individual to breathe. In a surveillance study that compiled data on asthma in the United States from 2006-2018, 8.3% of Americans have asthma (Pate et al., 2021). Among these, 20.4 million are adults, and 6.1 million are children making it the most common chronic disease for children. The study further shows that asthma has been the cause of 1.3 million emergency room visits per year.

Among the various respiratory diseases that can become aggravated by exposure to air pollution, studies suggest that asthma becomes detrimental when exposed to elevated $PM_{2.5}$ concentrations. A study examining associations between $PM_{2.5}$ and asthma in twenty-seven countries in 2015 using epidemiological meta-analysis showed that 5 to 10 million annual

asthma emergency room visits corresponded to exposure to $PM_{2.5}$ (Anenberg et al., 2018). Asthma-related emergency room visits accounted for 4% to 9% of global visits (Anenberg et al., 2018). Another cohort study conducted in 2022 tried to pinpoint at what instance during the first stages of life individuals were more susceptible to the effects created by $PM_{2.5}$ in that it could cause asthma and wheezing in a child (Khalili 2018). The data from this study suggested that the effects of $PM_{2.5}$ were more significant during the pseudo glandular stage (6-16 gestational weeks) and the canalicular stage (16-24 gestational weeks) than in any other stage of the baby's development. In addition, there was a statistical significance in the effects of $PM_{2.5}$ in the first three years after birth (Chen et al., 2022). These findings highlight the importance of the first years of development and how air quality during these times can significantly impact an individual's health and set a footprint that will last a lifetime. Not only has asthma put a strain on the livelihood of the individuals who contract this disease, but this disease also puts a burden on the country's economy. In 2013 alone, asthma accounted for $3 billion in losses due to missed work and school days, $29 billion due to asthma-related mortality, and $50.3 billion in medical costs, amounting to a total loss of $81.9 billion (Nurmagambetov et al., 2018). Not only does $PM_{2.5}$ take a toll on human health, but it also affects millions of families financially.

As previously mentioned, chronic obstructive pulmonary disease is a disease that affects millions of people worldwide. Chronic obstructive pulmonary disease (COPD) is a group of lung diseases that block airflow and make it difficult for the individual to breathe; the damage done to the lungs cannot be reverted. Among the studies that have examined the relationship between $PM_{2.5}$ and lung function, a cohort study found that an improvement in ambient $PM_{2.5}$ led to better lung function in various parameters (Bo et al., 2021). These parameters were forced respiratory volume in one second, forced vital capacity, and mid-expiratory flow between 25% and 75% of

the forced vital capacity. Furthermore, decreasing the $PM_{2.5}$ concentration every five $\mu g/m^3$ results in a 12% risk reduction of developing COPD (Bo et al., 2021). Therefore, reducing exposure to areas with a high concentration of $PM_{2.5}$ is critical in reducing the chances of aggravating any existing medical conditions relating to respiratory diseases.

Seasonal $PM_{2.5}$ also is a significant factor to consider in human exposure scenarios. In the winter, higher concentrations of $PM_{2.5}$ in urban areas are more concurrent in the western part of the United States; meanwhile, in the eastern United States, there is no trend in change in the concentration of $PM_{2.5}$ (Hand et al., 2014). This means that depending on the season; people should take the necessary precautions to prevent the aggravation of their health regarding their exposure to higher concentrations of $PM_{2.5}$.

Indoor- and outdoor-originating $PM_{2.5}$ exposure supplies different cardiopulmonary effects depending on the season (Chi et al., 2019). For example, during the heating season, indoor-originated $PM_{2.5}$ exposure led to a decrease in pulmonary function among COPD patients. During the same season, exposure to outdoor-originated $PM_{2.5}$ increased blood pressure among healthy elderly adults. However, during the non-heating season, exposure to outdoor-originated $PM_{2.5}$ was associated with decreased pulmonary function in healthy elderly adults.

Other than the repercussions of $PM_{2.5}$ exposure on blood pressure, there have also been associations between $PM_{2.5}$ exposure and cardiovascular diseases. *Cardiovascular diseases* are disorders that affect the heart and blood vessels, including structural problems and blood clots. Kaihara et al. (2021) found that $PM_{2.5}$ exposure is associated with cardiovascular events such as arrhythmias and hypertension. $PM_{2.5}$ can also prolong the length of cardiovascular disease-related hospitalizations. This prolongation of hospital stays also applied to short-term $PM_{2.5}$

exposure. In addition, compared hospitalizations were significantly more extended for elderly patients than younger patients.

The WHO places cancer as the leading cause of death worldwide and claims that 2020 alone was responsible for ten million deaths. The most common cancers worldwide include breast, colon, rectum, prostate, and lung cancers. Among these, studies have suggested that exposure to $PM_{2.5}$ can affect not only lung cancer but also colon and breast cancer. In a study that examined the effects of $PM_{2.5}$ exposure in pediatric, adolescent, and young adult (AYA) cancer patients, in the study, it was observed that an elevated $PM_{2.5}$ exposure than what is the EPA standard ($PM_{2.5} \geq 12\ \mu g/m^3$) can be exceptionally harmful to young patients with certain cancers (Ou et al., 2020). The study suggests that the risk for cancer mortality in colorectal cancer AYA patients with constant exposure to $PM_{2.5} \geq$ twelve $\mu g/m^3$ is 20-30% higher than in patients with less exposure. This study's association between $PM_{2.5}$ and mortality highlighted the most high-risk estimate. Other associations included a significant positive association with $PM_{2.5}$ and mortality among AYA patients who contracted CNS tumors, carcinomas, melanomas, and breast and colorectal cancer (Ou et al., 2020). Although the mechanisms that lead to these reactions in patients are not fully known, the data strongly suggests that $PM_{2.5}$ can aggravate cancer symptoms. This is especially alarming to learn, considering (as previously mentioned) that 99% of the population does not live in an area where the WHO's air quality guidelines are satisfactory. Additional extensive research is necessary to comprehend how $PM_{2.5}$ exposure affects patients with previously stated conditions such as but not limited to asthma, COPD, cancer, and cardiovascular diseases. However, with the current knowledge, it is enough to be conscious of the adverse effects $PM_{2.5}$ exposure can incur. Further action must be taken by the population, in general, to ensure that civilians, both healthy and unhealthy people, are not

chronically exposed to superior levels of $PM_{2.5}$, thus affecting their quality of life or causing premature death.

Resources worldwide have also been aimed to determine how PM2.5 affects the world around us. Specifically, how these pollutants affect the environment and may affect humanity's livelihood. Besides affecting human health, particulate matter such as $PM_{2.5}$ has reduced visibility in the form of haze and depleted soil nutrients, costing millions of dollars in the farming and meat industries. Not only has $PM_{2.5}$ been associated with the previously mentioned health hazards and environmental perils, but it continues to be a significant economic burden worldwide. The effects of $PM_{2.5}$ on human health and the environment have made it a regulated pollutant under the NAAQS in the United States and the world.

2.4 Transportation-Related Air Quality

Vehicles are the primary source of pollution generated in urban areas. The incomplete combustion of fossil fuels causes the pollution generated by vehicles. Heavy-duty and passenger vehicles negatively affect the air quality in near-road communities. The increment of vehicles produces higher concentrations of carbon monoxide (CO), carbon dioxide (CO_2), volatile organic compounds (VOCs), hydrocarbons (HCs), nitrogen dioxides (NO_x), and particulate matter ($PM_{2.5}$ and PM_{10}), among others.

Even with the improvement of engines and mechanical components the problem still prevails. In heavily trafficked roads, fine particles dominate the space occupied in comparison to larger particles; up to 80 times the concentration (Vasiliauskiené et al., 2021). The suspended time of larger particles is much less than fine particles. Petrol-fueled vehicles produce 10 to 100 times fewer emissions compared to diesel vehicles (Li et al., 2014). Even with the reduction of passenger vehicles, diesel vehicles could exceed the concentrations with far fewer vehicles on

the road. As particles are released into the air from exhaust pipes, they begin to change their chemical composition and physical characteristics as they react with other chemicals. Usually, as particles react, during coagulation and nucleation, secondary pollutants in the form of $PM_{2.5}$ are produced (Hodan et al., 2004). As vehicle usage increases year after year, transportation air quality becomes inadequate. Continuous analysis of $PM_{2.5}$ has proven the adverse effects on human health and how this problem continues to exist.

2.5 Near-Road Air Monitoring

In 1990 the Environmental Protection Agency began monitoring air quality and establishing an active data collection system. The system became what we know today as EPA's Air Quality System, AQS. In 2014, $PM_{2.5}$ data became more readily available as more stations monitoring the particulate matter and other chemicals were put into place by state and local governments. The Texas Commission on Environmental Quality (TCEQ) is the entity that monitors air quality in Texas and provides Texas air quality data to the EPA. TCEQ has a database called Texas Air Monitoring Information System (TAMIS). Users can generate and download reports stored within the database. Users can download parameters for wind speed, wind direction, solar radiation, and $PM_{2.5}$.

Meteorology, terrain, elevation, traffic, and type of vehicle, among others, contribute to concentrations of $PM_{2.5}$ becoming more complex. A study examining two stations with the highest $PM_{2.5}$ concentrations in the United States that included near-road monitoring stations found no correlation between the high concentrations of PM and traffic conditions (Brown et al., 2019). This displays the variability of $PM_{2.5}$ and that trying to identify a single factor to understand the reason behind high $PM_{2.5}$ is no simple task. Near-road sites are unrestricted to

account for emissions coming from vehicles only. Nonetheless, the $PM_{2.5}$ concentrations for near-road stations are significantly higher compared to other stations in proximity.

Chapter 3 Methodology & Study Approach

This study was conducted using reported $PM_{2.5}$ concentrations and evaluating them from 2015 to 2021 to highlight the distinction of how the conditions during the pandemic affected air quality. Urban and near-road stations were selected in four cities of interest (Austin, San Antonio, Houston, and Dallas–Fort Worth). The 24-hour average concentrations for each station in the targeted cities were calculated by averaging the 1-hour values. The determination of a significant difference using a Welch unpaired one-tail T-test would clarify a non-observable distinction between the concentrations of each year which will be explained in Chapter 4. The near-road station's emissions were compared to their respective urban monitoring station emissions from 2015 to 2021. The site descriptions, data processing, emission estimates, and meteorology are discussed in this chapter.

3.1 Site Description

This study used $PM_{2.5}$ data from 2015 to 2021 reported by the Texas Air Monitoring Information System (TAMIS) from four cities (Austin, San Antonio, Houston, and Dallas–Fort Worth). From the stations selected in those cities, four project sites are identified as near-road stations. Each station is identified by different numbering systems used by the EPA and TCEQ. EPA identifies stations as Air Quality Systems (AQS), and TCEQ identifies the stations as Continuous Ambient Monitoring Stations (CAMS). The four near-road stations are North Interstate 35 (CAMS 1068) in Austin, Interstate Highway 35 (CAMS 1069) in San Antonio, North Loop (CAMS 1052) in Houston, and California Parkway North (CAMS 1053) in Fort Worth. Figure 2 demonstrates a map with all the urban targeted stations in the four cities of interest. Table 1 shows an overview of near-road stations in each area of interest, including other parameters monitored by the stations other than $PM_{2.5}$.

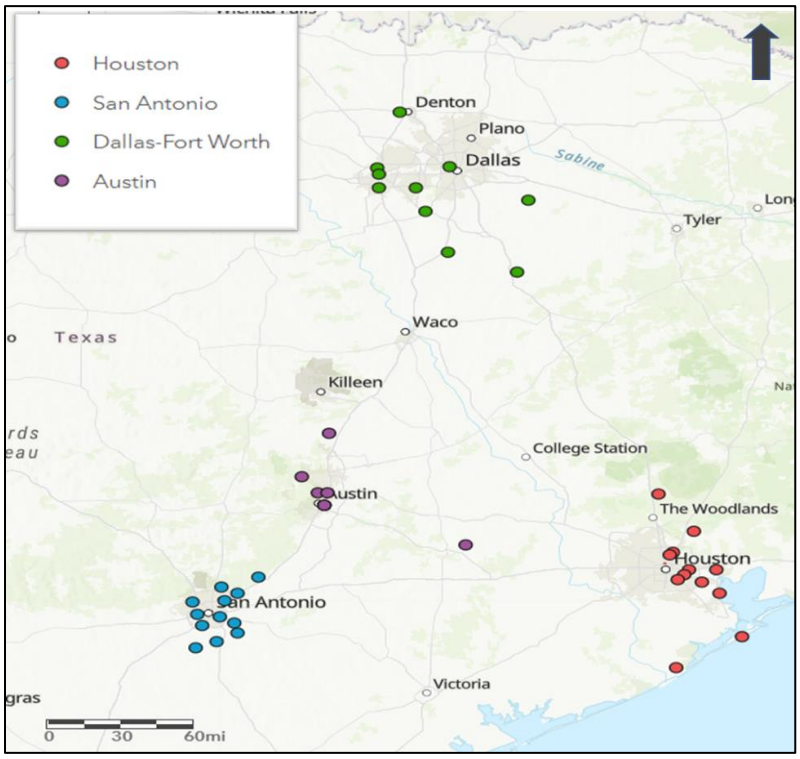

Figure 2 Location of PM Sites in Four Target Cities

Table 1 Site List of Near-Road $PM_{2.5}$ Monitors in Four Urban Areas

Core-Based Statistical Area	**Austin-Round Rock**	**San Antonio-New Braunfels**	**Houston-The Woodlands-Sugar Land**	**Dallas-Fort Worth-Arlington**
U.S. Census Bureau Pop. Est.	2,000,860	2,384,075	6,656,947	7,102,796
AQS CODE	484531068	480291069	482011052	484391053
CAMS	1068	1069	1052	1053
NAME	Austin North Interstate 35 C1068	San Antonio IH 35 C1069	Houston North Loop	Ft Worth California Parkway North C1053
LAT	30.3539	29.5294	29.8144	32.6647
LON	-97.6917	-98.3914	-95.3878	-97.3381
REGION	Austin	San Antonio	Houston	Dallas-Fort Worth
2015				
2016			x	
2017			x	
2018	x	x	x	
2019	x	x	x	x
2020	x	x	x	x
2021	x	x	x	x
Active	$PM_{2.5}$ (Local Conditions)	$PM_{2.5}$ (Local Conditions)	$PM_{2.5}$ (Local Conditions)	$PM_{2.5}$ (Local Conditions)
1 Hour	x	x	x	x
24 Hour	2017-2018	2017-2018	2015-2021	2015-2019
O_3				
CO	x	x	x	x
NO		x	x	x
NO_2	x	x	x	x
NO_x	x	x	x	x

3.1.1 Austin Stations Description

The Austin North Interstate 35 is a TCEQ continuous air monitoring station (CAMS) numbered 1068 and an EPA air quality system (AQS) numbered 48-453-1068 in Travis County, Austin, Texas. This station was first activated on April 15, 2014. The station is located at 8912 N IH 35, Austin, with latitude and longitude coordinates of 30.35384 and -97.69157. The station monitors CO, NO/NO_2/NO_X/, $PM_{2.5}$, outdoor temperature, wind direction, wind speed, and maximum wind gust. Figure 3 shows the near-road station's location and other urban ambient monitoring stations in Austin that monitor $PM_{2.5}$. Under the active column, there are two parameters, $PM_{2.5}$ local conditions and $PM_{2.5}$ acceptable. $PM_{2.5}$ local conditions only report data validated from Federal Reference Methods, Federal Equivalent Methods, or other methods that are to be used in making NAAQS. $PM_{2.5}$ acceptable recorded valid data that reasonably matches with the FRM (with or without corrections). FRM will be explained later in chapter 3 section 2. The summary of urban air monitoring sites in Austin that collected $PM_{2.5}$ data at any time between 2015 and 2021 is shown in Table 2.

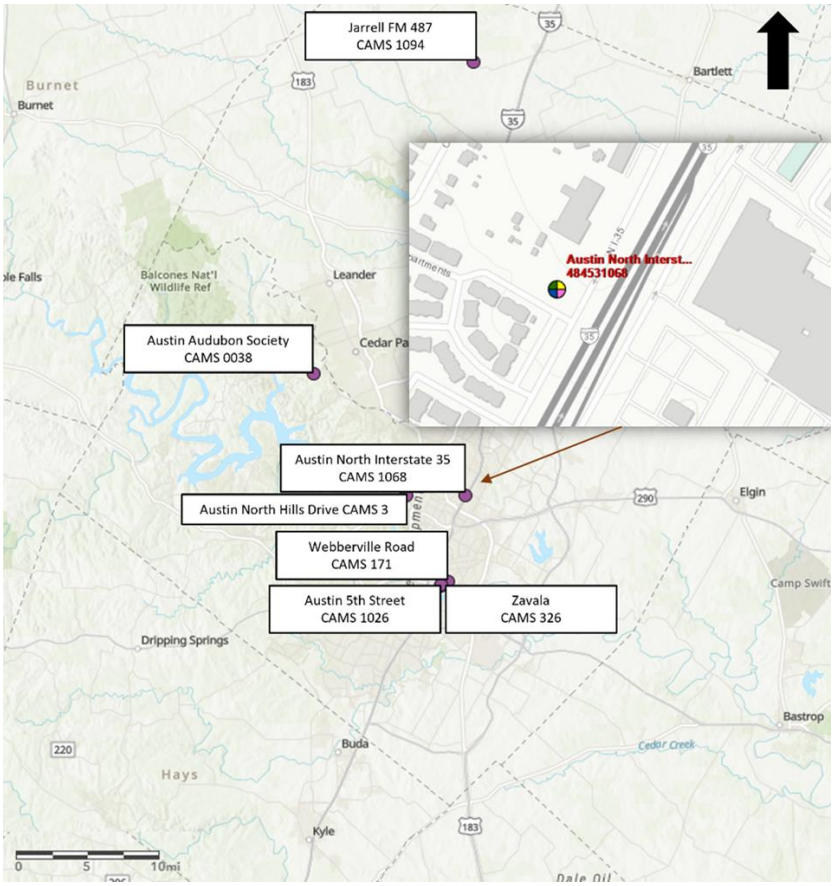

Figure 3 Austin Mapped Location of Urban Monitoring Sites

Table 2 Austin Summary of Urban $PM_{2.5}$ Sites

NAME	AQS CODE	CAMS	LAT	LON	2015	2016	2017	2018	2019	2020	2021	Active	1 Hour	24 Hour
Austin North Hills Drive C3/A322	484530014	3	30.3549	-97.7618	x	x	x	x	x	x	x	$PM_{2.5}$ (Local Conditions)	x	
Audubon C38	484530020	38	30.4832	-97.8723	x	x	x							x
Austin Webberville Road AF171	484530021	171	30.2632	-97.7129	x	x	x	x	x	x	x	$PM_{2.5}$ (Local Conditions)/Acceptable	x	x
Zavala C326	484530326	326	30.2583	-97.7203	x	x	x	x	May 3				x	
Fayette County C601	481490001	601	29.9625	-96.7459	x	x	x	Dec 4					x	
Austin 5th Street C1026	484531026	1026	30.2595	-97.7209	Oct 30								x	
Jarrell FM 487 C1094	484911094	1094	30.813	-97.6821						x	x	$PM_{2.5}$ (Local Conditions)		

3.1.2 San Antonio Stations Description

The San Antonio IH 35 is a continuous air monitoring station (CAMS) numbered 1069 and an EPA air quality system (AQS) numbered 48-029-1069 in Bexar County, San Antonio, Texas. This station was first activated on January 8, 2014. The station is located at 9904 IH 35 N, San Antonio, with latitude and longitude coordinates of 29.52943 and -98.39140. The station monitors CO, $NO/NO_2/NO_X/$, $PM_{2.5}$, outdoor temperature, wind direction, wind speed, standard deviation of horizontal wind direction, and maximum wind gust. Figure 4 shows the location of $PM_{2.5}$ monitoring sites in San Antonio. The summary of urban air monitoring sites in San Antonio that collected $PM_{2.5}$ data at any time between 2015 and 2021 is shown in Table 3.

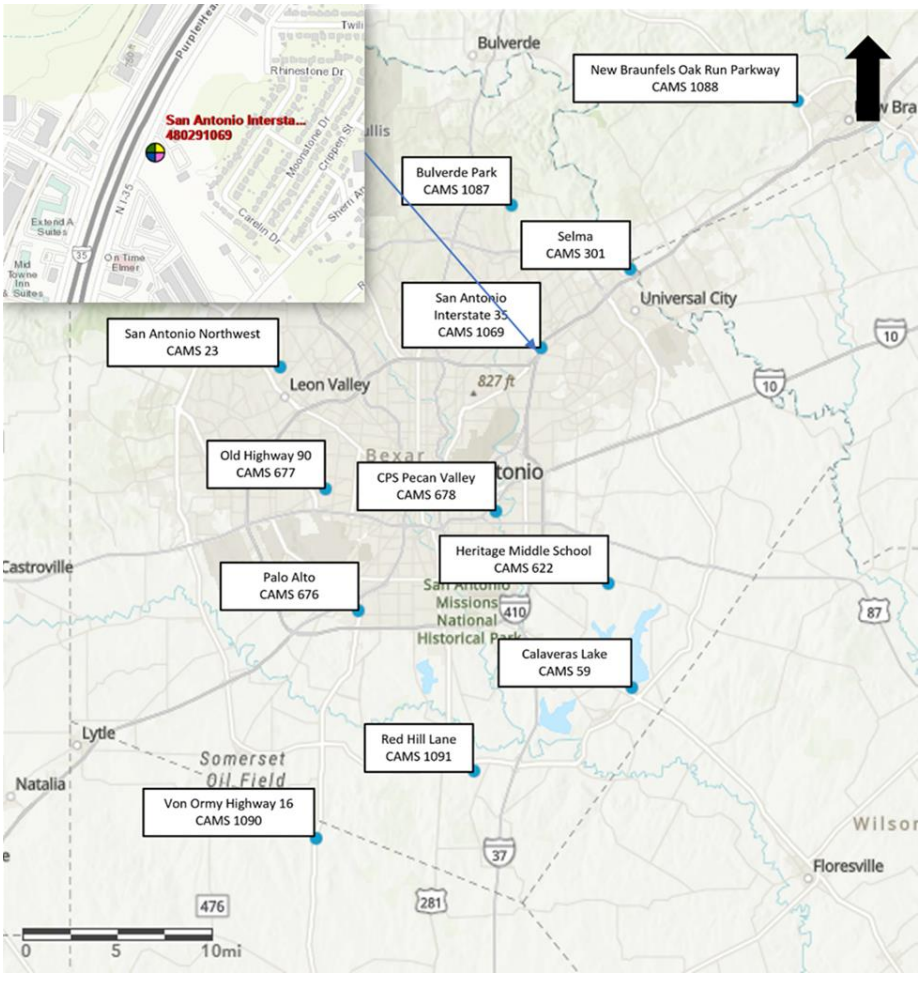

Figure 4 San Antonio Mapped Location of Urban Monitoring Sites

Table 3 San Antonio Summary of Urban $PM_{2.5}$ Sites

NAME	AQS CODE	CAMS	LAT	LON	2015	2016	2017	2018	2019	2020	2021	Active	1 Hour	24 Hour
San Antonio Northwest C23	480290032	23	29.5151	-98.6202	x	x	x	x	x	x	x	$PM_{2.5}$ (Local Conditions)	x	x
Calaveras Lake C59	480290059	59	29.2754	-98.3117	x	x	x	x	x	x	x	$PM_{2.5}$ (Local Conditions)	x	x
Selma C301	480290053	301	29.5877	-98.3125	x	x	x						x	
Heritage Middle School C622	480290622	622	29.3529	-98.3328	x	x	x	x	x	x	x	$PM_{2.5}$ Acceptable	x	
Palo Alto C676	480290676	676	29.3328	-98.5514	x	x	x	x	x	11-Jun				
Old Highway 90 C677/A319	480290677	677	29.4239	-98.5805	x	x	x	x	x	x	x	$PM_{2.5}$ Acceptable	x	
CPS Pecan Valley C678	480290055	678	29.4073	-98.4313	x								x	
San Antonio Bulverde Parkway	480291087	1087	29.635	-98.4177					x	x	x	$PM_{2.5}$ Acceptable	x	
New Braunfels Oak Run Parkway	480911088	1088	29.7132	-98.166					x	x	x	$PM_{2.5}$ Acceptable	x	
Von Ormy Highway 16 C1090	480131090	1090	29.163	-98.5892						x	x	$PM_{2.5}$ (Local Conditions)	x	
San Antonio Red Hill Lane C1091	480291091	1091	29.2129	-98.4502						x	x	$PM_{2.5}$ Acceptable	x	

3.1.3 Houston Stations Description

The Houston North Loop is a continuous air monitoring station (CAMS) numbered 1052 and an EPA air quality system (AQS) numbered 48-201-1052 in Harris County, Houston, Texas. This station was first activated on April 9, 2015. The station is located at 822 North Loop, Houston, with latitude and longitude coordinates of 29.81453 and -95.38769. The station monitors CO, NO/NO2/NOX/, $PM_{2.5}$, outdoor temperature, resultant wind direction, resultant wind speed, wind speed, standard deviation of horizontal wind direction, and maximum wind gust. Figure 5 shows the location of $PM_{2.5}$ monitoring sites in Houston. The summary of urban air monitoring sites in Houston that collected $PM_{2.5}$ data at any time between 2015 and 2021 is shown in Table 4.

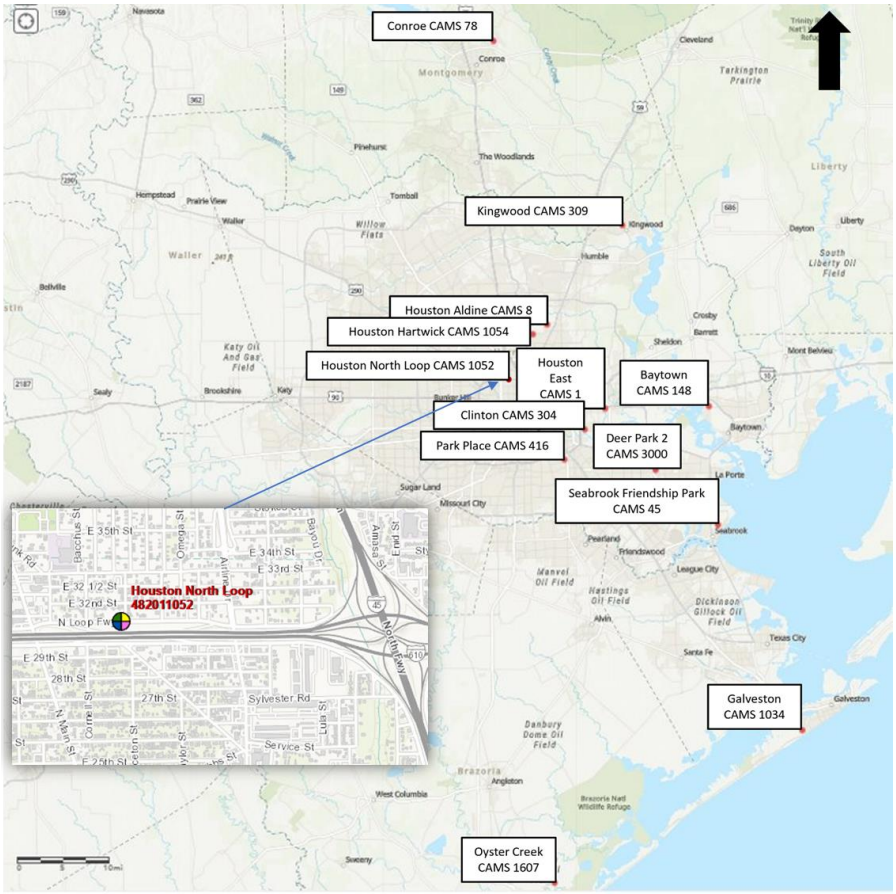

Figure 5 Houston Mapped Location of Urban Monitoring Sites

Table 4 Houston Summary of Urban $PM_{2.5}$ Sites

NAME	AQS CODE	CAMS	LAT	LON	2015	2016	2017	2018	2019	2020	2021	Active	1 Hour	24 Hour
Houston East C1/G316	482011034	1	29.768	-95.2206	x	x	x	x	x	x		$PM_{2.5}$ (Local Conditions)	x	
Houston Aldine C8/AF108/X150	482010024	8	29.901	-95.3261	x	x	x	x	x	x	x	$PM_{2.5}$ (Local Conditions)	x	x
Hou.DeerPrk2 C35/235/1001/AFH139FP239	482011039	35	29.6701	-95.1285	x	x	x	x	x	x	x	$PM_{2.5}$ (Local Conditions)/Acceptable	x	x
Seabrook Friendship Park C45	482011050	45	29.5831	-95.0155	x	x	x	x	x	x	x	$PM_{2.5}$ (Local Conditions)	x	
Clinton C403/C304/AH113	482011035	55	29.7337	-95.2576	x	x	x	x	x	x		$PM_{2.5}$ (Local Conditions)/Acceptable	x	x
Conroe Relocated C78/A321	483390078	78	30.3503	-95.4251	x	x	x	x	x	x	x	$PM_{2.5}$ (Local Conditions)	x	
Baytown A148	482010058	148	29.7707	-95.0312	x	x	x	x	x	x	x	$PM_{2.5}$ (Local Conditions)	x	x
Kingwood C309	482011042	309	30.0583	-95.1897	x	x	21-Jan						x	
Park Place C416	482010416	416	29.6864	-95.2947	x	x	x	x	x	x		$PM_{2.5}$ Acceptable	x	
Galveston 99th St. C1034/A320/X183	481671034	1034	29.2545	-94.8613	x	x	x	x	x	x	x	$PM_{2.5}$ (Local Conditions)	x	x
Houston Hartwick C1054	482011054	1054	29.8854	-95.3524		x	13-Apr						x	
Oyster Creek C1607	480291607	1607	29.0106	-95.3133			x	x	x	x		$PM_{2.5}$ (Local Conditions)	x	

3.1.4 Dallas – Fort Worth Stations Description

The Dallas – Fort Worth, California Parkway North is a continuous air monitoring station (CAMS) numbered 1053 and an EPA air quality system (AQS) numbered 48-439-1053 in Tarrant County, Fort Worth, Texas. This station was first activated on March 11, 2015. The station is located at 1198 California Parkway North, Fort Worth, with latitude and longitude coordinates of 32.66472 and -97.33806. The station monitors CO, NO/NO2/NOX/, $PM_{2.5}$, outdoor temperature, resultant wind direction, resultant wind speed, wind speed, standard deviation of horizontal wind direction, and maximum wind gust. Figure 6 shows the $PM_{2.5}$ monitoring sites in Dallas–Fort Worth. The summary of urban air monitoring sites in Dallas–Fort Worth that collected $PM_{2.5}$ data at any time between 2015 and 2021 is shown in Table 5.

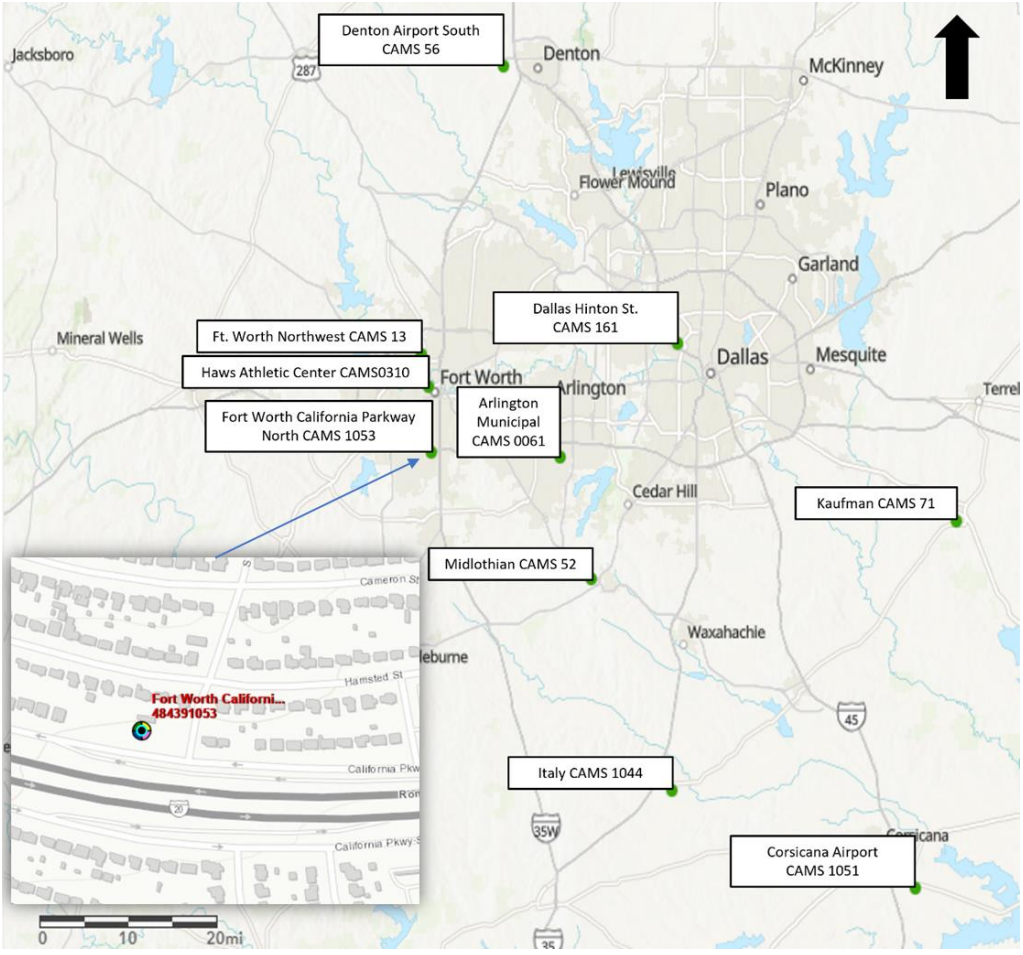

Figure 6 Dallas–Fort Worth Mapped Location of Urban Monitoring Sites

Table 5 Dallas–Fort Worth Summary of Urban $PM_{2.5}$ Sites

NAME	AQS CODE	CAMS	LAT	LON	2015	2016	2017	2018	2019	2020	2021	Active	1 Hour	24 Hour
Ft. Worth Northwest C13/AH302	484391002	13	32.8058	-97.3566					x	x	x	$PM_{2.5}$ (Local Conditions)	x	x
Midlothian OFW C52/A137	481390016	52	32.4821	-97.0269	x	x	x	x	x	x	x	$PM_{2.5}$ (Local Conditions)/ Acceptable	x	x
Denton Airport South C56/A163/X157	481210034	56	33.2191	-97.1963	x	x	x	x	x	x	x	$PM_{2.5}$ (Local Conditions)	x	
Dallas Hinton St. C401/C60/AH161	481130069	60	32.8201	-96.8601	x	x	x	x	x	x	x	$PM_{2.5}$ (Local Conditions)	x	x
Arlington Municipal Airport C61	484393011	61	32.6564	-97.0886	x	x	x	x	x				x	
Kaufman C71/A304/X071	482570005	71	32.565	-96.3177	x	x	x	x	x	x	x	$PM_{2.5}$ Acceptable	x	
Haws Athletic Center C310	484391006	310	32.7591	-97.3423	x	x	x	x	x	x	x	$PM_{2.5}$ (Local Conditions)	x	x
Italy C1044/A323	481391044	1044	32.1754	-96.8702	x	x							x	
Corsicana Airport C1051	483491051	1051	32.0319	-96.3991	x	x	x	x	x	x	x	$PM_{2.5}$ Acceptable	x	

3.2 URBAN AND NEAR-ROAD $PM_{2.5}$ MONITORING DATA PROCESSING

Burning fossil fuels generates particulate matter with an aerodynamic diameter of 2.5 microns or less. Activities relating the industrial and residential combustion produce significant amounts of emissions. Heavy-duty diesel vehicles and traffic are responsible for substantial concentrations on roadways. PM analysis is used to determine the concentrations to evaluate the air quality of a location. TCEQ is responsible for collecting PM data that can be downloaded from the Texas Air Monitoring Information System (TAMIS). TAMIS is state-operated and compiles data from the six commonly occurring pollutants with a network of monitoring stations.

Data downloaded from TAMIS was used in this study to evaluate $PM_{2.5}$ concentrations that were produced by vehicles captured at near-road and urban stations. The data collection instruments used in air monitoring sites must comply with either of two measurement principles, FRM or FEM, specified by the EPA's air monitoring methods. FRM and FEM have strict performance criteria for confident and accurate data collection. The Federal Reference Method (FRM) is a method designed using the best concentration measurement that is scientifically defensible and is defined as the gold standard as it serves as the basis of comparison in judging other measurement methods. The Federal Equivalent Method (FEM) is designed for a comparable level of compliance required to attain NAAQS. FEM is useful in implementing innovative technologies and providing cost-effective solutions as an alternative when measuring pollutant emissions.

To determine the difference between FRM and FEM data submission to the EPA, the EPA created two parameter codes numbered 88101 and 88502. $PM_{2.5}$ LOCAL CONDITIONS and ACCEPTABLE $PM_{2.5}$ AQI & SPECIATION MASS are the names of the parameter codes, respectively. Monitors that use the proper FRM/FEM and must comply with $PM_{2.5}$ NAAQS standards are assigned parameter code 88101, and other monitors that have valid data with an appropriate estimation to FRM (with or without corrections) with the difference of not having to satisfy the $PM_{2.5}$ NAAQS conditions are assigned to parameter code 88502.

TAMIS data was processed using hourly data to create 24-hour PM averages. Only hourly data were used if available. Days containing less than 75% of available data were not included in the 24-hour values. Negative hourly values were assigned a .5 limit value for quality assurance. This was done for all stations with available $PM_{2.5}$ data, as various stations were deactivated or added in different years. Appendix A shows all $PM_{2.5}$ urban monitoring station data as time series from 2015 to 2021 for Austin, San Antonio, Houston, and Dallas–Fort Worth. The focus of providing a time series was to demonstrate if there was a pattern or trend between the sets of data. However, the provided data sets did not allow for an effective visual demonstration of any trend or pattern for urban stations due to the overlapping of values. Additionally, meteorology affecting each station further influences $PM_{2.5}$ concentrations which will be explained in Chapter 3.

To visualize the distinction of $PM_{2.5}$ concentrations in each of the four cities, the three most concurrent years to the COVID-19 pandemic (2019-2021) data were used for all near-road monitoring sites. A series of box plots were prepared to show the monthly and seasonal variation of PM concentrations in each city. A box plot shows the distribution through data percentages and averages. The plot is divided into four sections, each representing twenty-five percent of the data available. Each section is separated by a quartile, and depending on the size of the section, the dispersion is easier to identify. Bivariate polar plots of $PM_{2.5}$ concentrations were also used. In these plots the angle represents the wind direction, the wind inclines in a cardinal direction. The circle's location specifies the wind speed as it lies within a set of rings. The wind speed is in m/s (from 0 to 10 m/s as each ring has a specified speed). The intensity of the color states the average hourly $PM_{2.5}$ values over each month in the color code provided in the figures: red, high concentration, and blue, low concentration.

$PM_{2.5}$ concentrations of near-road stations in each city are illustrated by the following:

1. Time Series of hourly averages
2. Box plots
    - Before Lockdown (January 1st to March 20th, 2015-2021)
    - Lockdown Phase I (March 21st to April 30th, 2015-2021)

- Lockdown Phase II (May 1st to September 30th, 2015-2021)
- After Lockdown (October 1st to December 31st, 2015-2021)

3. Polar $PM_{2.5}$ concentration annulus plots for near-road stations from 2019 to 2021
4. Monthly polar $PM_{2.5}$ concentration plots for near-road stations from 2019 to 2021

3.2.1 Austin Data Processing

Austin's near-road station CAMS1068 data of 24-hour values is shown as a yearly time series graph in Figure 7. Yearly $PM_{2.5}$ concentrations from 2018 to 2021 are higher between mid-May and late July. One notices that the station was installed in October 2018, so PM data was available only after October 15, 2018. There is no observable trend between each year. Data from 2018 was limited starting mid-October.

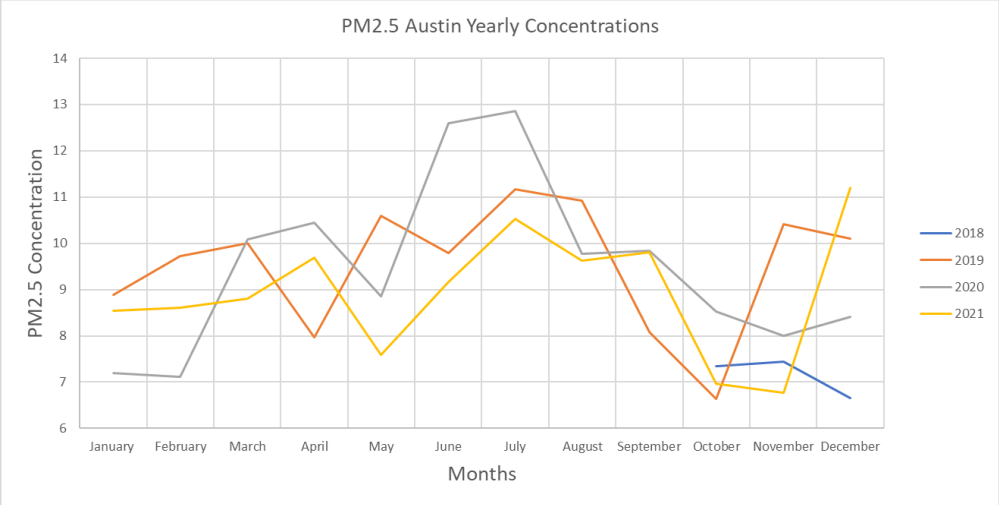

Figure 7 Austin 2018-2021 Near-Road CAMS 1068 $PM_{2.5}$ Time Series Comparison Yearly Concentrations (µg/m3)

Figure 8 shows a box plot from 2019 to 2021 with the hourly average of $PM_{2.5}$ concentrations at the Austin near-road site 1068. The hourly averages are the color circles. During the Lockdown Phase 1 and Phase 2 in 2020, the concentrations of $PM_{2.5}$ were slightly higher in comparison to 2019 and 2021.

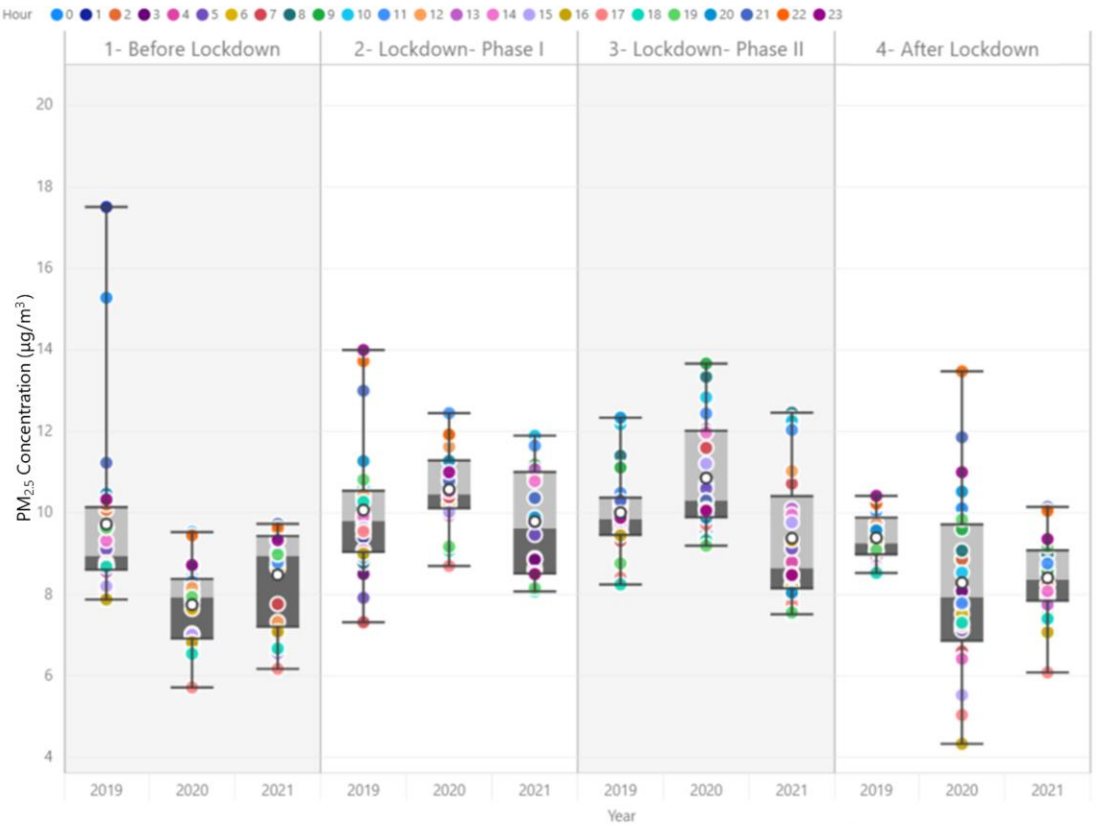

Figure 8 Austin Near-Road Site 1068 Hourly Average $PM_{2.5}$

Figures 9, 10, and 11 provide polar $PM_{2.5}$ concentration annulus plots for CAMS 1068 by month and wind direction. In all years, southerly winds prevail with high $PM_{2.5}$ concentrations. This is because CAMS 1068 is located northwest of Interstate Highway 35, as shown in Figure 3. The early months of 2020, shown in Figure 16, depict elevated $PM_{2.5}$ concentrations compared to other months in that year. The high concentrations were observed during the lockdown's first and second phase periods caused by the COVID-19 pandemic. In comparison to 2019 and 2021, elevated concentrations during these periods are apparent.

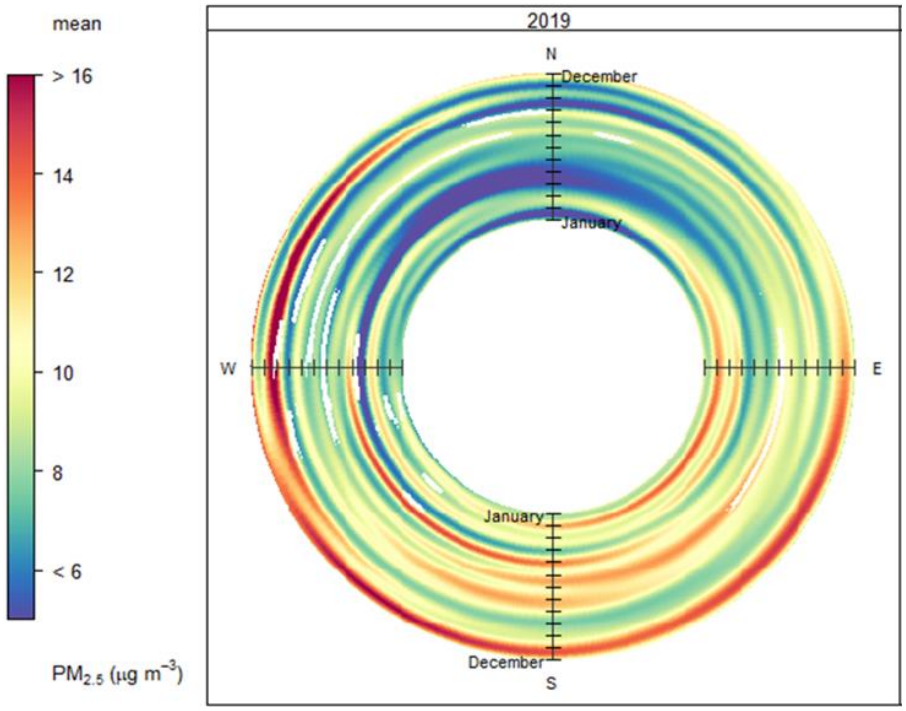

Figure 9 Austin 2019 Near-Road CAMS 1068 Polar Annulus Plot for $PM_{2.5}$ Concentrations (µg/m3) in Corresponding Wind Direction and Month

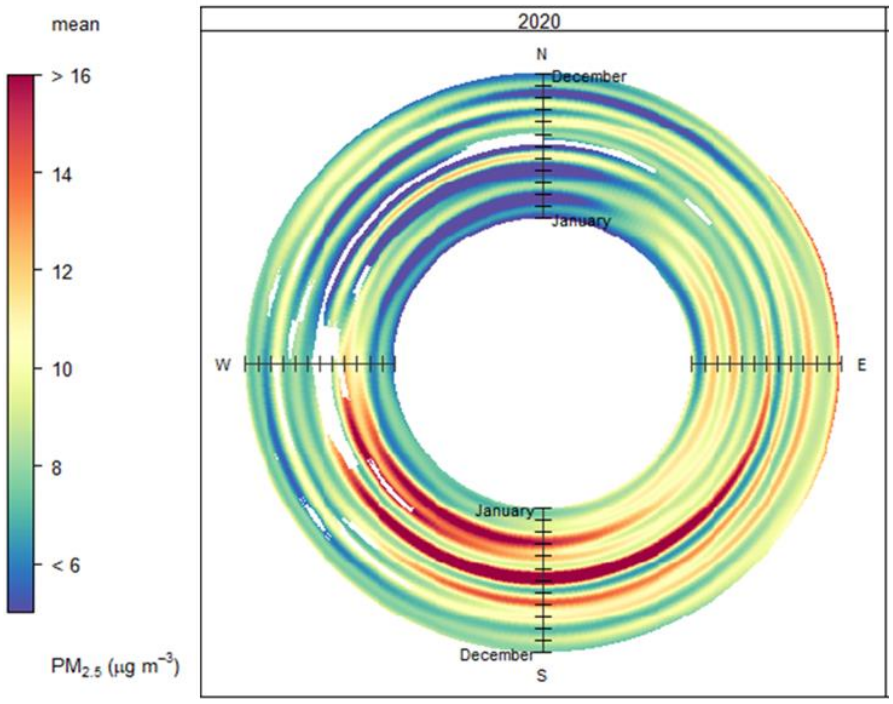

Figure 10 Austin 2020 Near-Road CAMS 1068 Polar Annulus Plot for $PM_{2.5}$ Concentrations (µg/m3) in Corresponding Wind Direction and Month

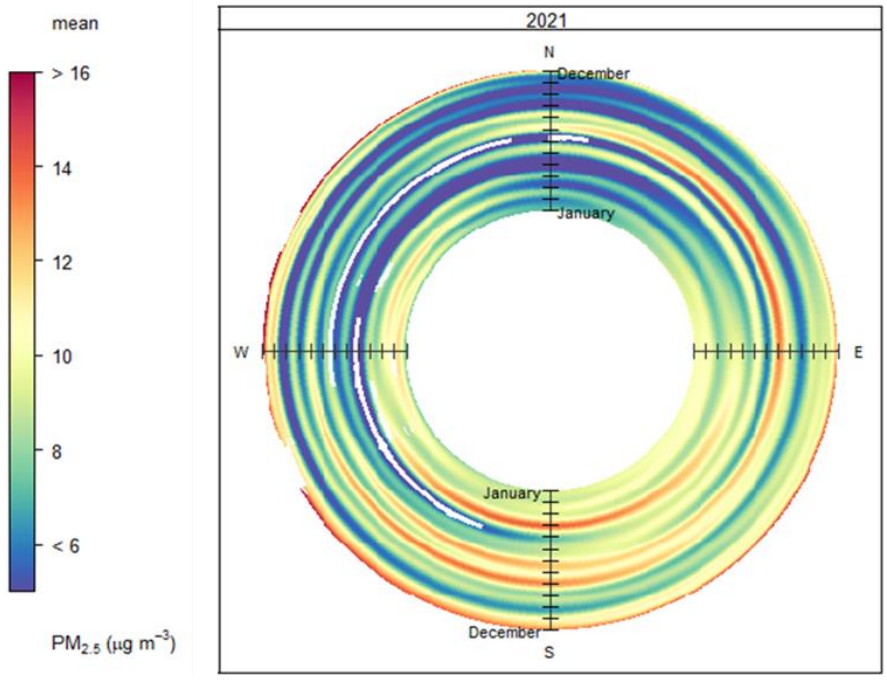

Figure 11 Austin 2021 Near-Road CAMS 1068 Polar Annulus Plot for $PM_{2.5}$ Concentrations (µg/m3) in Corresponding Wind Direction and Month

Figures 12, 13, 14, and 15 show the monthly polar $PM_{2.5}$ concentration plots concerning wind speed and direction for 2019 to 2021. The tables are organized according to the lockdown phase periods. Figure 14 suggests higher $PM_{2.5}$ concentrations coming from southern winds between the months of May to July, which supports the information shown in Figure 10.

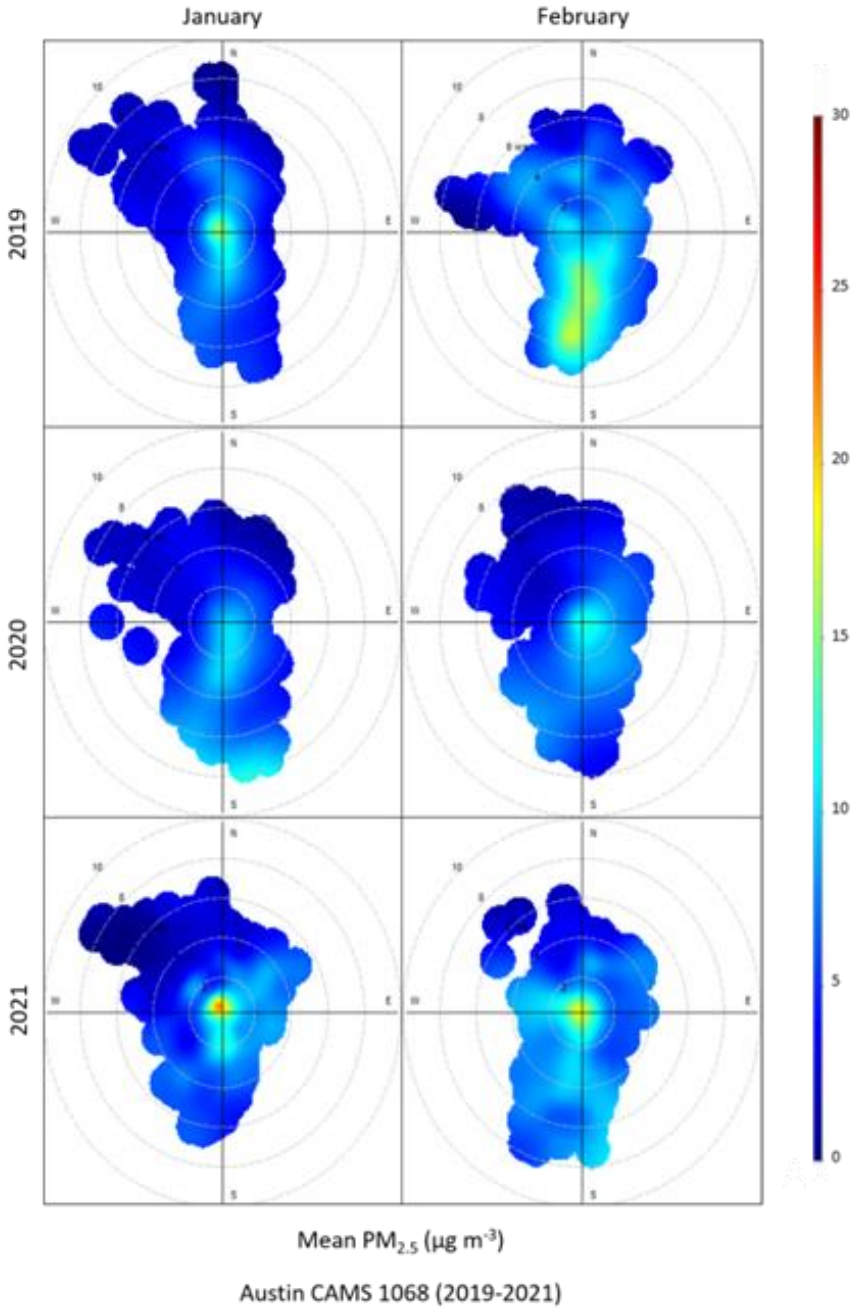

Figure 12 Austin 2019-2021 Near-Road CAMS 1068 $PM_{2.5}$ Concentrations (µg/m3) in Corresponding Wind Direction for January and February

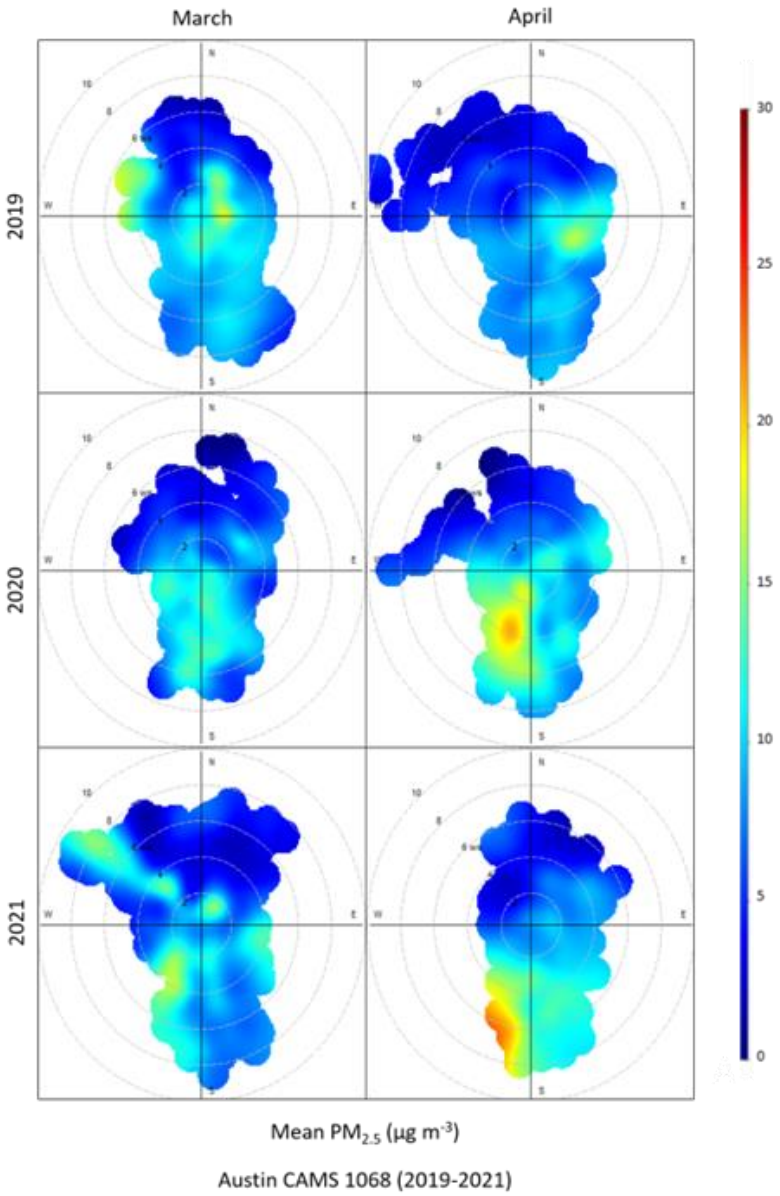

Figure 13 Austin 2019-2021 Near-Road CAMS 1068 $PM_{2.5}$ concentrations ($\mu g/m^3$) in Corresponding Wind Direction for March and April

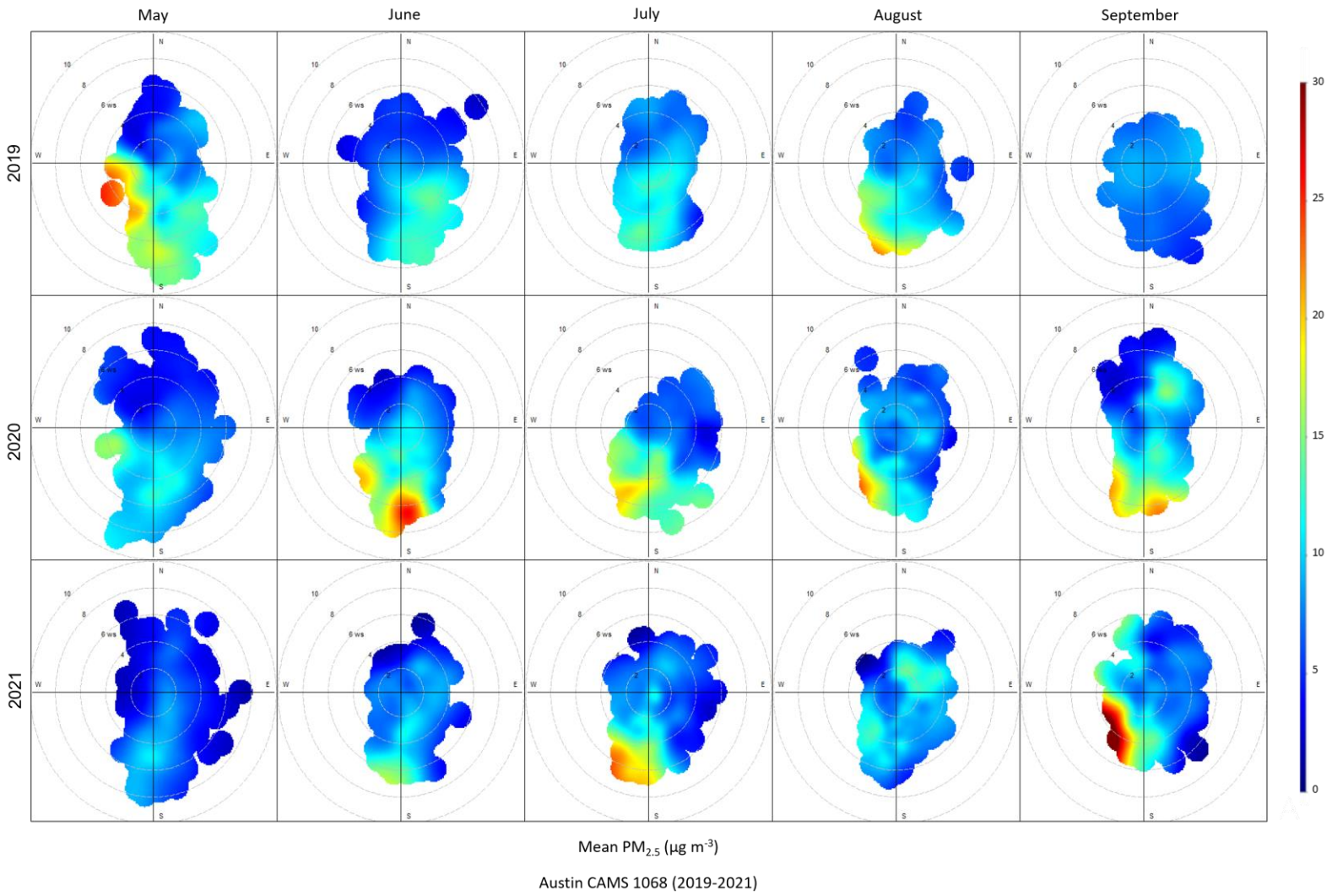

Figure 14 Austin 2019-2021 Near-Road Station CAMS 1068 $PM_{2.5}$ concentrations ($\mu g/m^3$) in Corresponding Wind Direction for May to September

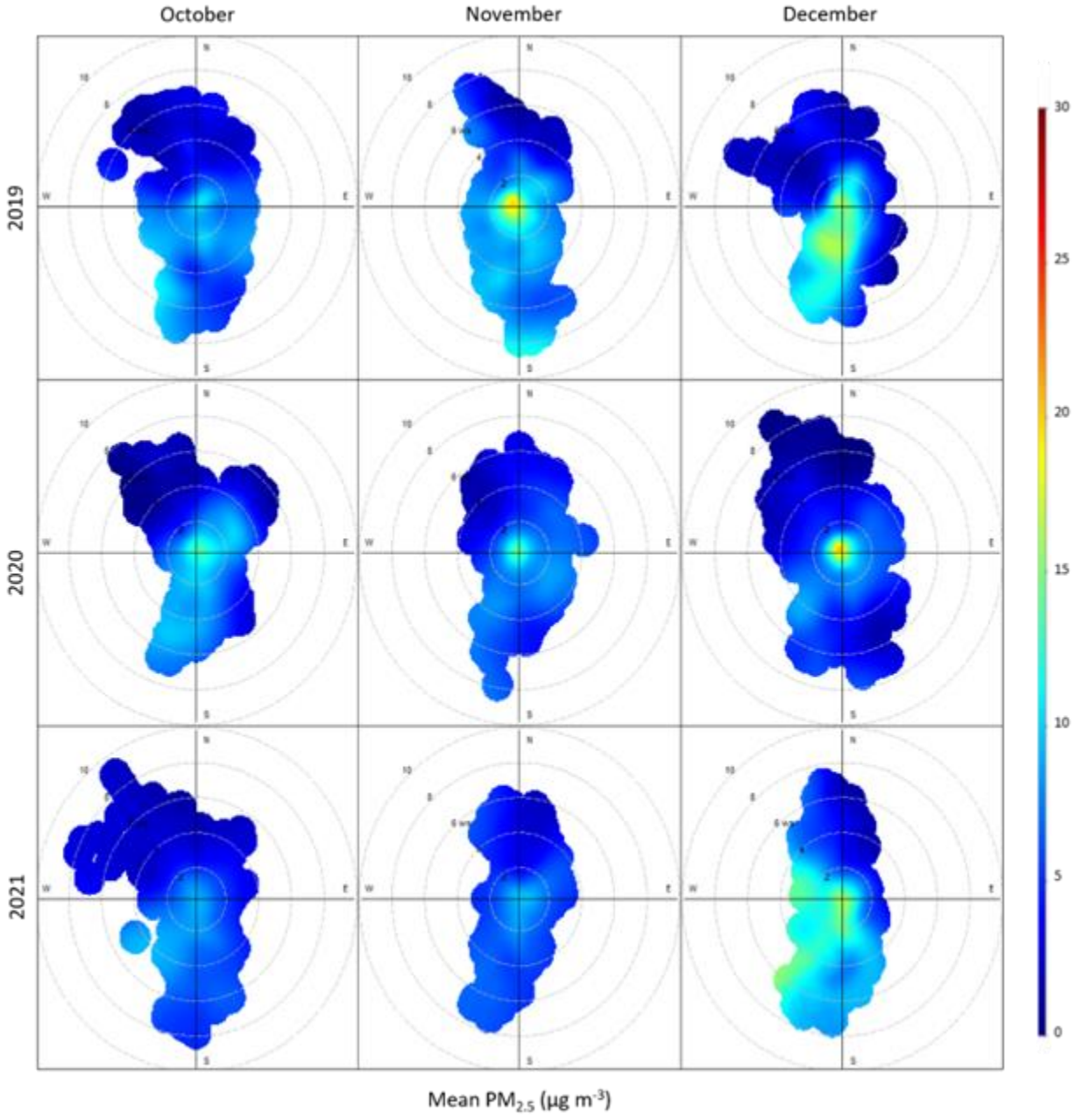

Figure 15 Austin 2019-2021 Near-Road CAMS 1068 $PM_{2.5}$ Concentrations ($\mu g/m^3$) in Corresponding Wind Direction for October to December

3.2.2 San Antonio Data Processing

San Antonio's near-road station CAMS1069 data of 24-hour values are shown in Figure 16 as a yearly time series. Yearly concentrations between 2018 and 2019 highlight no observable trend but an increase during the summer months. Data from 2018 was limited starting mid-November.

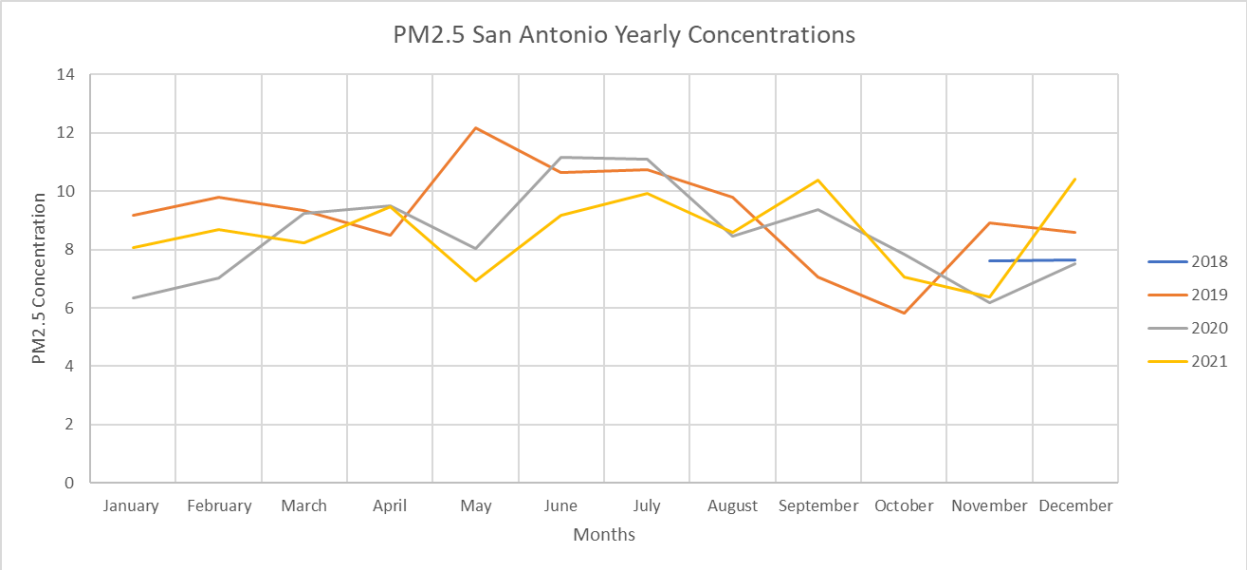

Figure 16 San Antonio 2018-2021 Near-Road CAMS 1069 $PM_{2.5}$ Time Series Yearly Concentrations (µg/m3)

Figure 17 shows the hourly average of $PM_{2.5}$ concentrations at the San Antonio near-road site 1069. During Lockdown Phase 1, concentrations increased between 2019 and 2020. In this period in 2021, the hourly concentrations showed much higher variation. In Lockdown Phase 2, there was a higher variation in 2020 and 2021.

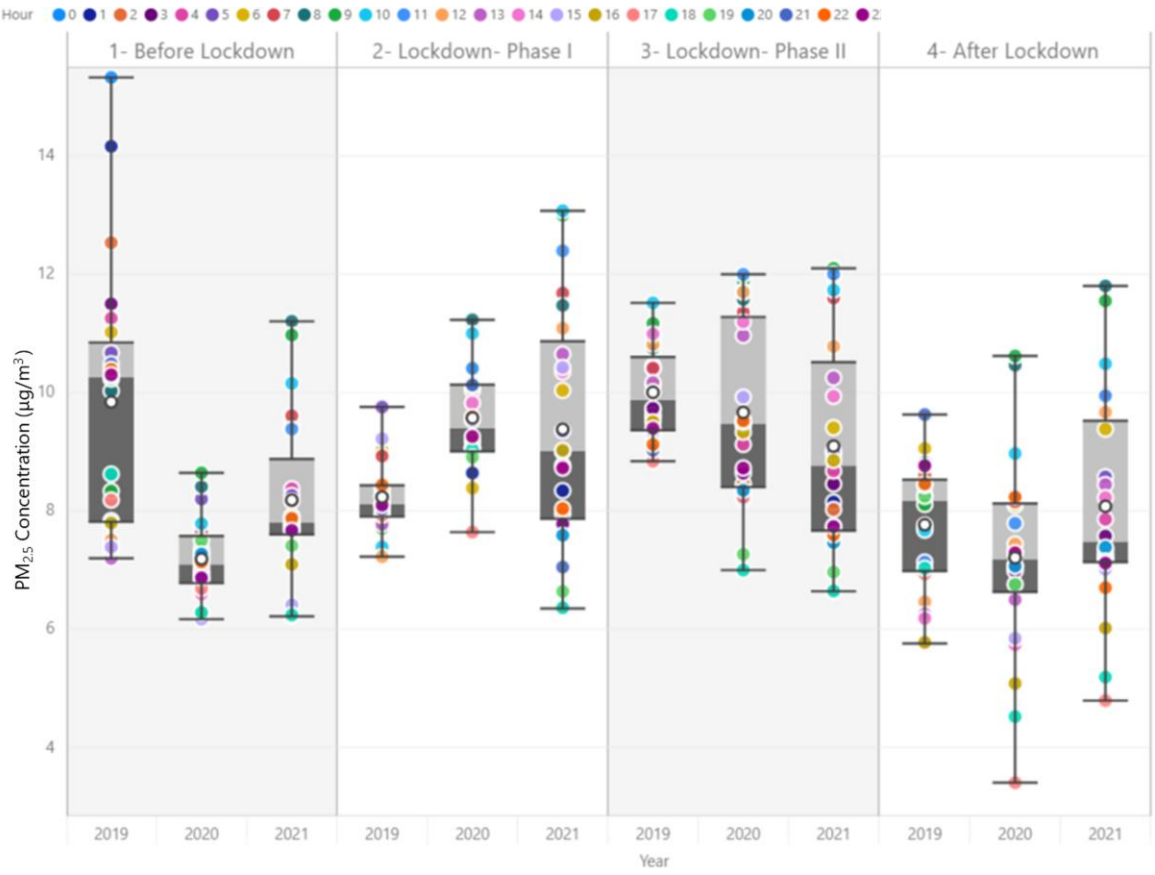

Figure 17 San Antonio Near-Road CAMS 1069 Hourly Average $PM_{2.5}$

Figures 18, 19, and 20 provide polar $PM_{2.5}$ concentration annulus plots for CAMS 1069 by month and wind direction. In 2020 and 2021, southern and northern winds prevail, with high $PM_{2.5}$ concentrations observed during the summer and early fall. CAMS 1069 is located southeast of Interstate Highway 35, as shown in Figure 4. As Interstate Highway 35 curves at this location high concentrations of $PM_{2.5}$ data are observed at CAMS 1069. These high concentrations are observed in the south, west, and north directions apparent in Figure 19 and Figure 20.

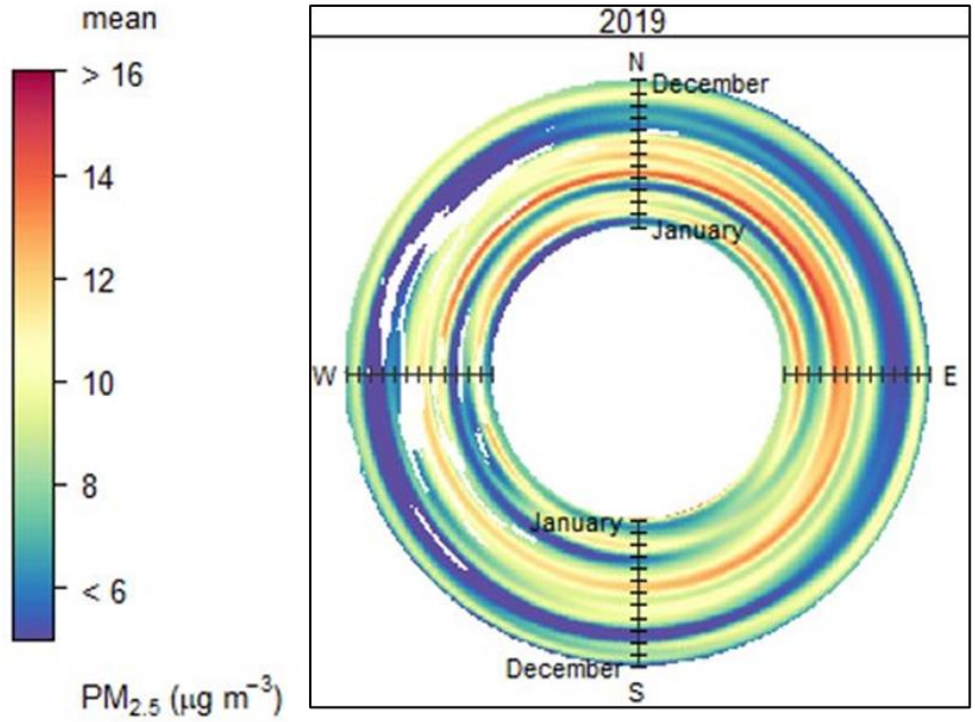

Figure 18 San Antonio 2019 Near-Road Station CAMS 1069 Polar Annulus plot for $PM_{2.5}$ Concentrations (µg/m3) in Corresponding Wind Direction and Month

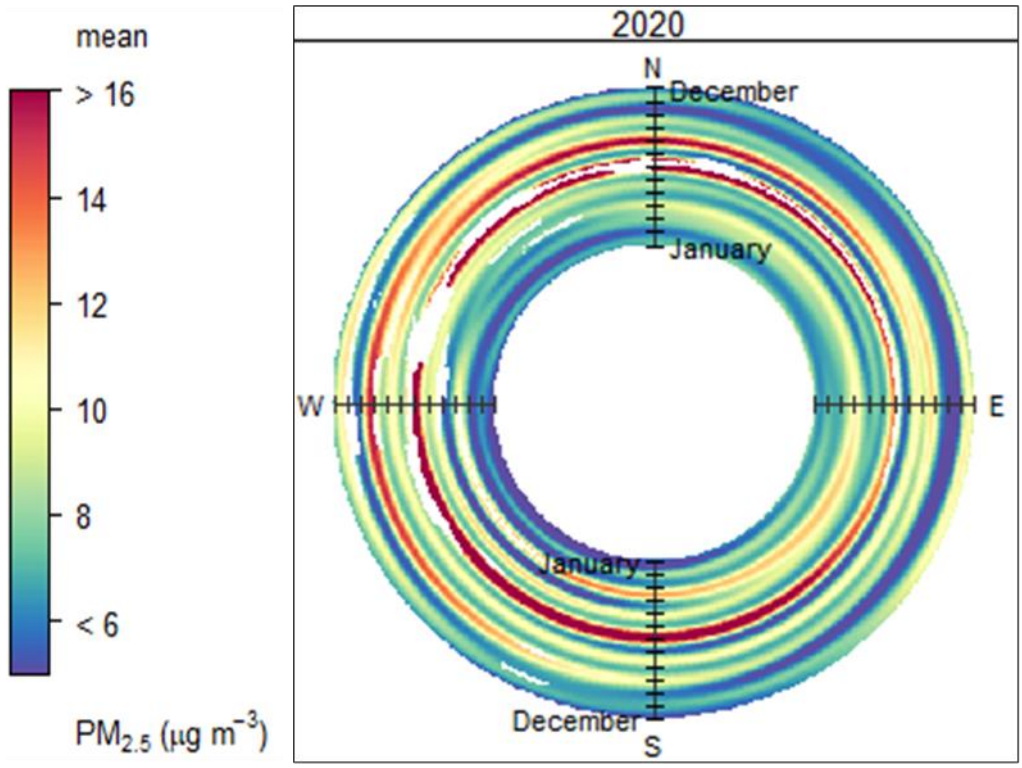

Figure 19 San Antonio 2020 Near-Road Station CAMS 1069 polar annulus plot for $PM_{2.5}$ Concentrations (µg/m3) in Corresponding Wind Direction and Month

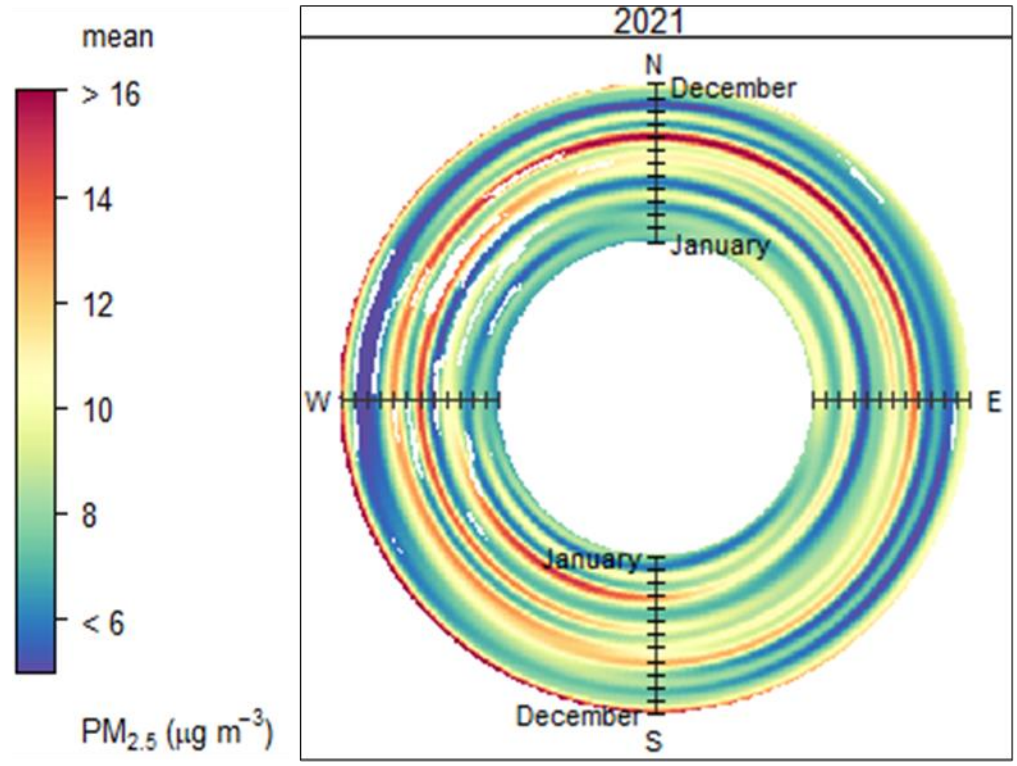

Figure 20 San Antonio 2021 Near-Road Station CAMS 1069 Polar Annulus Plot for $PM_{2.5}$ Concentrations (µg/m3) in Corresponding Wind Direction and Month

Figures 21, 22, 23, and 24 show the monthly polar $PM_{2.5}$ concentration plots concerning wind direction and speed for 2019 to 2021. Figure 22 suggests higher $PM_{2.5}$ concentrations coming from north winds in May and from the south in June, which supports the information shown in Figure 19.

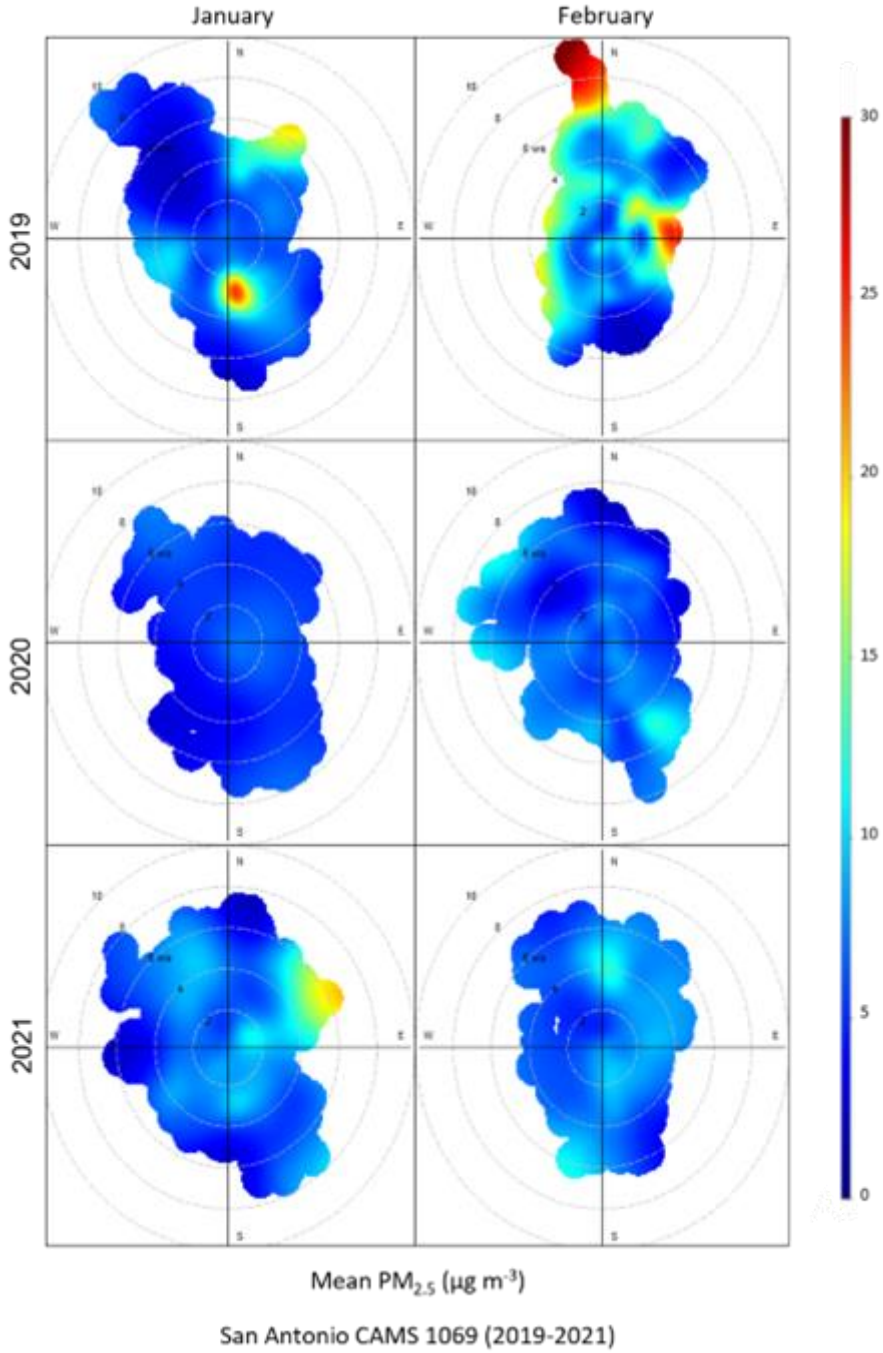

Figure 21 San Antonio 2019-2021 Near-Road CAMS 1069 $PM_{2.5}$ Concentrations ($\mu g/m^3$) in Corresponding Wind Direction for January and February

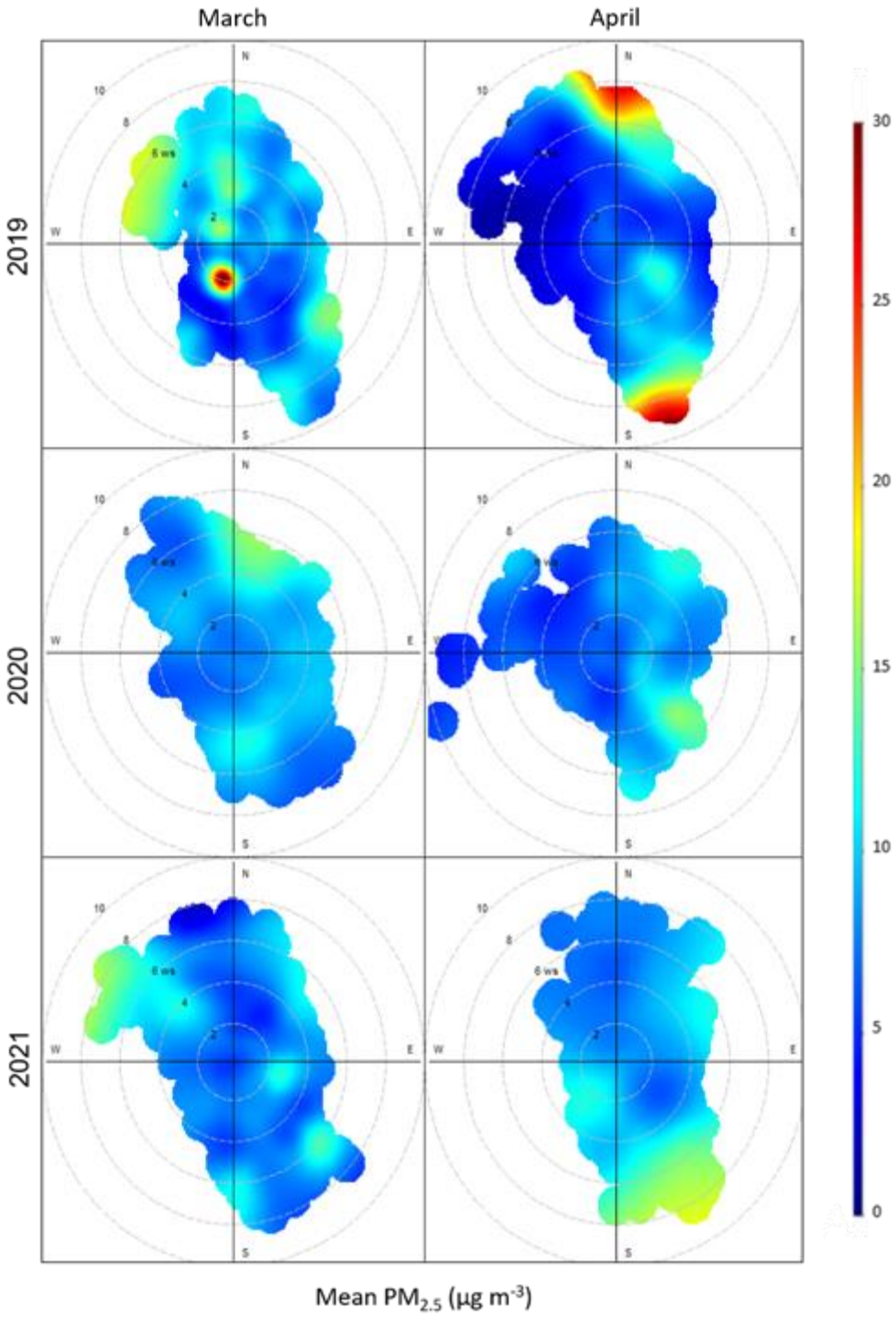

Figure 22 San Antonio 2019-2021 Near-Road CAMS 1069 $PM_{2.5}$ Concentrations ($\mu g/m^3$) in Corresponding Wind Direction for March and April

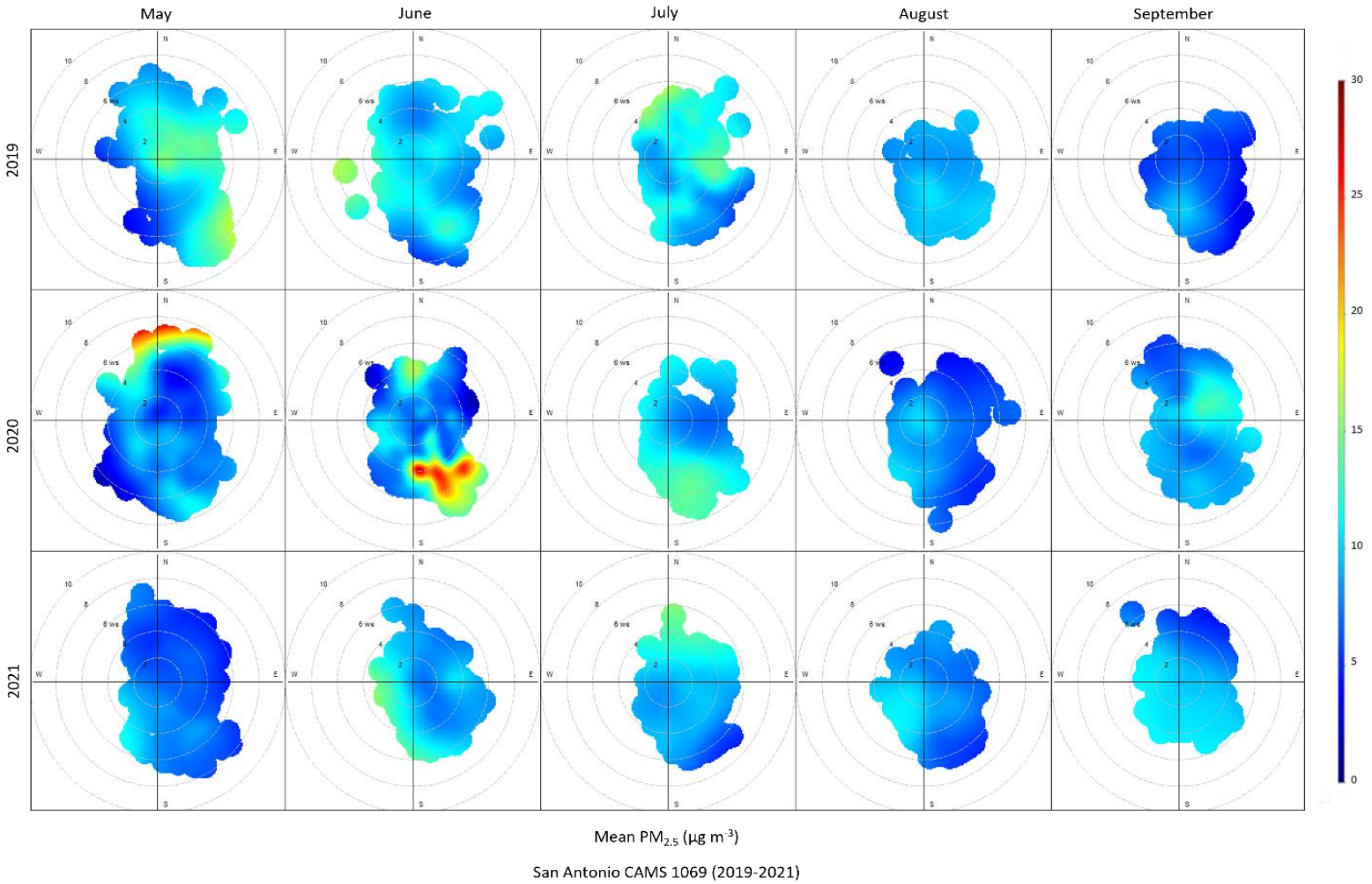

Figure 23 San Antonio 2019-2021 Near-Road CAMS1069 $PM_{2.5}$ Concentrations ($\mu g/m^3$) in Corresponding Wind Direction for May to September

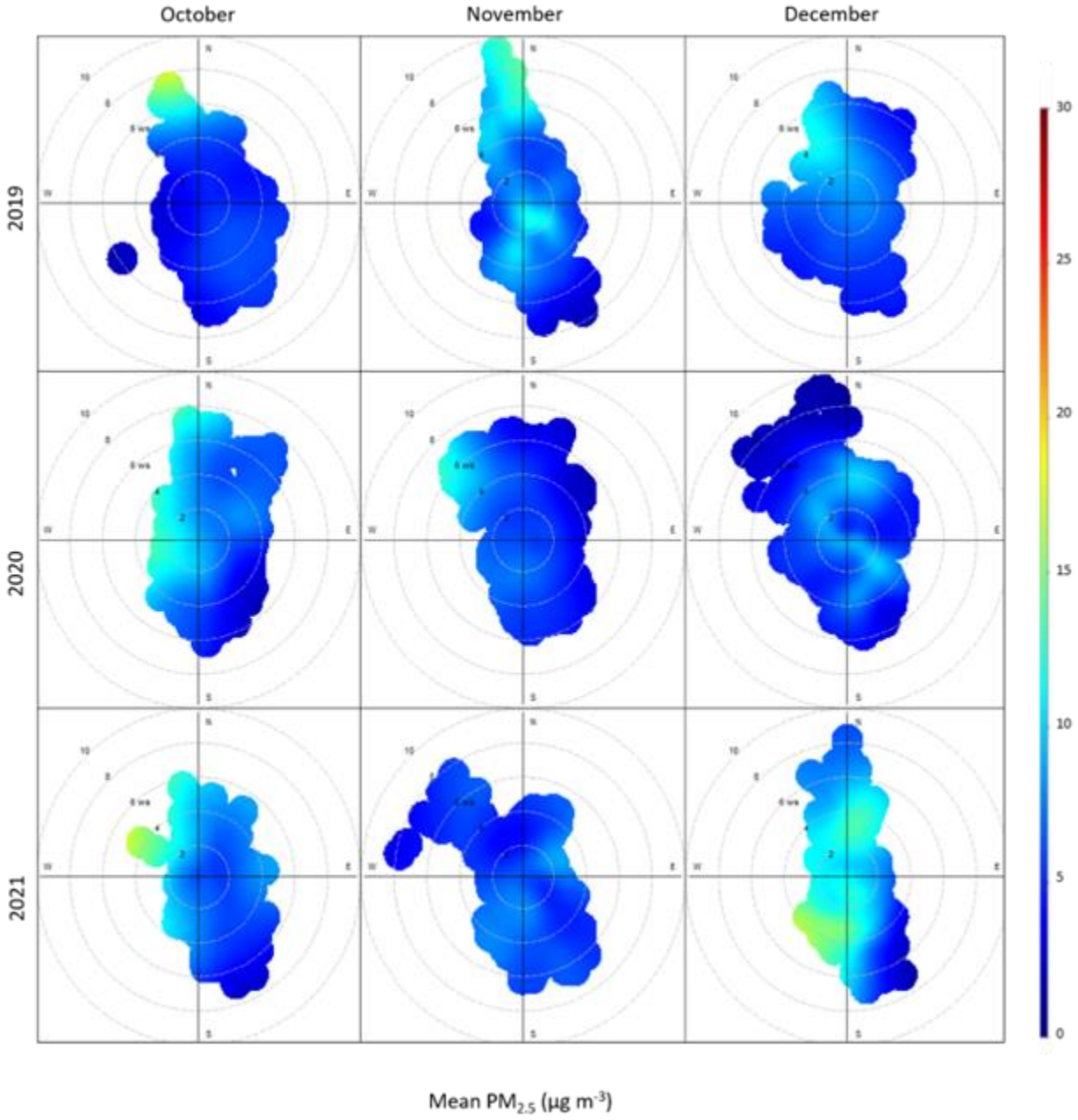

Figure 24 San Antonio 2019-2021 Near-Road CAMS 1069 $PM_{2.5}$ Concentrations ($\mu g/m^3$) in Corresponding Wind Direction for October to December

3.2.3 Houston Data Processing

Houston's near-road station CAMS1052 data is shown in Figure 25 as a yearly time series. Yearly concentrations between 2018 and 2019 highlight no observable trend, but an increase during the summer months. In 2020 an increase from mid-March to mid-April was observed. This site recorded 24-hr values every 3 or 6 days. CAMS 1052 was omitted from polar annulus plots and monthly polar $PM_{2.5}$ concentration plots as no hourly data was available.

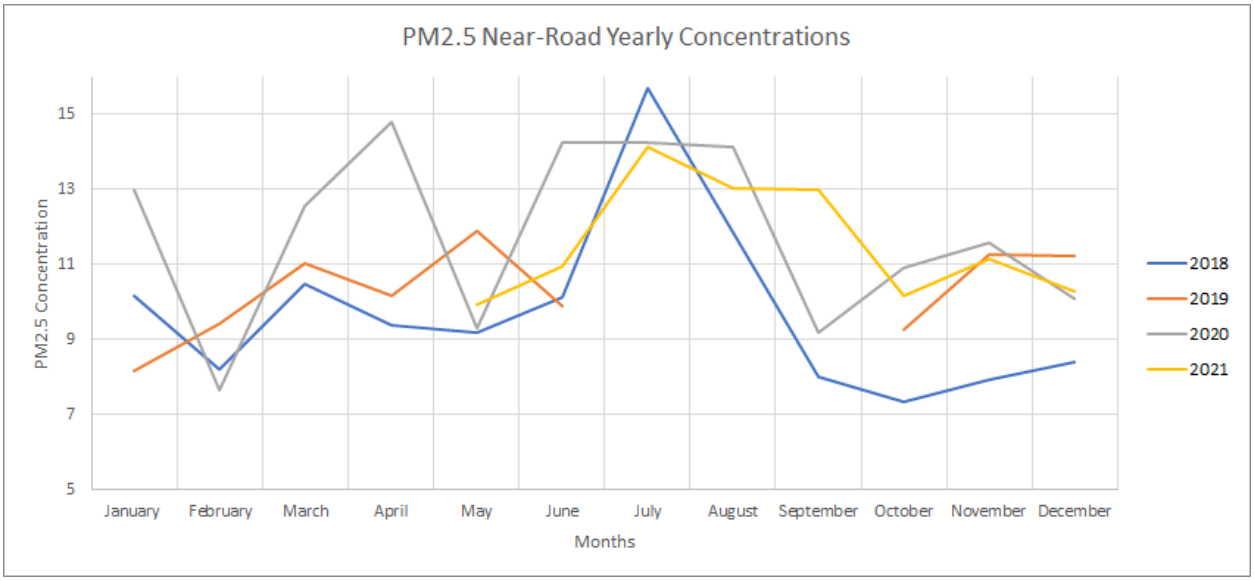

Figure 25 Houston 2018-2021 Near-Road CAMS 1052 $PM_{2.5}$ Time Series Comparison Yearly Concentrations (µg/m3)

Figure 26 shows the hourly average of $PM_{2.5}$ concentrations at the Houston near-road site 1052. Hourly data started being reported in 2021.

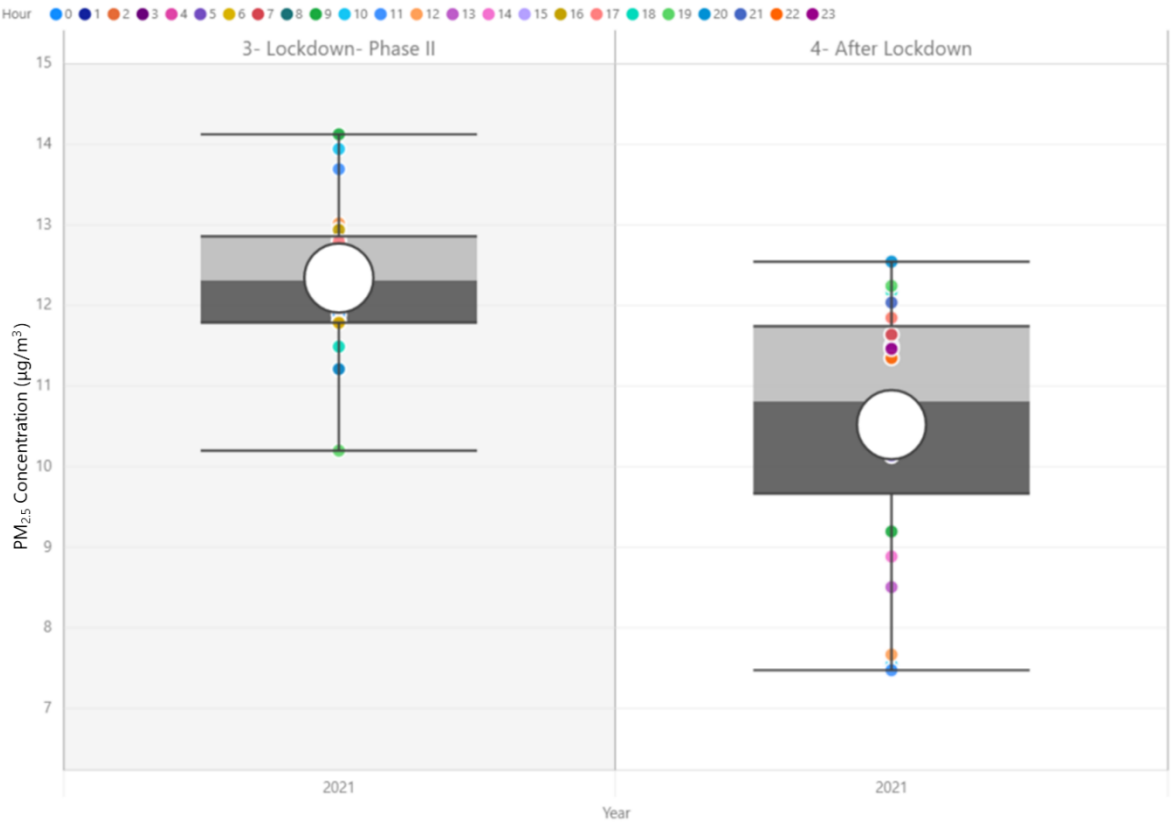

Figure 26 Houston Near-road CAMS 1052 Hourly Average $PM_{2.5}$

3.2.4 Dallas – Fort Worth Data Processing

Dallas–Fort Worth's near-road station CAMS1052 data of 24-hour values are shown in Figure 27 as a yearly time series. Yearly concentrations between 2018 and 2019 highlight no observable trend but an increase during the summer months. In 2020 an increase from mid-March to mid-April was visible.

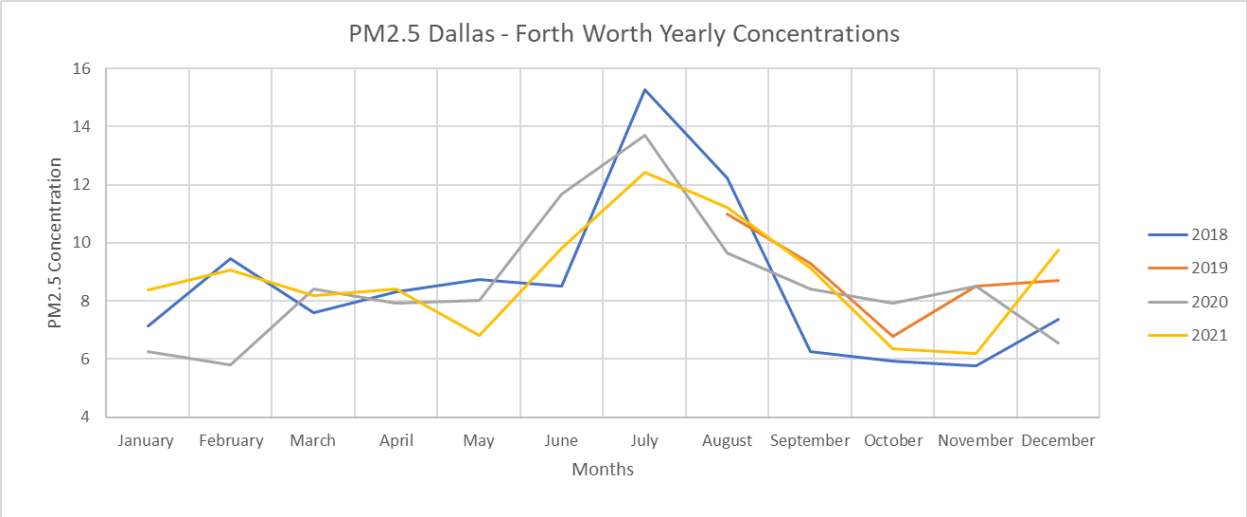

Figure 27 Dallas – Fort Worth 2018-2021 Near-Road CAMS 1053 $PM_{2.5}$ Time Series Comparison Yearly Concentrations (µg/m3)

Figure 28 shows the hourly average of $PM_{2.5}$ concentrations at the Dallas-Fort Worth near-road site 1053. During Lockdown Phase 2, concentrations were higher in comparison to other periods but remained similar throughout the three years.

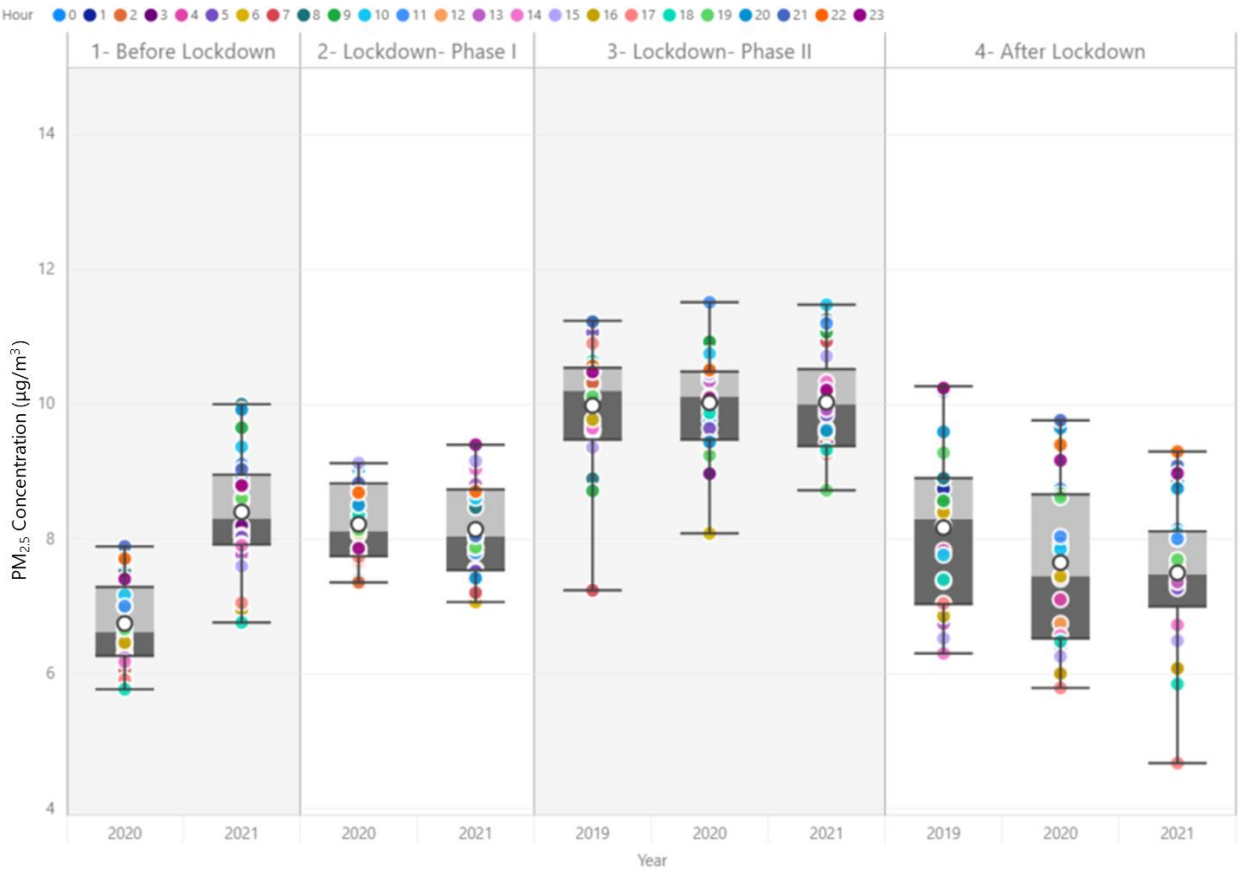

Figure 28 Dallas-Fort Worth Near-road CAMS 1053 Hourly Average $PM_{2.5}$

Figure 29 and Figure 30 provide polar $PM_{2.5}$ concentration annulus plots for CAMS 1053 by month and wind direction. In 2020, southern winds during the months of June and July prevail in comparison to other months in that year. In 2021, eastern winds in July and late winter months prevail with high $PM_{2.5}$ concentrations. CAMS 1053 is located north of Interstate Highway 610, as shown in Figure 6. High concentrations are observed in the south direction apparent in Figure 29 and the east direction in Figure 30.

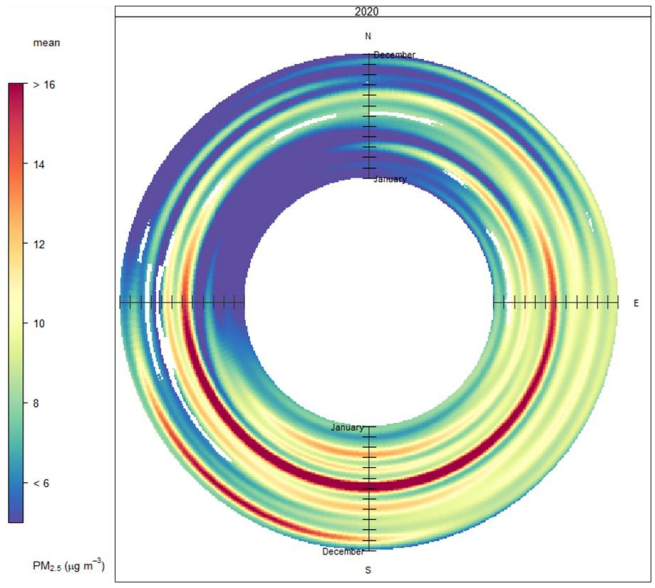

Figure 29 Dallas–Fort Worth Near-Road Station CAMS 1053 Polar Annulus Plot for $PM_{2.5}$ Concentrations (µg/m3) in Corresponding Wind direction and Season for 2020

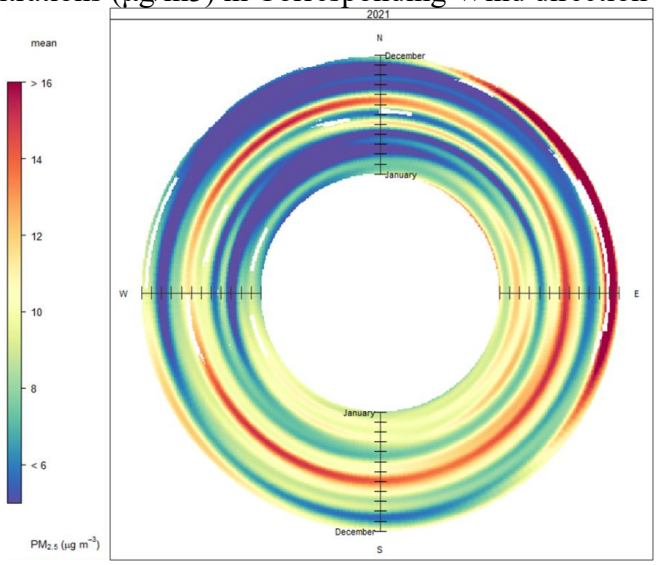

Figure 30 Dallas–Fort Worth Near-Road Station CAMS 1053 Polar Annulus Plot for $PM_{2.5}$ Concentrations (µg/m3) in Corresponding Wind direction and Season for 2021

Figures 31, 32, 33, and 34 show the monthly polar $PM_{2.5}$ concentration plots concerning wind direction and speed for 2020 to 2021. Figure 33 in the months of June to September depicts a higher concentration in 2020 compared to 2021.

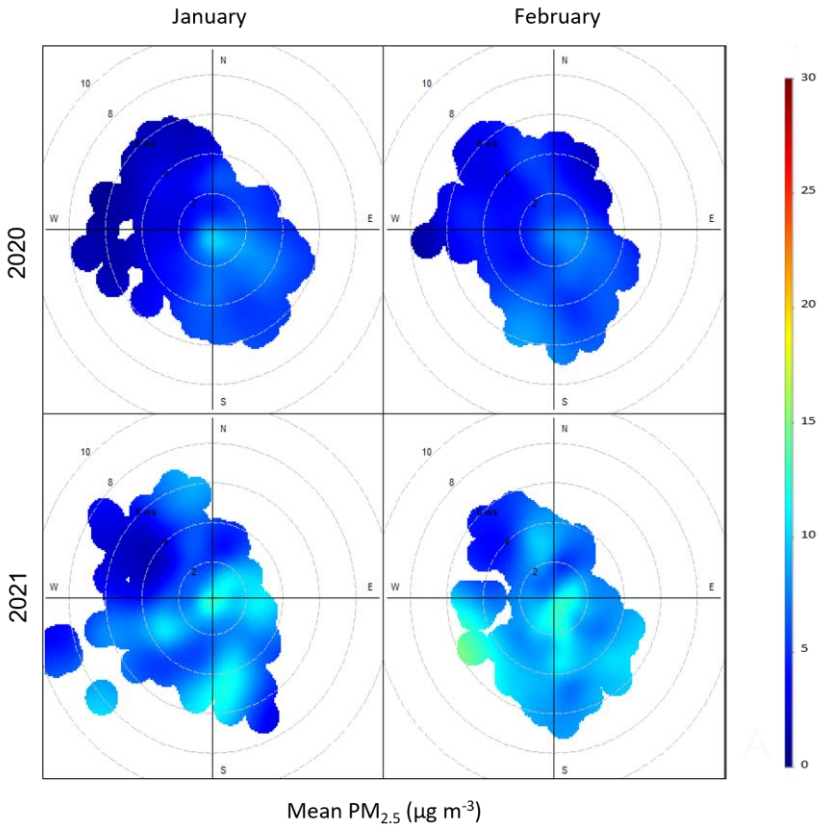

Figure 31 Dallas–Fort Worth 2020-2021 Near-Road CAMS 1053 $PM_{2.5}$ Concentrations ($\mu g/m^3$) in Corresponding Wind Direction for January and February

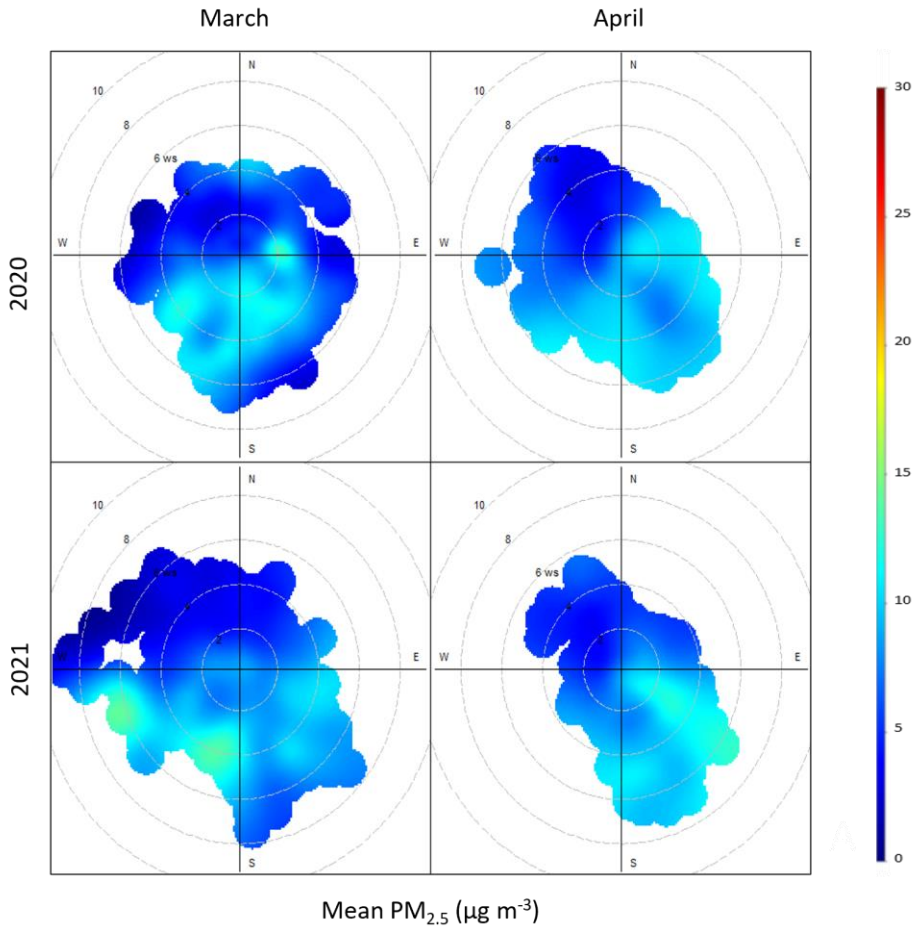

Figure 32 Dallas–Fort Worth 2020-2021 Near-Road CAMS 1053 $PM_{2.5}$ Concentrations ($\mu g/m^3$) in Corresponding Wind Direction for March and April

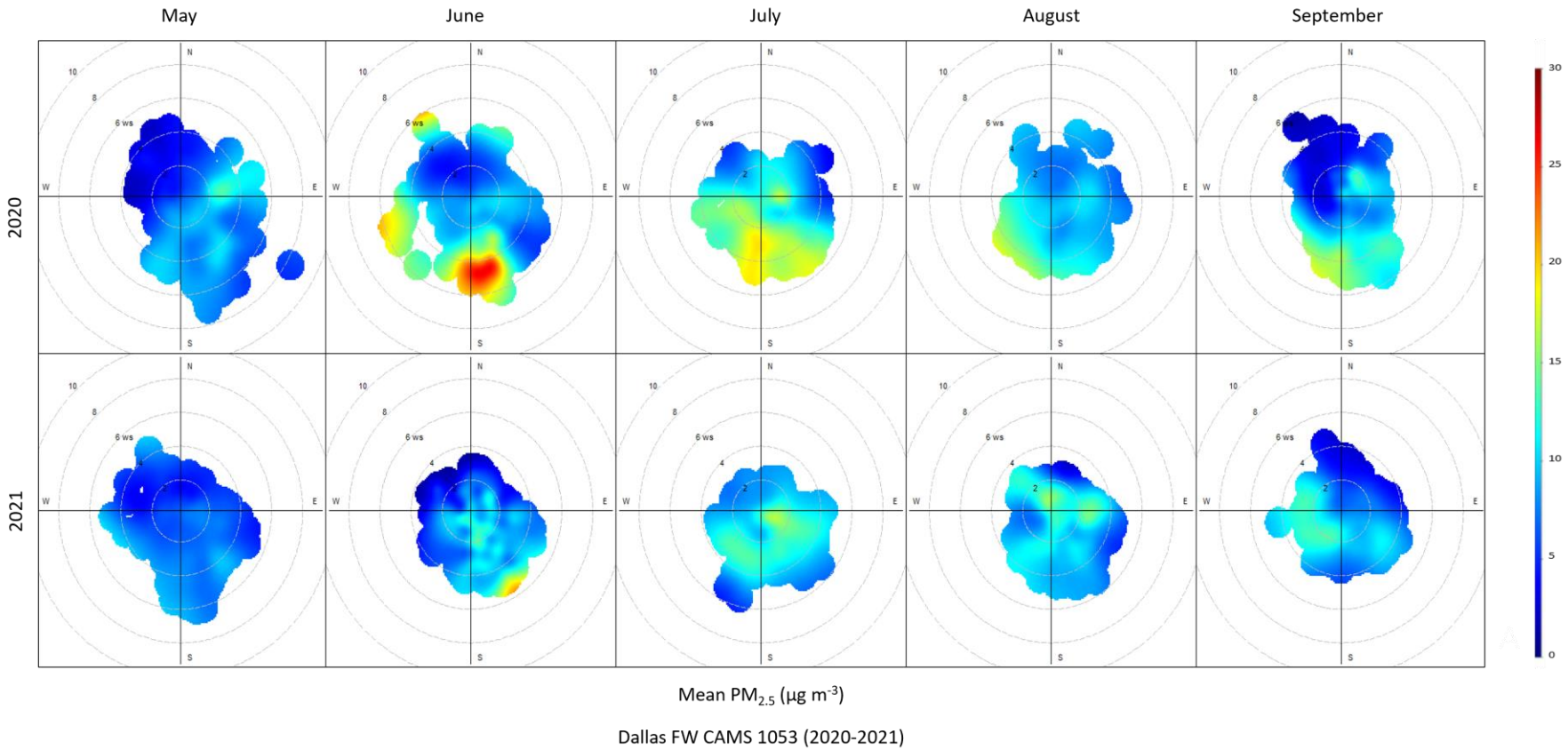

Figure 33 Dallas–Fort Worth 2020-2021 Near-Road CAMS 1053 $PM_{2.5}$ Concentrations ($\mu g/m^3$) in Corresponding Wind Direction for May to September

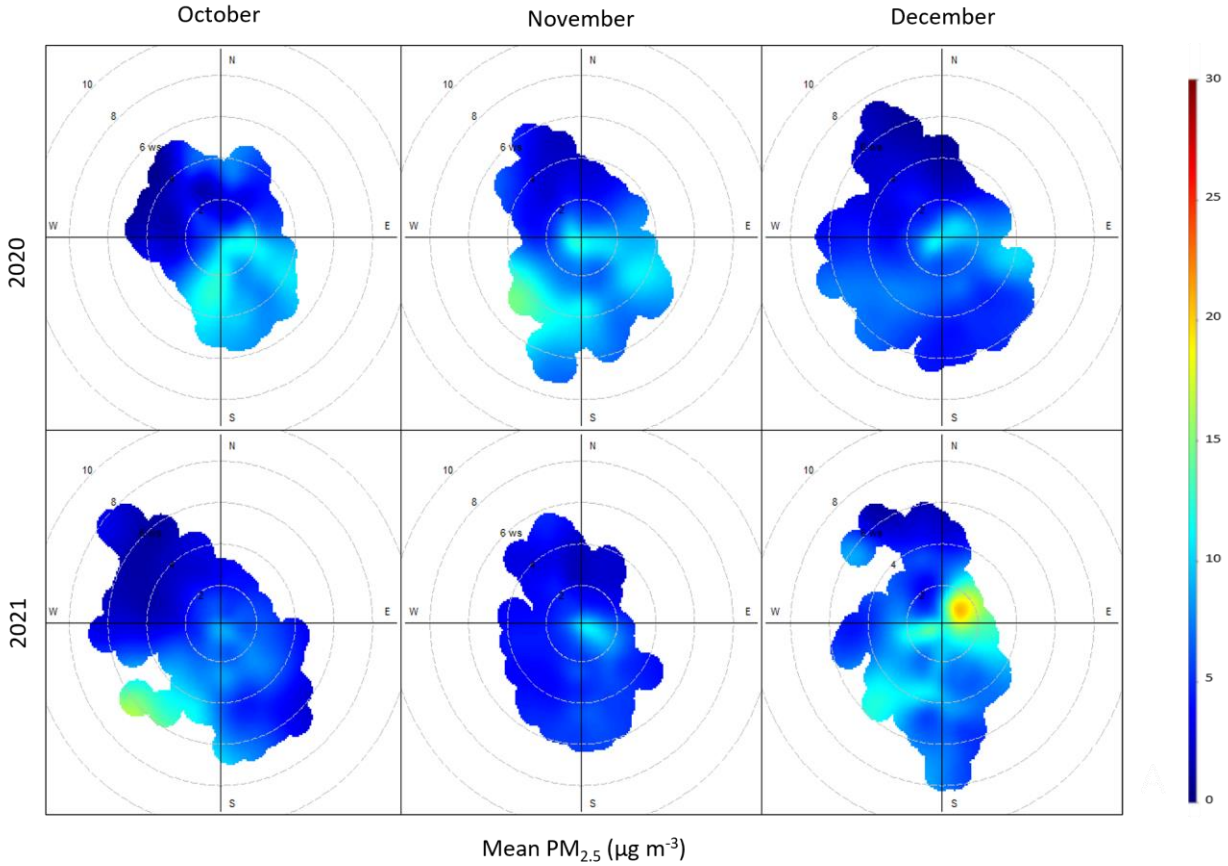

Figure 34 Dallas–Fort Worth 2020-2021 Near-Road CAMS 1053 $PM_{2.5}$ Concentrations ($\mu g/m^3$) in Corresponding Wind Direction for October to December

3.3 METEOROLOGICAL DATA ANALYSIS

Meteorology significantly affects the concentration of $PM_{2.5}$ in the atmosphere. Local weather patterns influence the behavior of particulate matter and other chemicals in the air. Identifying the sources of pollution is easier when meteorology is analyzed. Understanding wind speed and direction patterns are helpful as it allows for a better understanding of where the pollution is produced.

The meteorology parameters collected at the monitoring stations are not limited to wind speed and direction. Temperature, relative humidity, solar radiation, and pressure data are also collected as they influence the particles' concentration in the air. Meteorology parameters undergo quality control checks by TCEQ and EPA to validate the data. TCEQ follows air monitoring protocols imposed by the federal government under the EPA. Meteorology data submitted to TAMIS and AQS is formatted and coded as $PM_{2.5}$ data. Each parameter mentioned has its number ID consisting of five digits, the same as mentioned for $PM_{2.5}$ data submitted to TCEQ and EPA. Description and AQS number IDs are shown in Table 6. Each station measures different meteorological parameters depending on location and usage.

Table 6 Meteorological Parameters: Description and AQS

AQS	Description	Standard Units
61101	Wind Speed Scalar	Knots
61102	Wind Direction Scalar	Degrees Compass
61103	Wind Speed Resultant	Knots
61104	Wind Direction Resultant	Degrees Compass
62101	Temperature	Degrees Fahrenheit
62201	Relative Humidity	Percent relative humidity
63301	Solar Radiation	Langley's/minute
64101	Pressure	Millibars

Different sensors are used in each station to collect the diverse types of meteorology parameters that affect $PM_{2.5}$ concentrations. Anemometers (cup, blade, or sonic) measure wind speed with a range of 0.5 to 50 m/s and a minimum sampling frequency of 1 hour. Vane or sonic anemometers with a range of 0-359 degrees and a minimum sampling frequency of one hour are used to measure wind direction. A thermistor sensor allows for a one-hour frequency sampling with an operational range of -20 to 40 degrees Celsius to measure ambient temperature. A hygrometer with a 0 to 100% operating range and a minimum sampling frequency of one hour is used to measure relative humidity. A UV (A and B) radiometer with a 0 to 12 watts/m^2 working range is used to measure solar radiation. These parameters are used to understand the air quality trend of an area to highlight the variability between years. This section describes the procedure and usage of the data for this research.

The meteorology of each city is illustrated by the following:

1. Area map with available wind rose for 2020
2. A meteorological monitoring data summary (near-road stations are shown in bold letters)

3.3.1 Austin Meteorological Data Analysis

In Austin, eight urban air monitoring stations were active in 2015 and 2021 which provides a good background level of PM concentrations in the city. Figure 35 exhibits the only two archivable available wind roses at CAMS 3 and CAMS 171 in 2020 with concurrent data collection of $PM_{2.5}$ and wind speed and direction. Wind roses plot the frequency of occurrence of wind direction and wind speed categories using hourly data. Both stations display a more significant wind speed frequency and direction from the south. Table 7 shows a site summary of $PM_{2.5}$ sites that collected meteorological data between 2015 to 2021 in Austin. CAMS stations 601, 326, 1026, and 1094 did not record meteorological data, as seen in Table 7.

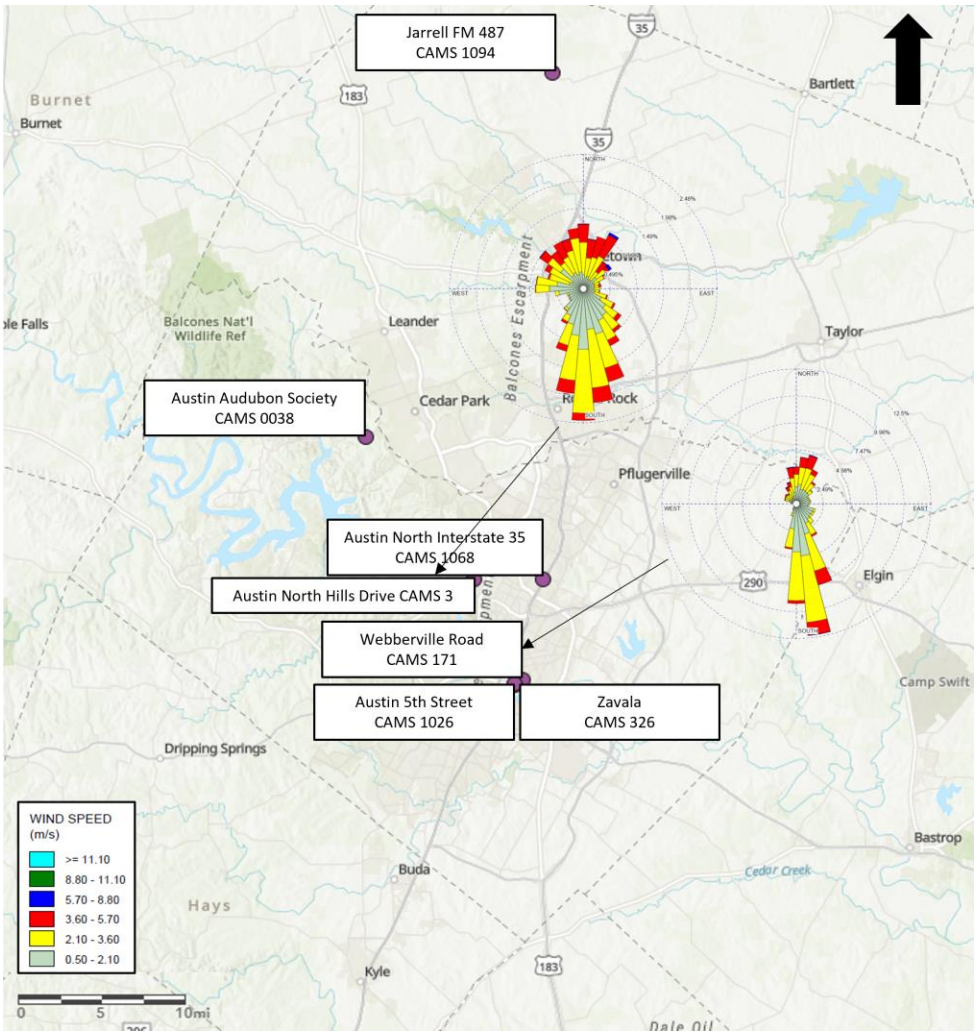

Figure 35 Austin 2020 Wind Rose Map for $PM_{2.5}$ Sites

Table 7 Austin Meteorological Monitoring Data Summary

Name	AQS Code	CAMS	Lat	Lon	Wind Speed	Wind Direction	Temperature	Pressure	Relative Humidity	Solar Radiation
Austin North Hills Drive C3/A322	484530014	3	30.35	-97.76	x	x				
Audubon C38	484530020	38	30.48	-97.87	x	x	x			x
Austin Webberville Road AF171	484530021	171	30.26	-97.71	x	x	x			
Zavala C326	484530326	326	30.26	-97.72						
Fayette County C601	481490001	601	29.96	-96.75						
Austin 5th Street C1026	484531026	1026	30.26	-97.72						
Austin North Interstate 35 C1068	**484531068**	**1068**	**30.35**	**-97.69**	**x**	**x**	**x**			
Jarrell FM 487 C1094	484911094	1094	30.81	-97.68						

3.3.2 San Antonio Meteorological Data Analysis

In San Antonio, thirteen monitoring stations were active between 2015 and 2021. Figure 36 exhibits wind roses for 7 CAMS stations (23, 59, 622, 677, 1087, 1088, and 1091) in 2020 with concurrent data collection of $PM_{2.5}$ and wind speed and direction. Table 8 shows a site summary of $PM_{2.5}$ sites that collected meteorological data between 2015 to 2021 in San Antonio. From the previous twelve stations, two stations (CAMS 301 and CAMS 676) were not recollecting meteorological data, as seen in Table 8.

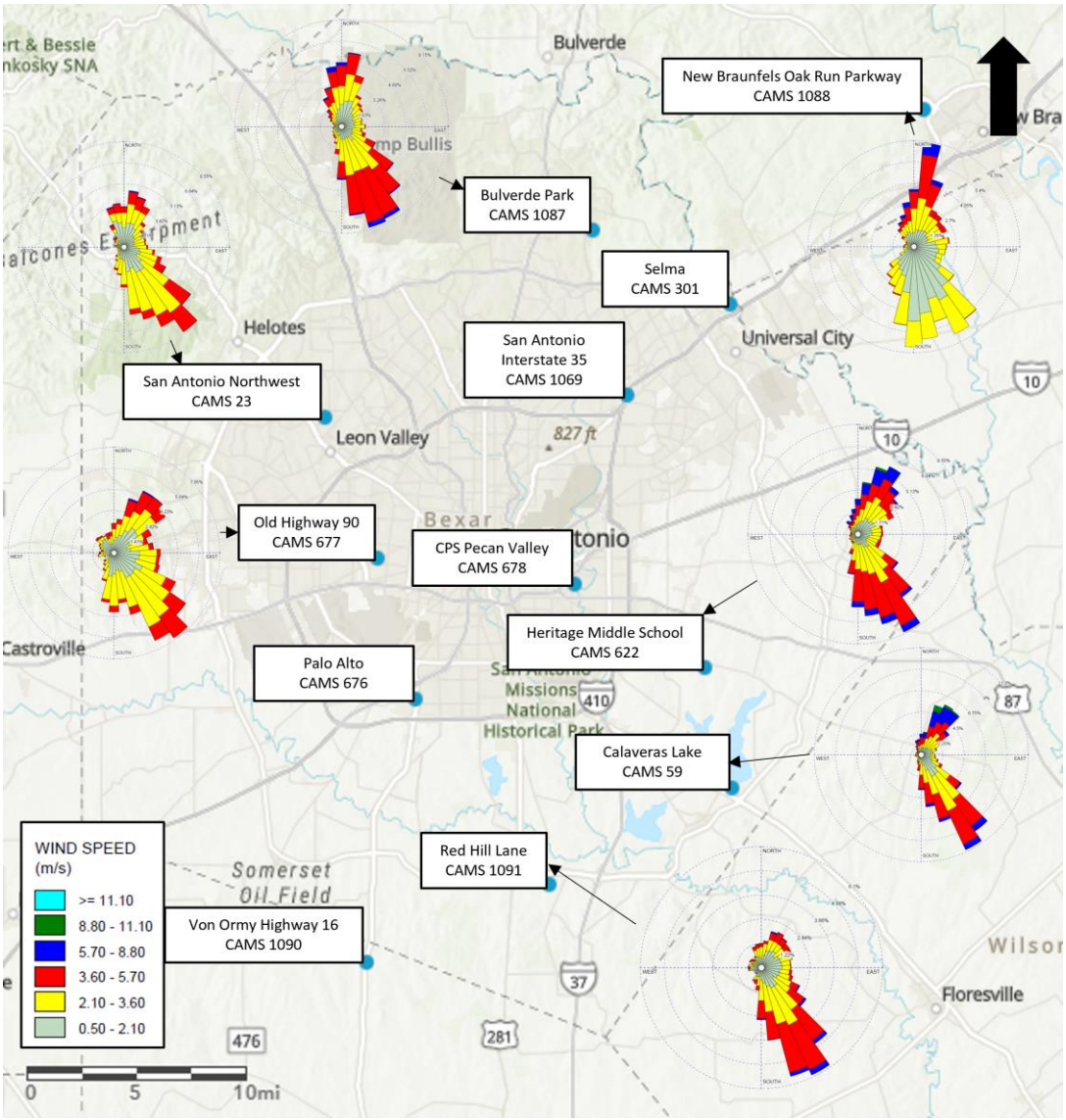

Figure 36 San Antonio 2020 Wind Rose Map for $PM_{2.5}$ Sites

Table 8 San Antonio Meteorological Monitoring Data Summary

Name	AQS Code	CAMS	Lat	Lon	Wind Speed	Wind Direction	Temperature	Pressure	Relative Humidity	Solar Radiation
San Antonio Northwest C23	480290032	23	29.52	-98.62	x	x	x			
Selma C301	480290053	301	29.59	-98.31						
CPS Pecan Valley C678	480290055	678	29.41	-98.43	x	x	x		x	x
Calaveras Lake C59	480290059	59	29.28	-98.31	x	x	x			
Heritage Middle School C622	480290622	622	29.35	-98.33	x	x	x			
Palo Alto C676	480290676	676	29.33	-98.55						
Old Highway 90 C677/A319	480290677	677	29.42	-98.58	x	x	x			
San Antonio IH 35 C1069	**480291069**	**1069**	**29.53**	**-98.39**	**x**	**x**	**x**			
San Antonio Bulverde Parkway	480291087	1087	29.64	-98.42	x	x	x			
New Braunfels Oak Run Parkway	480911088	1088	29.71	-98.17	x	x	x			
Von Ormy Highway 16 C1090	480131090	1090	29.16	-98.59	x	x	x			
San Antonio Red Hill Lane C1091	480291091	1091	29.21	-98.45	x	x	x			

3.3.3 Houston Meteorological Data Analysis

In Houston, thirteen monitoring stations were active between 2015 and 2021. Figure 37 exhibits wind roses for 10 CAMS stations (1, 8, 45, 78, 148, 304, 416, 1034, 1607, and 3000) in 2020 with concurrent data collection of $PM_{2.5}$ and wind speed and direction. Two stations (CAMS 1044 and CAMS 1054) have been inactive since January 20th, 2017, and April 13th, 2017. Table 9 shows a site summary of $PM_{2.5}$ sites that collected meteorological data between 2015 to 2021 in Houston. It is observable that south winds prevail in the stations. CAMS 1054 did not recollect meteorological data, as seen in Table 9. CAMS 1034 and CAMS 1607 have prevailing winds from the southeast due to their proximity to the Gulf of Mexico.

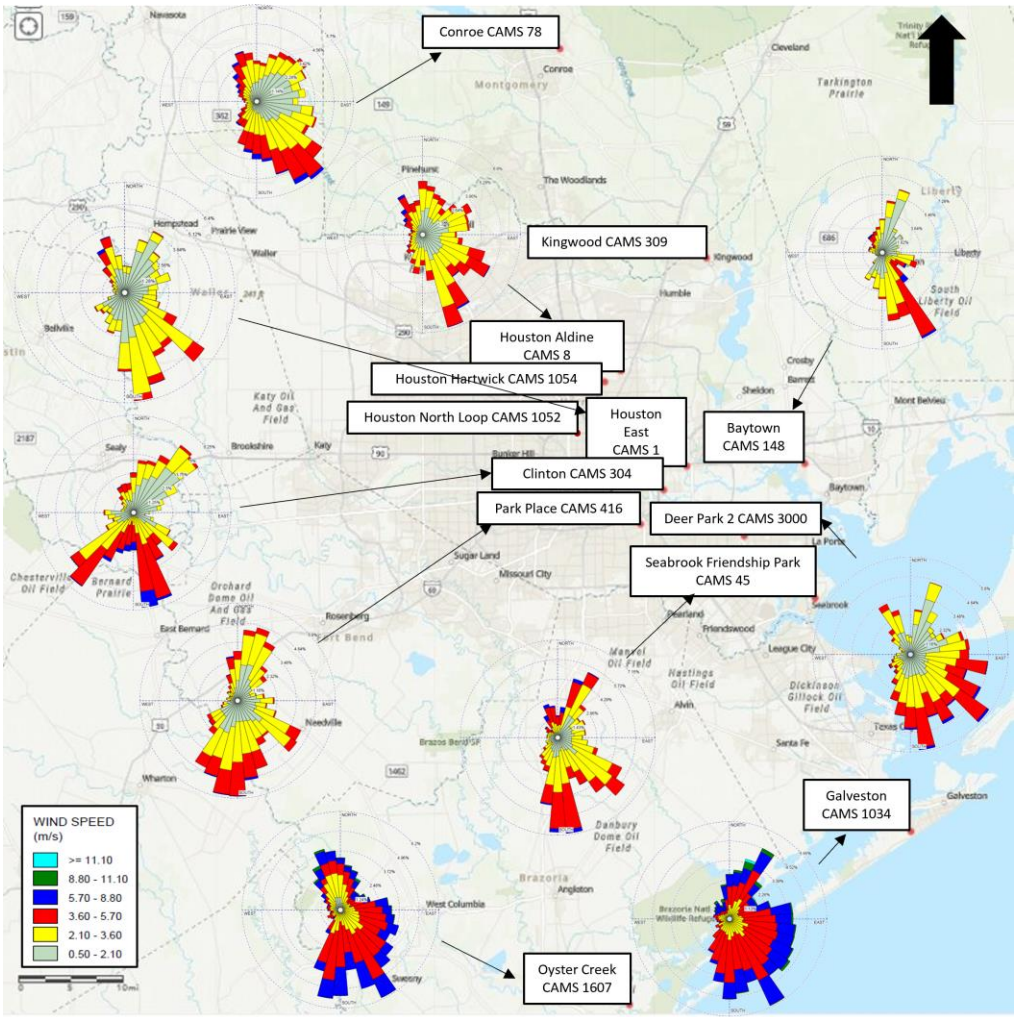

Figure 37 Houston 2020 Wind Rose Map for $PM_{2.5}$ sites

Table 9 Houston Meteorological Monitoring Data Summary

Name	AQS Code	CAMS	Lat	Lon	Wind Speed	Wind Direction	Temperature	Pressure	Relative Humidity	Solar Radiation
Houston East C1/G316	482011034	1	29.77	-95.22	x	x	x			
Houston Aldine C8/AF108/X150	482010024	8	29.90	-95.33	x	x	x	x	x	x
Hou.DeerPrk2 C35/235/1001/AFH139FP239	482011039	35	29.67	-95.13	x	x	x	x	x	x
Seabrook Friendship Park C45	482011050	45	29.58	-95.02	x	x	x			x
Clinton C403/C304/AH113	482011035	55	29.73	-95.26	x	x	x	x	x	x
Conroe Relocated C78/A321	483390078	78	30.35	-95.43	x	x	x			x
Baytown A148	482010058	148	29.77	-95.03	x	x	x			
Kingwood C309	482011042	309	30.06	-95.19						
Park Place C416	482010416	416	29.69	-95.30	x	x	x	x	x	x
Galveston 99th St. C1034/A320/X183	481671034	1034	29.25	-94.86	x	x	x		x	x
Houston North Loop C1052	**482011052**	**1052**	**29.81**	**-95.39**	**x**	**x**	**x**			
Houston Hartwick C1054	482011054	1054	29.89	-95.35						
Oyster Creek C1607	480291607	1607	29.01	-95.31	x	x	x			

3.3.4 Dallas – Fort Worth Meteorological Data Analysis

In Dallas – Fort Worth, ten monitoring stations were active between 2015 and 2021. Figure 38 exhibits wind roses for 6 CAMS stations (13, 52, 56, 71, 161, and 1051) in 2020 with concurrent data collection of $PM_{2.5}$ and wind speed and direction. Table 10 shows a site summary of $PM_{2.5}$ sites that collected meteorological data between 2015 to 2021 sites in Dallas – Fort Worth. It is observable that south winds prevail in the stations. CAMS 310 did not collect wind speed and direction parameters as shown in Table 10.

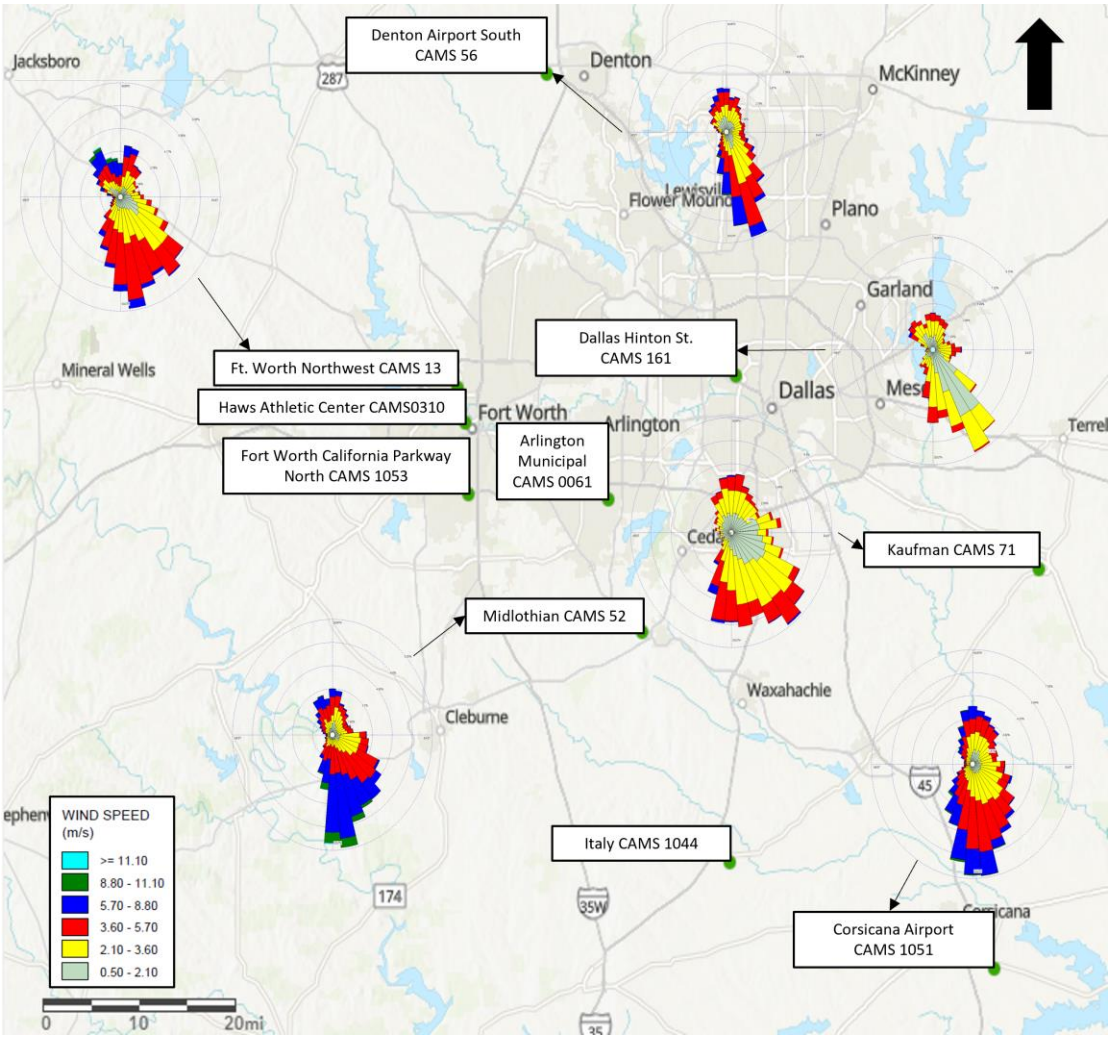

Figure 38 Dallas – Fort Worth 2020 Wind Rose Map for $PM_{2.5}$ sites

Table 10 Dallas–Fort Worth Meteorological Monitoring Data Summary

Name	AQS Code	CAMS	Lat	Lon	Wind Speed	Wind Direction	Temperature	Pressure	Relative Humidity	Solar Radiation
Ft. Worth Northwest C13/AH302	484391002	13	32.81	-97.36	x	x	x		x	x
Midlothian OFW C52/A137	481390016	52	32.48	-97.03	x	x	x			x
Denton Airport South C56/A163/X157	481210034	56	33.22	-97.20	x	x	x		x	x
Dallas Hinton St. C401/C60/AH161	481130069	60	32.82	-96.86	x	x	x		x	x
Arlington Municipal Airport C61	484393011	61	32.66	-97.09	x	x	x			x
Kaufman C71/A304/X071	482570005	71	32.57	-96.32	x	x	x		x	x
Haws Athletic Center C310	484391006	310	32.76	-97.34						x
Italy C1044/A323	481391044	1044	32.18	-96.87	x	x	x		x	x
Corsicana Airport C1051	483491051	1051	32.03	-96.40	x	x	x		x	
Ft Worth California Parkway North C1053	**484391053**	**1053**	**32.67**	**-97.34**	**x**	**x**	**x**			

Chapter 4 Results & Discussion

The assumption of more cars on the road has been correlated to the increase of emissions in traffic on highways and urban areas. The lockdown period in 2020 allows for the testing of this assumption as restrictions were imposed that limited the number of people on highways. This causes a change in countries' air quality including the United States.

Impacts of the COVID-19 pandemic on PM air quality in urban regions are evaluated using the annual PM concentrations observed at urban and near-road air monitoring stations in four metropolitan cities in Texas. To effectively analyze the impact of the COVID-19 pandemic it was necessary to adhere to the time period in which the restrictions were placed in effect. After deciding the time periods used for this analysis, a series of Welch's t-tests were performed for all urban stations within each city from 2015 to 2021. Additionally, the same was performed for near-road stations for the years with available data. This chapter will further explain the usage and the results from the evaluation of the stations in this study.

4.1 Impacts of Covid-19 Lockdown on $PM_{2.5}$ Pollution

In this chapter the following time periods were used for urban stations:

- Before Lockdown (January 1st to March 20th, 2015-2021)
- Lockdown Phase I (March 21st to April 30th, 2015-2021)
- Lockdown Phase II (May 1st to September 30th, 2015-2021)
- After Lockdown (October 1st to December 31st, 2015-2021)

These period sets adhere to the pandemic period in the state of Texas as restrictions were imposed. Average period values for each period were found using average daily $PM_{2.5}$ concentrations. Near-road stations did not have sufficient data to be analyzed using the same time periods. Therefore, Welch's one-tail t-tests performed for near-road stations used average monthly $PM_{2.5}$ concentrations from 2015 to 2021 for near-road stations.

Performing a time series analysis was not sufficient to differentiate the effects of seasonal variations caused by traffic activity, temperature, and pressure. For each time period and station, the mean values were calculated ($C_{i,j,k}$), where *i* represents the station, *j* the year, and *k* the time period. Thus, a dataset consisting of $C_{i,j,k}$ values for all 31 urban sites in Houston, Austin, San Antonio, and Dallas-Fort Worth, *i*: 1-31; *j*:1-6 (i.e., 2015-2021); and *k*: 1-4 were created. The same was performed for the 4 near-road stations with their respective available data. The average, count, and standard deviation were needed to calculate the degrees of freedom, t-statistics, and p-values to perform a series of one-tail unequal variance t-tests. The unequal variance t-test is also known as Welch's t-test. Welch's t-tests were used since the number of available stations did not remain constant from year to year. This type of test demonstrates the significant difference between group means for each of the years between 2015 to 2021, for all the urban and near-road stations, respectively (e.g., $C_{i,2020,\text{ Lockdown Phase 1}}$, vs. $C_{i,2015,\text{ Lockdown Phase 1}}$).

The Welch's one-tail t-test allows testing of an alternative hypothesis which in this case is to determine whether one year is significantly different from another. This type of test allows for the determination if one of the population means is greater than the other. If there is no impact (increase or decrease) in PM concentrations, then urban nor near-road stations will experience any statistically significant change.

A Welch's t-test can be either left-tailed or right-tailed. The direction of the t-value determines the side the test will be assigned, a left-tailed test is assigned when the alternative hypothesis asserts that the true value of the parameter indicated in the null hypothesis is lower than what the null hypothesis suggests. When the alternative hypothesis asserts that the true value of the parameter stated in the null hypothesis is higher than the null hypothesis claims, a right-tailed test is utilized.

The values of t-stat, P-value, and t-critical one-tail per year are shown in each square section, respectively, as shown in Table 11. P-values less than .05 are considered statistically significant in this study. The comparison between the t-stat and the t-critical values allows for the determination of whether the null hypothesis should be accepted or rejected. Moreover, if P-value

< .05 it will result in the rejection of the null hypothesis, and the acceptance of the alternative hypothesis.

Table 11 T-Test Matrix Example

Example	
Years	2016
2015	t-stat
	P-value
	t-critical

Tables 12, 13, 14, and 15 show Welch's t-test performed for all urban stations between 2015 to 2021. Table 12 shows how the matrix was separated into two sections by a diagonal set of gray squares. The top-right side of the matrix shows the values generated by the t-test. The bottom-left side of Table 12 displays the results. Three possible outcomes are shown in the top-right section; for example, year 1 is greater than year 2, year 1 is less than year 2, or NSD (no significant difference), and the test statistics are listed in the opposite upper triangular section of the table. Table 12 shows the performance assessed by Welch's t-test of the mean values from January 1st to March 20th.

Table 12 showed no significant difference for the compared years except on the following occasions: 2017 being significantly greater than 2015 and 2016, 2018 being greater than 2016, and 2021 having a greater mean than the years 2015, 2016, and 2020. As shown in Table 13, there was a significant difference between March 21st to April 30th for the years 2020 and 2021 compared to previous years in the overall urban station across the four cities. The quarantine lockdown was performed during this period in the state of Texas. Table 14 exhibits 2015 as the most remarkable significant difference between each year, but 2020 had a highly significant difference compared to other years except for 2015 and 2018. Table 15 presents no significant differences for any of the years except when we reached the year 2018, which had the lowest mean value. It is interesting to note that no significant variations in mean values during the Before Lockdown phase occurred

in 2020, indicating that background $PM_{2.5}$ concentrations were consistent with usual level concentrations before the COVID-19 pandemic outbreak.

Table 12 Welch's T-Test Urban Stations – Before Lockdown (January to March 20th, 2015-2021)

Urban Stations Welch's T-Test Jan 1 - March 20							
Years	**2015**	**2016**	**2017**	**2018**	**2019**	**2020**	**2021**
Mean Con.	7.1	7.1	8.1	7.8	7.7	7.4	8.0
		0.053	-2.239	-1.595	-1.311	-0.835	-2.451
2015		0.479	**0.015**	0.059	0.099	0.204	**0.009**
		1.673	1.677	1.680	1.686	1.674	1.673
			-2.433	-1.739	-1.420	-0.974	-2.784
2016	**NSD**		**0.010**	**0.045**	0.083	0.168	**0.004**
			1.682	1.687	1.694	1.679	1.676
				0.506	0.631	1.499	0.272
2017	**2015<2017**	**2016<2017**		0.308	0.265	0.070	0.394
				1.674	1.677	1.676	1.676
					0.150	0.894	-0.318
2018	**NSD**	**2016<2018**	**NSD**		0.441	0.188	0.376
					1.678	1.679	1.680
						0.666	-0.469
2019	**NSD**	**NSD**	**NSD**	**NSD**		0.255	0.321
						1.684	1.685
							-1.512
2020	**NSD**	**NSD**	**NSD**	**NSD**	**NSD**		**0.068**
							1.675
2021	**2015<2021**	**2016<2021**	**NSD**	**NSD**	**NSD**	**2020<2021**	

Table 13 Welch's T-Test Urban Stations – Lockdown Phase 1 (March 21st to April 30th, 2015-2021)

Urban Stations Welch's T-Test March 21 -April 30							
Years	**2015**	**2016**	**2017**	**2018**	**2019**	**2020**	**2021**
Mean Con.	8.1	8.4	8.8	8.4	8.1	9.4	9.3
		-0.901	-1.313	-0.731	-0.031	-3.362	-3.373
2015		0.186	0.098	0.234	0.488	**0.001**	**0.001**
		1.673	1.686	1.682	1.675	1.679	1.673
			-0.852	-0.106	0.827	-2.847	-2.822
2016	**NSD**		0.200	0.458	0.206	**0.003**	**0.003**
			1.691	1.687	1.679	1.685	1.676
				0.670	1.276	-0.971	-0.781
2017	**NSD**	**NSD**		0.253	0.105	0.168	0.220
				1.677	1.685	1.680	1.684
					0.690	-2.083	-1.936
2018	**NSD**	**NSD**	**NSD**		0.247	**0.021**	**0.030**
					1.681	1.679	1.680
						-3.241	-3.226
2019	**NSD**	**NSD**	**NSD**	**NSD**		**0.001**	**0.001**
						1.680	1.676
							0.330
2020	**2015<2020**	**2016<2020**	**NSD**	**2018<2020**	**2019<2020**		0.371
							1.678
2021	**2015<2021**	**2016<2021**	**NSD**	**2018<2021**	**2019<2021**	**NSD**	

Table 14 Welch's T-Test Urban Stations – Lockdown Phase 2 (May 1st to September 30th, 2015-2021)

Urban Stations Welch's T-Test May 1 to September 30							
Years	**2015**	**2016**	**2017**	**2018**	**2019**	**2020**	**2021**
Mean Con.	10.8	9.0	8.9	10.2	9.2	10.0	9.2
		7.132	6.168	1.683	4.308	2.872	4.849
2015		**0.000**	**0.000**	**0.050**	**0.000**	**0.003**	**0.000**
		1.675	1.673	1.681	1.682	1.672	1.672
			0.396	-3.324	-0.378	-3.907	-0.682
2016	**2015>2016**		0.347	**0.001**	0.354	**0.000**	0.249
			1.679	1.692	1.692	1.677	1.679
				-3.229	-0.604	-3.513	-0.891
2017	**2015>2017**	**NSD**		**0.001**	0.275	**0.000**	0.188
				1.680	1.680	1.674	1.673
					2.249	0.517	2.349
2018	**2015>2018**	**2016<2018**	**2017<2018**		**0.015**	0.304	**0.011**
					1.677	1.683	1.677
						-2.165	-0.157
2019	**2015>2019**	**NSD**	**NSD**	**2018>2019**		**0.018**	0.438
						1.683	1.677
							2.346
2020	**2015>2020**	**2016<2020**	**2017<2020**	**NSD**	**2019<2020**		**0.011**
							1.674
2021	**2015>2021**	**NSD**	**NSD**	**2018>2021**	**NSD**	**2020>2021**	

Table 15 Welch's T-Test Urban Stations – After Lockdown (October 1st to December 31st, 2015-2021)

Urban Stations Welch's T-Test October 1 - December 31							
Years	**2015**	**2016**	**2017**	**2018**	**2019**	**2020**	**2021**
Mean Con.	7.5	7.6	7.7	6.1	7.9	7.6	7.7
		-0.087	-0.381	4.263	-1.018	-0.260	-0.255
2015		0.465	0.352	**0.000**	0.157	0.398	0.400
		1.673	1.679	1.675	1.681	1.678	1.684
			-0.300	4.129	-0.913	-0.178	-0.194
2016	**NSD**		0.383	**0.000**	0.183	0.430	0.424
			1.677	1.675	1.679	1.677	1.681
				3.719	-0.531	0.119	0.047
2017	**NSD**	**NSD**		**0.000**	0.299	0.453	0.481
				1.676	1.675	1.674	1.675
					-4.323	-3.784	-3.022
2018	**2015>2018**	**2016>2018**	**2017>2018**		**0.000**	**0.000**	**0.002**
					1.678	1.676	1.679
						0.672	0.500
2019	**NSD**	**NSD**	**NSD**	**2018<2019**		0.252	0.310
						1.676	1.675
							-0.052
2020	**NSD**	**NSD**	**NSD**	**2018<2020**	**NSD**		0.479
							1.677
2021	**NSD**	**NSD**	**NSD**	**2018<2021**	**NSD**	**NSD**	

Welch's one-tail t-tests were performed for near-road stations using monthly averages of $PM_{2.5}$ concentrations. The monthly concentrations were tested to determine whether the concentration in one year is significantly higher than another year's concentration. There was not sufficient data to run the test for the specific periods used for urban stations. Tables 16, 17, 18, and 19 show Welch's t-tests performed for near-road stations in Austin, San Antonio, Houston, and Dallas – Fort Worth, respectively. Tables 16, 17, and 19 did not show any significant differences between the years for their respective stations. Hourly values for the years 2015 and 2016 were not available for Austin's near-road station CAMS 1068 and San Antonio's near-road station CAMS 1069. Table 18 displays CAMS 1052 for the years 2015 to 2021. From this table, 2015, 2020, and 2021 showed significant differences in comparison to previous years which could result from the pandemic lockdown.

Table 16 Welch's T-Test Austin Near-Road Station CAMS 1068 2017-2021

Welch's T-Test Austin CAMS1068 2015-2021							
Years	**2015**	**2016**	**2017**	**2018**	**2019**	**2020**	**2021**
Mean Con.			9.2	9.7	9.5	9.5	8.9
2015							
2016							
				-0.311	-0.530	-0.371	0.490
2017				0.381	0.301	0.357	0.314
				1.812	1.717	1.721	1.717
					0.112	0.142	0.497
2018			**NSD**		0.456	0.445	0.315
					1.812	1.796	1.812
						0.077	1.051
2019			**NSD**	**NSD**		0.470	0.152
						1.725	1.717
							0.800
2020			**NSD**	**NSD**	**NSD**		0.217
							1.725
2021			**NSD**	**NSD**	**NSD**	**NSD**	

Table 17 Welch's T-Test San Antonio Near-Road Station CAMS 1069 for 2017 to 2021

Welch's T-Test San Antonio CAMS 1069 2015-2021							
Years	**2015**	**2016**	**2017**	**2018**	**2019**	**2020**	**2021**
Mean Con.			8.9	9.7	9.2	8.5	8.6
2015							
2016							
				-1.117	-0.506	0.737	0.590
2017				0.140	0.309	0.235	0.281
				1.746	1.725	1.725	1.717
					0.646	1.545	1.476
2018			**NSD**		0.263	0.069	0.079
					1.725	1.725	1.734
						1.072	0.969
2019			**NSD**	**NSD**		0.148	0.172
						1.717	1.721
							-0.207
2020			**NSD**	**NSD**	**NSD**		0.419
							1.721
2021			**NSD**	**NSD**	**NSD**	**NSD**	

Table 18 Welch's T-Test Houston Near-Road Station CAMS 1052 for 2015 to 2021

Welch's T-Test Houston CAMS 1052 2015-2021							
Years	**2015**	**2016**	**2017**	**2018**	**2019**	**2020**	**2021**
Mean Con.	12.6	10.2	9.6	9.7	10.3	11.8	11.7
		2.468	3.073	2.653	2.478	0.736	0.872
2015		**0.014**	**0.004**	**0.009**	**0.015**	0.236	0.200
		1.771	1.771	1.746	1.796	1.746	1.782
			0.851	0.516	-0.161	-1.953	-1.972
2016	**2015>2016**		0.202	0.306	0.437	**0.032**	**0.038**
			1.717	1.725	1.729	1.725	1.812
				-0.201	-1.105	-2.669	-2.747
2017	**2015>2017**	**NSD**		0.421	0.141	**0.007**	**0.011**
				1.725	1.729	1.725	1.833
					-0.686	-2.184	-2.198
2018	**2015>2018**	**NSD**	**NSD**		0.251	**0.020**	**0.023**
					1.740	1.717	1.771
						-1.957	-1.990
2019	**2015>2019**	**NSD**	**NSD**	**NSD**		**0.033**	**0.043**
						1.740	1.895
							0.119
2020	**NSD**	**2016<2020**	**2017<2020**	**2018<2020**	**2019<2020**		0.453
							1.771
2021	**NSD**	**2016<2021**	**2017<2021**	**2018<2021**	**2019<2021**	**NSD**	

Table 19 Welch's T-Test Dallas – Fort Worth Near-Road Station CAMS 1053 for 2015 to 2021

Welch's T-Test Dallas – Fort Worth CAMS 1053 2015-2021							
Years	**2015**	**2016**	**2017**	**2018**	**2019**	**2020**	**2021**
Mean Con.	9.2	8.5	8.8	8.6	8.2	8.6	8.8
		0.671	0.508	0.568	1.011	0.601	0.407
2015		0.256	0.311	0.288	0.165	0.278	0.345
		1.753	1.796	1.729	1.771	1.740	1.753
			-0.369	-0.031	0.419	-0.055	-0.368
2016	**NSD**		0.358	0.488	0.340	0.478	0.358
			1.746	1.725	1.725	1.717	1.717
				0.240	1.044	0.263	-0.088
2017	**NSD**	**NSD**		0.407	0.155	0.398	0.466
				1.761	1.734	1.753	1.740
					0.359	-0.016	-0.267
2018	**NSD**	**NSD**	**NSD**		0.362	0.493	0.396
					1.746	1.721	1.729
						-0.442	-0.852
2019	**NSD**	**NSD**	**NSD**	**NSD**		0.332	0.202
						1.734	1.725
							-0.285
2020	**NSD**	**NSD**	**NSD**	**NSD**	**NSD**		0.389
							1.721
2021	**NSD**	**NSD**	**NSD**	**NSD**	**NSD**	**NSD**	

During the events of the 2019 pandemic caused by COVID-19, countries experienced changes in their overall air quality. The lockdown measures caused the shutdown of industries, diminished vehicular usage, and influenced human activities which caused considerable improvement in air quality. Different studies analyzed one or several pollutants from the six commonly occurring pollutants. In Asian and European countries, the overall NO_2 concentrations were reduced by up to 30% (Gautam, 2020). In Brazil, CO, NO, and NO_2 concentrations were reduced by 64.8, 77.3, and 54.3%, respectively (Nakada and Urban, 2020). Spain experienced a reduction of PM_{10} and NO_2 by 28 and 57%, respectively (Tobías et al., 2020). Reduced concentrations of $PM_{2.5}$ were observed in South Korea by up to 25% (Kwak et al., 2021). In India, the concentrations of $PM_{2.5}$, PM_{10}, CO, and NO_2 were reduced by 43, 31, 10, and 18%, respectively (Sharma et al., 2020). $PM_{2.5}$ concentrations increased, especially in the Midwestern and Southern regions of the United States (Chen et al., 2021, Archer et al., 2020).

For this study, the analysis was conducted in Texas to evaluate the influence of the quarantine period on $PM_{2.5}$ for the cities of Austin, San Antonio, Houston, and Dallas-Fort Worth from 2015 to 2021 for urban and near-road stations using a series of Welch's t-tests. Our study found that in Houston's near-road station CAMS 1052 the $PM_{2.5}$ concentrations were significantly higher compared to the near-road stations located in the other three cities. For the urban stations, during Lockdown Phases I and II, $PM_{2.5}$ concentrations were higher. This increment may not be limited to the variability in traffic activity and local meteorology. According to Chen et al., (2021), stationary sources produced significant amounts of primary $PM_{2.5}$ emissions in comparison to mobile sources. $PM_{2.5}$ has a non-linear formation which makes it difficult to pinpoint a specific emission source. Secondary pollutants are also of concern as they are mainly created in the atmosphere and are significant sources of $PM_{2.5}$ besides the fact that the formulation of $PM_{2.5}$ is directly emitted. $PM_{2.5}$ production by stationary sources and the complex chemical reactions that produce $PM_{2.5}$ in the air are substantial. Therefore, it is important to mention that decreasing mobility (car usage only) may not cause a significant reduction in $PM_{2.5}$ concentrations.

Chapter 5 Conclusion and Future Work

$PM_{2.5}$ emissions have been detrimental to human health posing severe health risks. PM concentration evaluations are necessary to impose regulations to lower PM concentrations in areas in which high concentrations of PM are observed. These regulations will reduce health complications and other related problems as production sources are identified.

In this study, a series of analyses evaluated the $PM_{2.5}$ concentrations for the events of the COVID-19 pandemic in 2020 before, during, and after. The analyses included:

1. Time Series of hourly averages – showed changes in $PM_{2.5}$ concentrations over time for all four cities
2. Box plots – demonstrated the variation in concentrations for sites with hourly data
3. Polar $PM_{2.5}$ concentration annulus plots for near-road stations from 2019 to 2021 – reflected the effects of wind direction on $PM_{2.5}$ concentrations at near-road sites
4. Monthly polar $PM_{2.5}$ concentration plots for near-road stations from 2019 to 2021 – illustrated $PM_{2.5}$ concentrations based on wind speed and direction
5. Welch's one-tail t-test – evaluated if the mean concentration of a year was significantly greater than another year

In each city, the number of monitoring stations varied from year to year as stations were deactivated or added. Each city included a near-road station and several urban stations; near-road stations had been selected based on a set of parameters including the distance between the station and a target roadway. $PM_{2.5}$ concentrations monitored by near-road stations were actively influenced by highway emissions which present a contrast to $PM_{2.5}$ concentrations monitored by urban stations. Each station recollected hourly $PM_{2.5}$ data or 24-hour values every 3 or 6 days depending on the type of equipment the monitoring station had.

Four time periods were evaluated to reflect the concentration differences caused by the imposed restrictions on vehicle usage for box plots and Welch's one-tail t-tests:

- Before Lockdown (January 1st to March 20th, 2015-2021)
- Lockdown Phase I (March 21st to April 30th, 2015-2021)
- Lockdown Phase II (May 1st to September 30th, 2015-2021)
- After Lockdown (October 1st to December 31st, 2015-2021)

This study has observed, using Welch's one-tail t-tests, an increase of $PM_{2.5}$ concentrations in Texas for urban areas as well in Houston's CAMS 1052 near-road station. In comparison to other near-road stations in Austin, San Antonio, and Dallas-Fort Worth no significant increase was observed. It can be inferred that even though mobile sources have an impact on increasing $PM_{2.5}$ concentrations at near-road stations, many other factors influence PM concentrations such as meteorology, human activity, etc. Emissions from mobile sources might have a considerable influence on the reduction or the increase of the overall production of $PM_{2.5}$, but $PM_{2.5}$ production was not the only pollutant that was affected by events caused by the COVID-19 pandemic. The results of this study illustrate that traffic emissions may not be entirely responsible for the entire production of $PM_{2.5}$ as concentrations observed, through the different analyses performed, increased. Meteorology and traffic conditions have, to a certain extent, an influence on the production of $PM_{2.5}$, but even if vehicle usage is constrained, other sources might still produce more emissions.

This study focused on emission changes produced by mobile sources rather than determining an impact produced by stationary sources. Future work could include the effects caused by the COVID-19 pandemic on the output of $PM_{2.5}$ emissions by stationary sources. Another factor to take into consideration would be the modeling of concentrations in near-road stations and see the comparison between the model and real-life measurements during the COVID-19 pandemic. This would further reflect the effects of transportation on air quality.

References

Anenberg, S. C., Henze, D. K., Tinney, V., Kinney, P. L., Raich, W., Fann, N., Malley, C. S., Roman, H., Lamsal, L., Duncan, B., Martin, R. V., van Donkelaar, A., Brauer, M., Doherty, R., Jonson, J. E., Davila, Y., Sudo, K., & Kuylenstierna, J. C. I. (2018). Estimates of the global burden of ambient PM2.5, Ozone, and no2 on asthma incidence and emergency room visits. *Environmental Health Perspectives*, *126*(10), 107004. https://doi.org/10.1289/ehp3766

Archer, C.L., Cervone, G., Golbazi, M., Fahel, N.A., Hultquist, C. (2020). Changes in air quality and human mobility in the U.S. during the COVID-19 pandemic. arXiv.org.

Bo, Chang, L., Guo, C., Lin, C., Lau, A. K. H., Tam, T., & Lao, X. Q. (2021). Reduced ambient PM2.5, better lung function, and decreased chronic obstructive pulmonary disease risk. *Environment International*, *156*, 106706–106706. https://doi.org/10.1016/j.envint.2021.106706

Brown, Penfold, B., Mukherjee, A., Landsberg, K., & Eisinger, D. S. (2019). Conditions Leading to Elevated PM2.5 at Near-Road Monitoring Sites: Case Studies in Denver and Indianapolis. *International Journal of Environmental Research and Public Health*, *16*(9), 1634–. https://doi.org/10.3390/ijerph16091634

Brown, Penfold, B., Mukherjee, A., Landsberg, K., & Eisinger, D. S. (2019). Conditions Leading to Elevated PM 2.5 at Near-Road Monitoring Sites: Case Studies in Denver and Indianapolis. *International Journal of Environmental Research and Public Health*, *16*(9).

Chen, G., Zhou, H., He, G., Zhu, S., Sun, X., Ye, Y., Chen, H., Xiao, J., Hu, J., Zeng, F., Yang, P., Gao, Y., He, Z., Wang, J., Cao, G., Chen, Y., Feng, H., Ma, W., Liu, C., & Liu, T. (2022). Effect of early-life exposure to PM2.5 on childhood asthma/wheezing: a birth

cohort study. (2022). *Pediatric Allergy and Immunology.*, *33*(6). https://doi.org/10.1111/pai.13822

Chen, Henneman, L. R. F., & Nethery, R. C. (2021). Differential impacts of COVID-19 lockdowns on PM2.5 across the United States. *Environmental Advances*, *6*, 100122–. https://doi.org/10.1016/j.envadv.2021.100122

Chi, Chen, C., Li, H., Pan, L., Zhao, B., Deng, F., & Guo, X. (2019). Different health effects of indoor- and outdoor-originated PM 2.5 on cardiopulmonary function in COPD patients and healthy elderly adults. *Indoor Air*, *29*(2), 192–201. https://doi.org/10.1111/ina.12521

Cortez-Lugo, M., Escamilla-Núñez, C., Barraza-Villarreal, A., Texcalac-Sangrador, J. L., Chow, J., Watson, J., Hernández-Cadena, L., & Romieu, I. (2013). Association between light absorption measurements of PM2.5 and distance from heavy traffic roads in the Mexico City metropolitan area Asociación entre las mediciones de PM2.5 por absorbancia y la distancia a vías de alto tráfico en la zona metropolitana de la Ciudad de México. *Salud Pública de México*, *55*(2), 155–161.

DeWinter, Brown, S. G., Seagram, A. F., Landsberg, K., & Eisinger, D. S. (2018). A national-scale review of air pollutant concentrations measured in the U.S. near-road monitoring network during 2014 and 2015. *Atmospheric Environment (1994)*, *183*, 94–105. https://doi.org/10.1016/j.atmosenv.2018.04.003

Environmental Protection Agency. (n.d.). Health and Environmental Effects of Particulate Matter (PM). EPA. Retrieved April 20, 2022, from https://www.epa.gov/pm-pollution/health-and-environmental-effects-particulate-matter-pm

Gautam. (2020). COVID-19: air pollution remains low as people stay at home. *Air Quality, Atmosphere and Health*, *13*(7), 853–857. https://doi.org/10.1007/s11869-020-00842-6

Hand, Schichtel, B. A., Malm, W. C., Pitchford, M., & Frank, N. H. (2014). Spatial and seasonal patterns in urban influence on regional concentrations of speciated aerosols across the United States. *Journal of Geophysical Research. Atmospheres*, *119*(22), 12,832–12,849. https://doi.org/10.1002/2014JD022328

Hodan, W. M., & Barnard, W. R. (2004). Evaluating the Contribution of PM2.5 Precursor Gases and Re-entrained Road Emissions to Mobile Source PM2.5 Particulate Matter Emissions. *13th International Emission Inventory Conference*. EPA. Retrieved September 9, 2022, from https://www3.epa.gov/ttnchie1/conference/ei13/

Hua, Yin, Y., Peng, L., Du, L., Geng, F., & Zhu, L. (2014). Acute effects of black carbon and PM2.5 on children asthma admissions: A time-series study in a Chinese city. *The Science of the Total Environment*, *481*, 433–438. https://doi.org/10.1016/j.scitotenv.2014.02.070

Hua, Yin, Y., Peng, L., Du, L., Geng, F., & Zhu, L. (2014). Acute effects of black carbon and PM2.5 on children asthma admissions: A time-series study in a Chinese city. *The Science of the Total Environment*, *481*, 433–438. https://doi.org/10.1016/j.scitotenv.2014.02.070

Jain, Sharma, S. K., Vijayan, N., & Mandal, T. K. (2020). Seasonal characteristics of aerosols (PM2.5 and PM10) and their source apportionment using PMF: A four year study over Delhi, India. *Environmental Pollution (1987)*, *262*, 114337–114337. https://doi.org/10.1016/j.envpol.2020.114337

Kaihara, Yoneyama, K., Nakai, M., Higuma, T., Sumita, Y., Miyamoto, Y., Watanabe, M., Izumo, M., Ishibashi, Y., Tanabe, Y., Harada, T., Yasuda, S., Ogawa, H., & Akashi, Y. J. (2021). Association of PM2.5 exposure with hospitalization for cardiovascular disease in elderly individuals in Japan. *Scientific Reports*, *11*(1), 9897–9897. https://doi.org/10.1038/s41598-021-89290-5

Khalili, Bartell, S. M., Hu, X., Liu, Y., Chang, H. H., Belanoff, C., Strickland, M. J., & Vieira, V. M. (2018). Early-life exposure to PM2.5 and risk of acute asthma clinical encounters among children in Massachusetts: a case-crossover analysis. *Environmental Health*, *17*(1), 20–20. https://doi.org/10.1186/s12940-018-0361-6

Kwak, Han, B.-S., Park, K., Moon, S., Jin, H.-G., Park, S.-B., & Baik, J.-J. (2021). Inter- and intra-city comparisons of PM2.5 concentration changes under COVID-19 social distancing in seven major cities of South Korea. *Air Quality, Atmosphere and Health*, *14*(8), 1155–1168. https://doi.org/10.1007/s11869-021-01006-w

Li, H., Zhou, L., Ren, M., Sheng, G., Fu, J., & Peng, P. (2014). Levels, profiles and gas–particle distribution of atmospheric PCDD/Fs in vehicle parking lots of a South China metropolitan area. *Chemosphere (Oxford)*, *94*, 128–134. https://doi.org/10.1016/j.chemosphere.2013.09.061

Nakada, & Urban, R. C. (2020). COVID-19 pandemic: Impacts on the air quality during the partial lockdown in São Paulo state, Brazil. *The Science of the Total Environment*, *730*, 139087–139087. https://doi.org/10.1016/j.scitotenv.2020.139087

Nurmagambetov, Kuwahara, R., & Garbe, P. (2018). The Economic Burden of Asthma in the United States, 2008-2013. *Annals of the American Thoracic Society*, *15*(3), 348–356. https://doi.org/10.1513/AnnalsATS.201703-259OC

Ou, Hanson, H. A., Ramsay, J. M., Kaddas, H. K., Pope, 3rd, Leiser, C. L., VanDerslice, J., & Kirchhoff, A. C. (2020). Fine Particulate Matter Air Pollution and Mortality among Pediatric, Adolescent, and Young Adult Cancer Patients. *Cancer Epidemiology, Biomarkers & Prevention*, *29*(10), 1929–1939. https://doi.org/10.1158/1055-9965.EPI-19-1363

Oyana, Minso, J., Jones, T. L., McCullers, J. A., Arnold, S. R., & Cormier, S. A. (2021). Particulate matter exposure predicts residence in high-risk areas for community acquired pneumonia among hospitalized children. *Experimental Biology and Medicine (Maywood, N.J.)*, *246*(17), 1907–1916. https://doi.org/10.1177/15353702211014456

Pate, Zahran, H. S., Qin, X., Johnson, C., Hummelman, E., & Malilay, J. (2021). Asthma Surveillance — United States, 2006–2018. *MMWR. Surveillance Summaries*, *70*(5), 1–32. https://doi.org/10.15585/mmwr.ss7005a1

Sharma, Zhang, M., Anshika, Gao, J., Zhang, H., & Kota, S. H. (2020). Effect of restricted emissions during COVID-19 on air quality in India. *The Science of the Total Environment*, *728*, 138878–138878. https://doi.org/10.1016/j.scitotenv.2020.138878

Tobías, Carnerero, C., Reche, C., Massagué, J., Via, M., Minguillón, M. C., Alastuey, A., & Querol, X. (2020). Changes in air quality during the lockdown in Barcelona (Spain) one month into the SARS-CoV-2 epidemic. *The Science of the Total Environment*, *726*, 138540–138540. https://doi.org/10.1016/j.scitotenv.2020.138540

Vasiliauskienė, V., Pečiulienė, M., & Jasaitis, D. (2021). Influence of Meteorological Parameters on the Dynamics of Ozone and Aerosol Particles Near a Road Transport Street. *Water, Air, and Soil Pollution*, *232*(9). https://doi.org/10.1007/s11270-021-05304-y

Wang, Zhang, R., Tan, Y., & Yu, W. (2021). Dominant synoptic patterns associated with the decay process of PM 2.5 pollution episodes around Beijing. *Atmospheric Chemistry and Physics*, *21*(4), 2491–2508. https://doi.org/10.5194/acp-21-2491-2021

Weber, Insaf, T. Z., Hall, E. S., Talbot, T. O., & Huff, A. K. (2016). Using Hierarchical Bayesian Model estimates to assess the impact of fine particulate matter (PM2.5) on respiratory-

cardiovascular chronic diseases in the New York City Metropolitan area. *Environmental Research*, *151*, 399–409. https://doi.org/10.1016/j.envres.2016.07.012

Wei, Liang, F., Cheng, W., Zhou, R., Wu, X., Feng, Y., & Wang, Y. (2017). The mechanisms for lung cancer risk of PM2.5: Induction of epithelial-mesenchymal transition and cancer stem cell properties in human non-small cell lung cancer cells. *Environmental Toxicology*, *32*(11), 2341–2351. https://doi.org/10.1002/tox.22437

World Health Organization. (n.d.). *Cancer*. World Health Organization. Retrieved May 30, 2022, from https://www.who.int/news-room/fact-sheets/detail/cancer

World Health Organization. (n.d.). *Chronic respiratory diseases*. World Health Organization. Retrieved April 20, 2022, from https://www.who.int/health-topics/chronic-respiratory-diseases#tab=tab_1

Xie, Liu, Z., Wen, T., Huang, X., Liu, J., Tang, G., Yang, Y., Li, X., Shen, R., Hu, B., & Wang, Y. (2019). Characteristics of chemical composition and seasonal variations of PM2.5 in Shijiazhuang, China: Impact of primary emissions and secondary formation. *The Science of the Total Environment*, *677*, 215–229. https://doi.org/10.1016/j.scitotenv.2019.04.300

Appendix A

AUSTIN TIME SERIES BETWEEN 2015 TO 2021

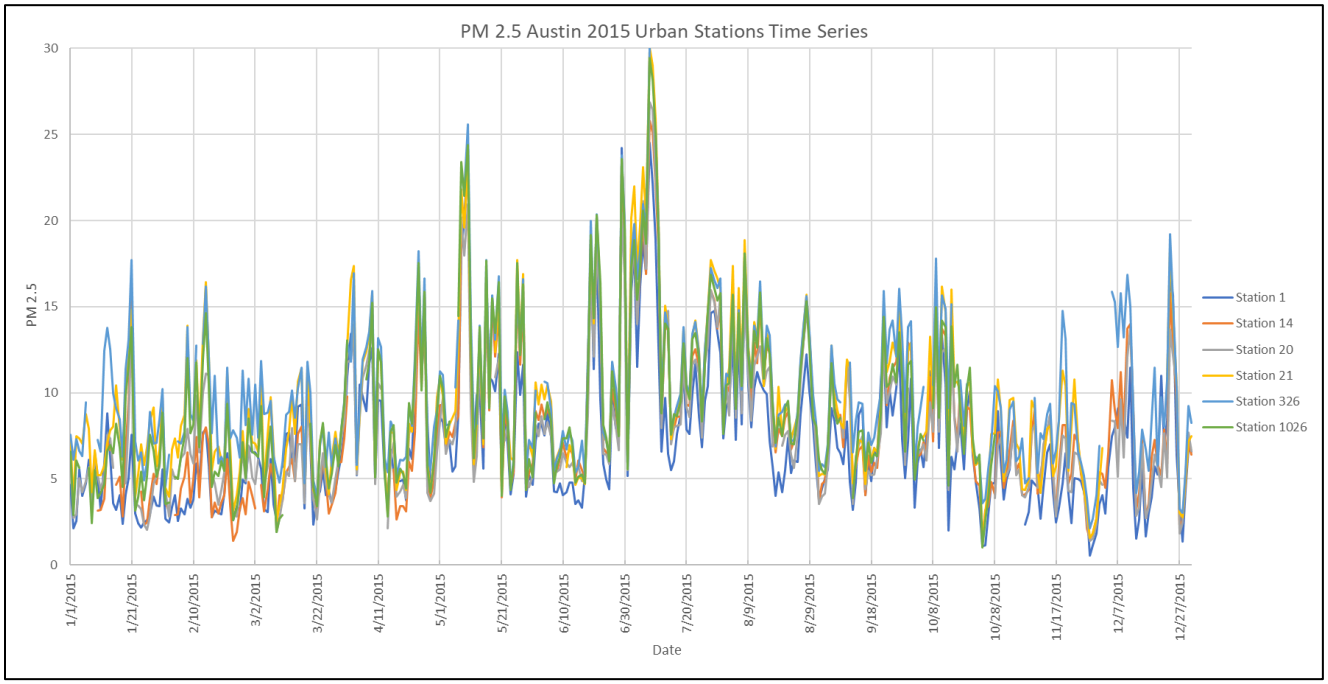

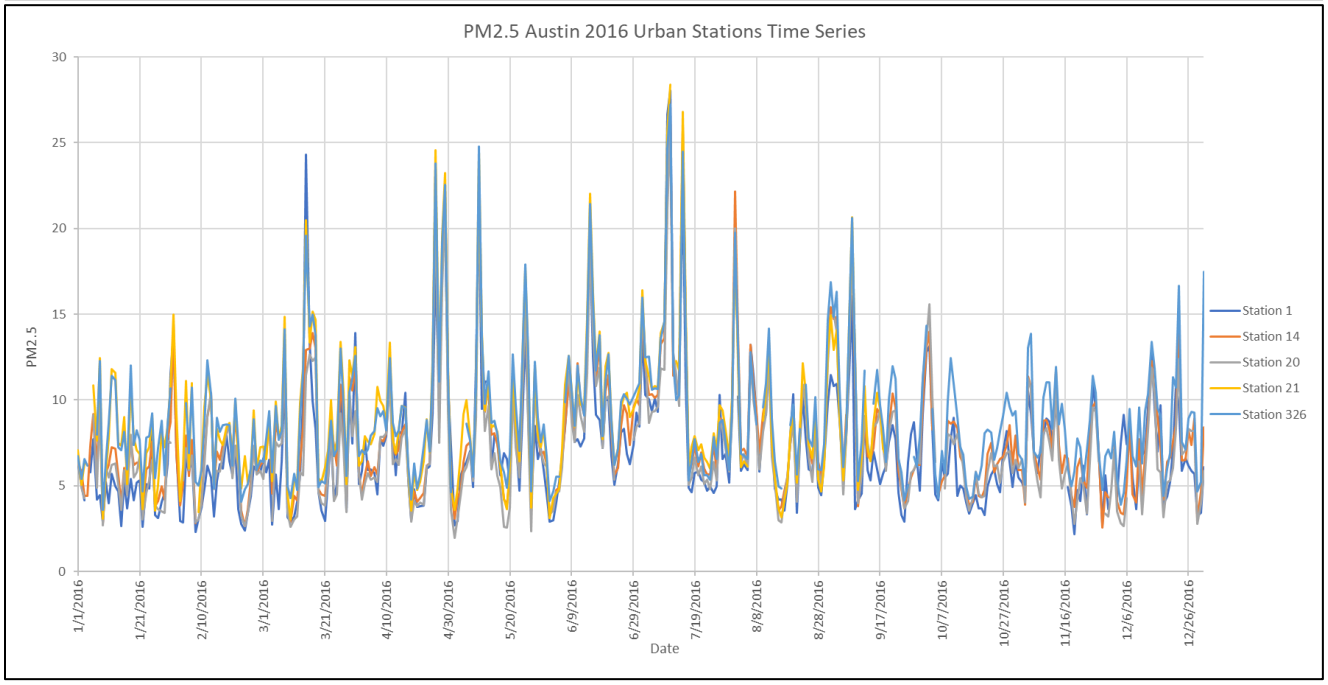

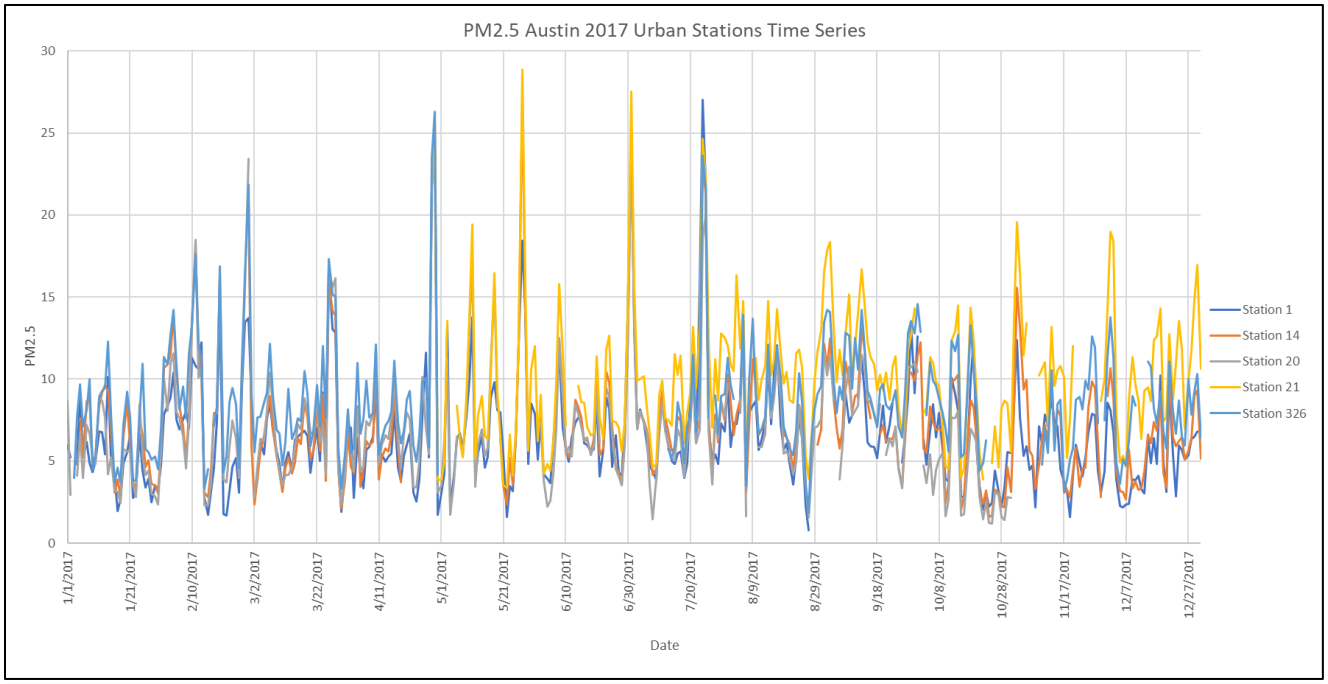
PM2.5 Austin 2017 Urban Stations Time Series
PM2.5
Date
Station 1
Station 14
Station 20
Station 21
Station 326

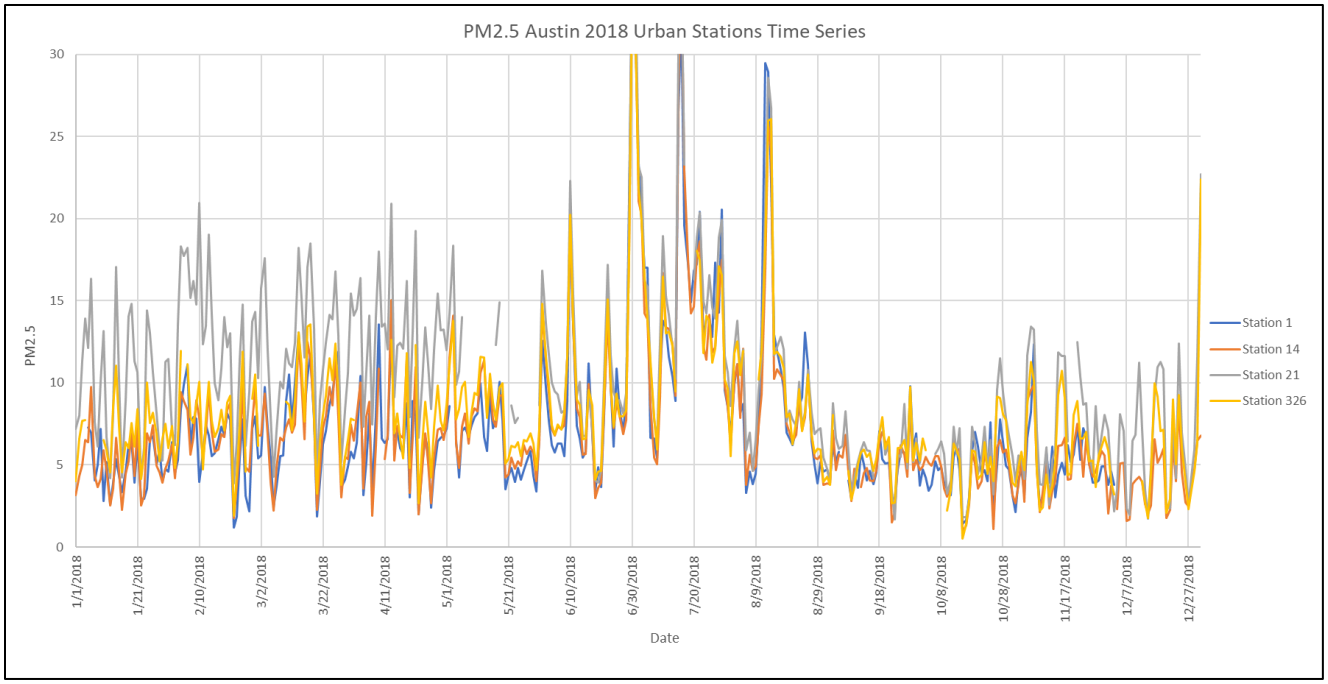
PM2.5 Austin 2018 Urban Stations Time Series
PM2.5
Date
Station 1
Station 14
Station 21
Station 326

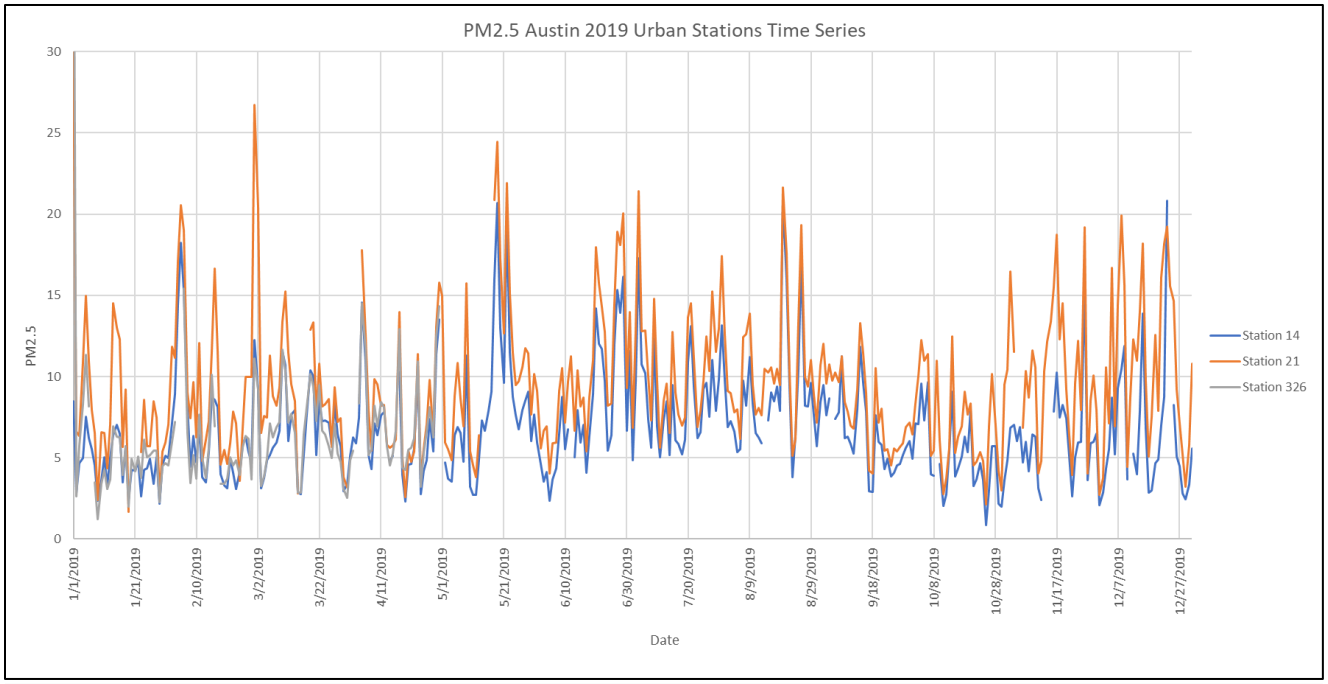
PM2.5 Austin 2019 Urban Stations Time Series
PM2.5
Date
Station 14
Station 21
Station 326

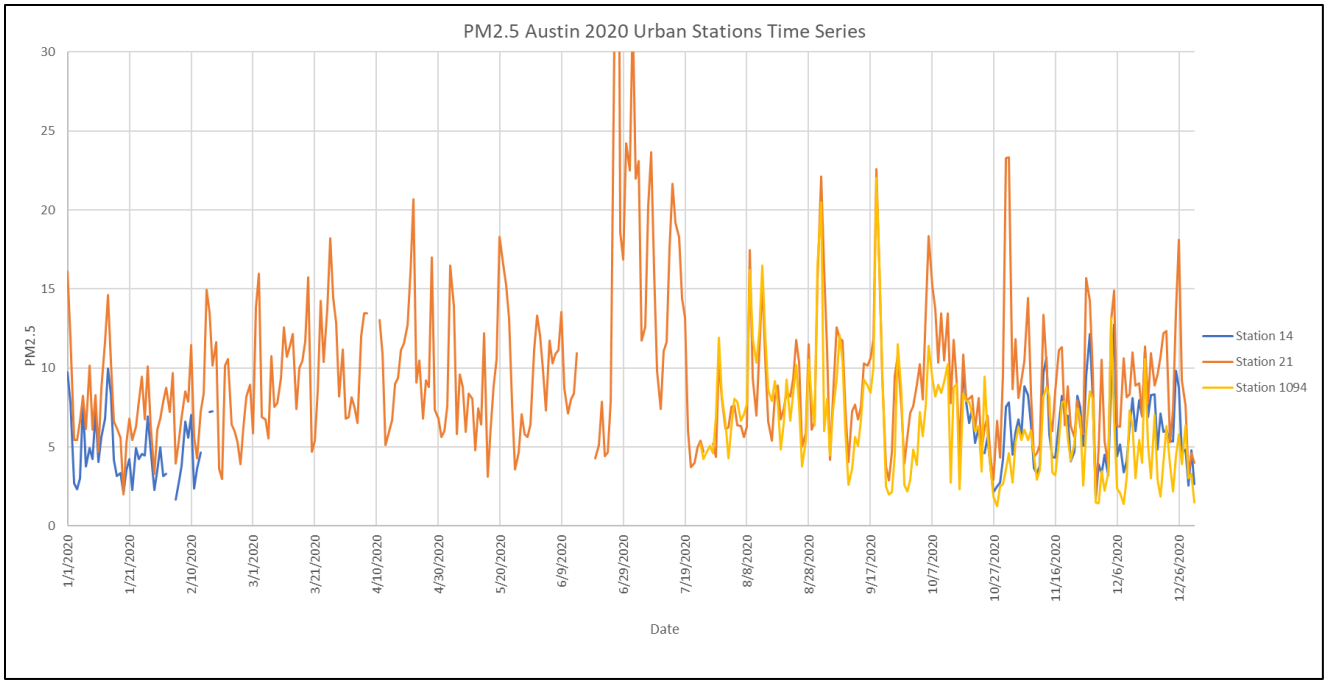
PM2.5 Austin 2020 Urban Stations Time Series
PM2.5
Date
Station 14
Station 21
Station 1094

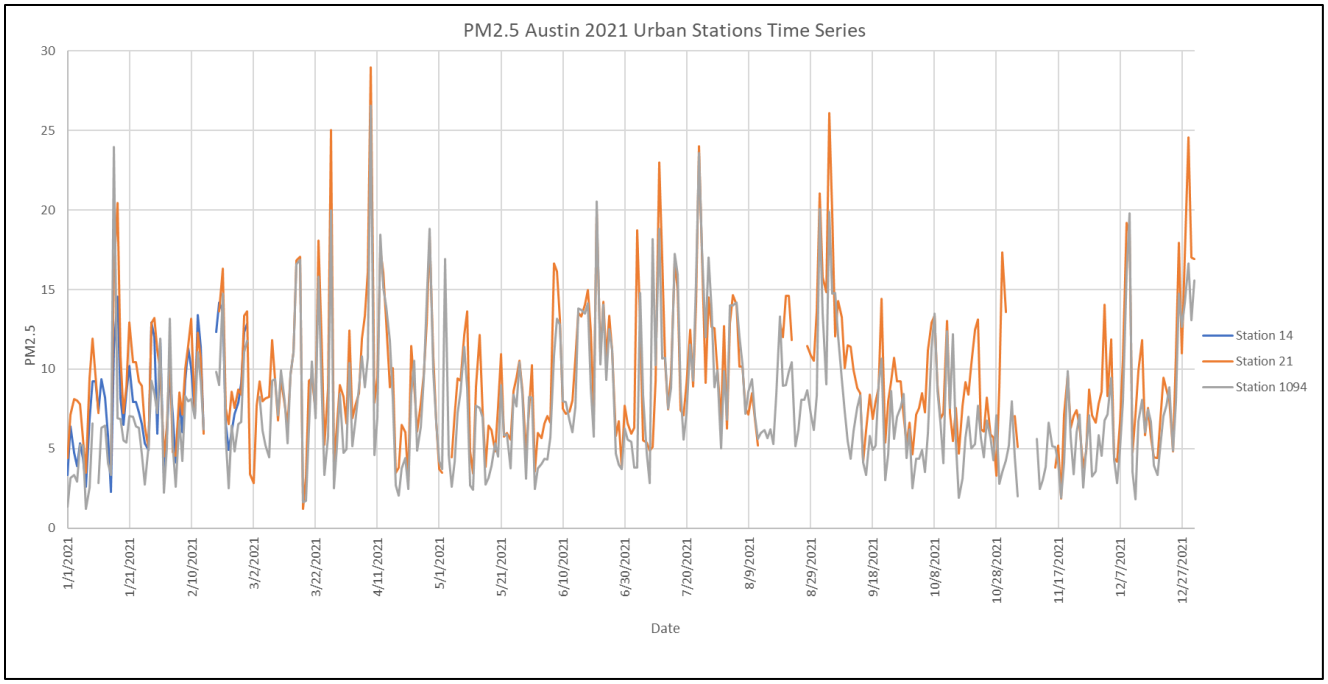

SAN ANTONIO TIME SERIES BETWEEN 2015 TO 2021

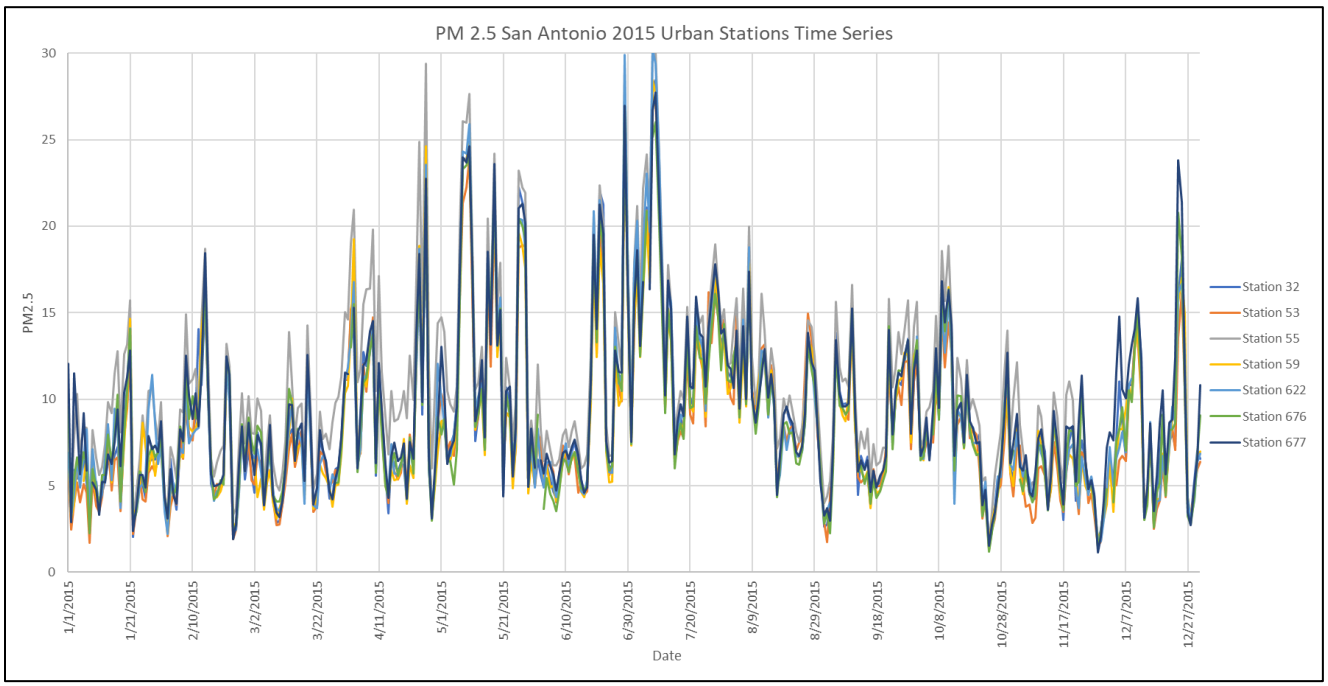

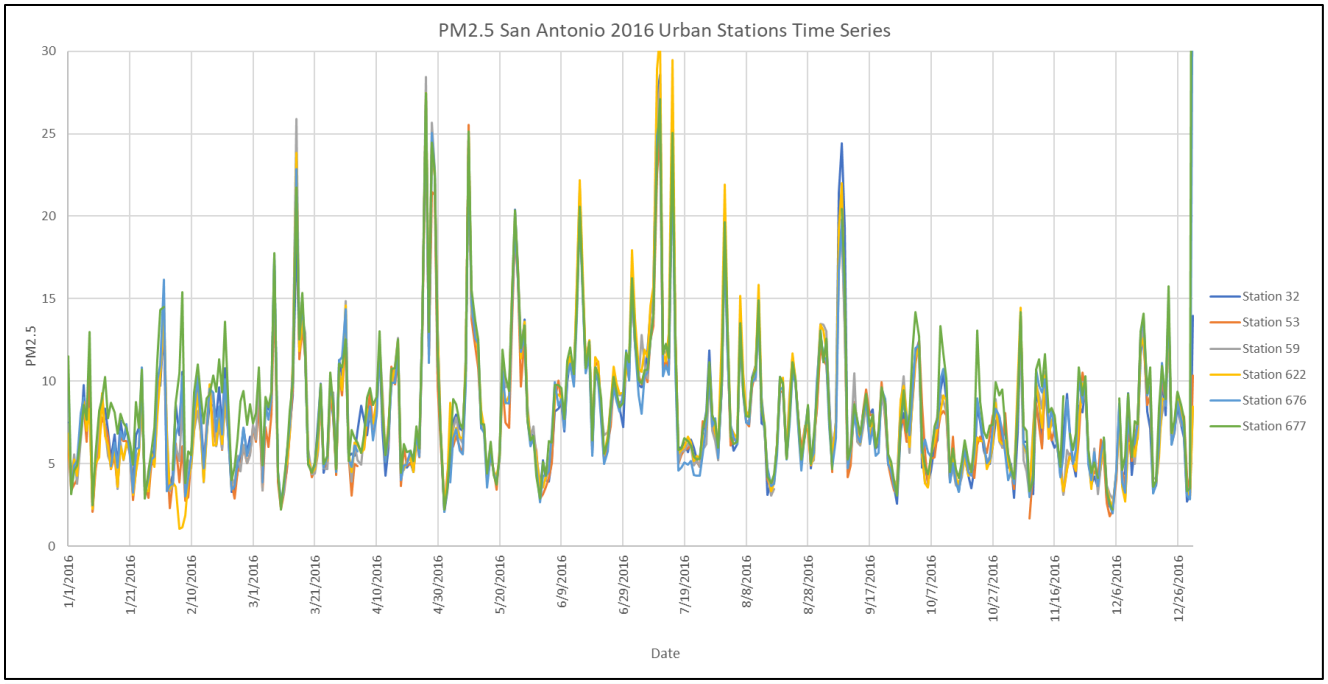
PM2.5 San Antonio 2016 Urban Stations Time Series
PM2.5
Date
Station 32
Station 53
Station 59
Station 622
Station 676
Station 677

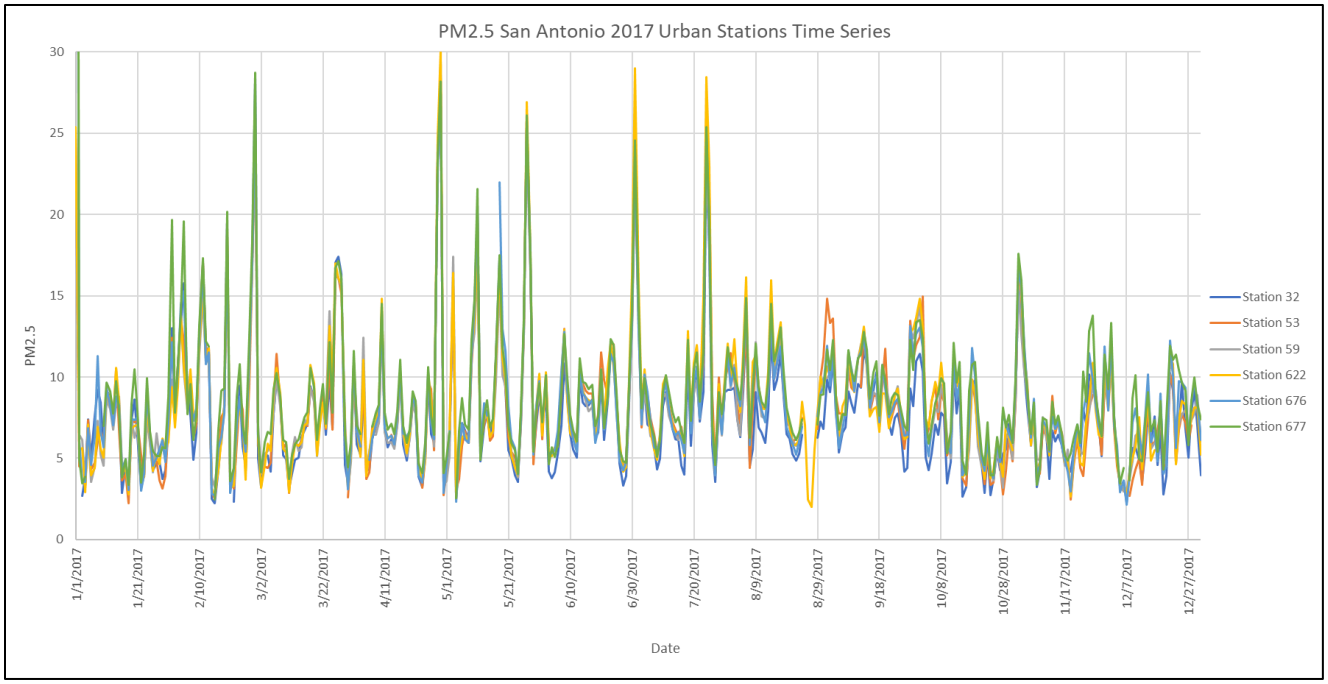
PM2.5 San Antonio 2017 Urban Stations Time Series
PM2.5
Date
Station 32
Station 53
Station 59
Station 622
Station 676
Station 677

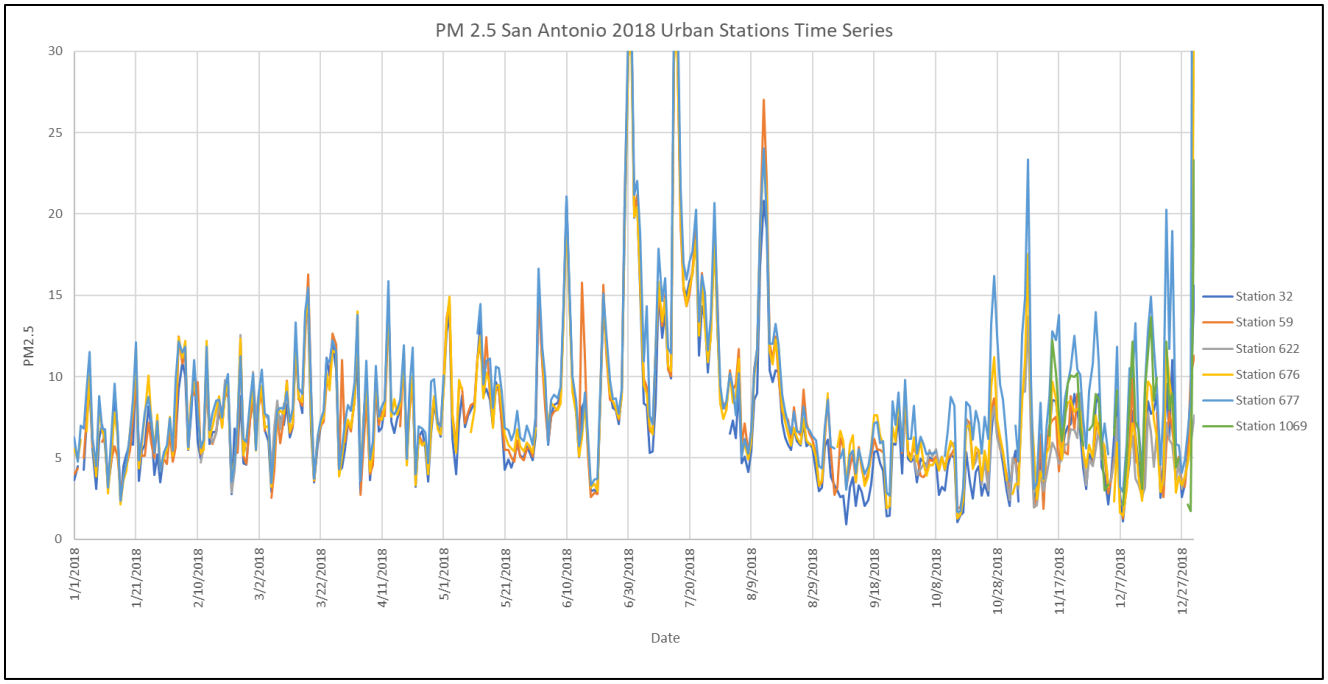
PM 2.5 San Antonio 2018 Urban Stations Time Series
PM2.5
Date
Station 32
Station 59
Station 622
Station 676
Station 677
Station 1069

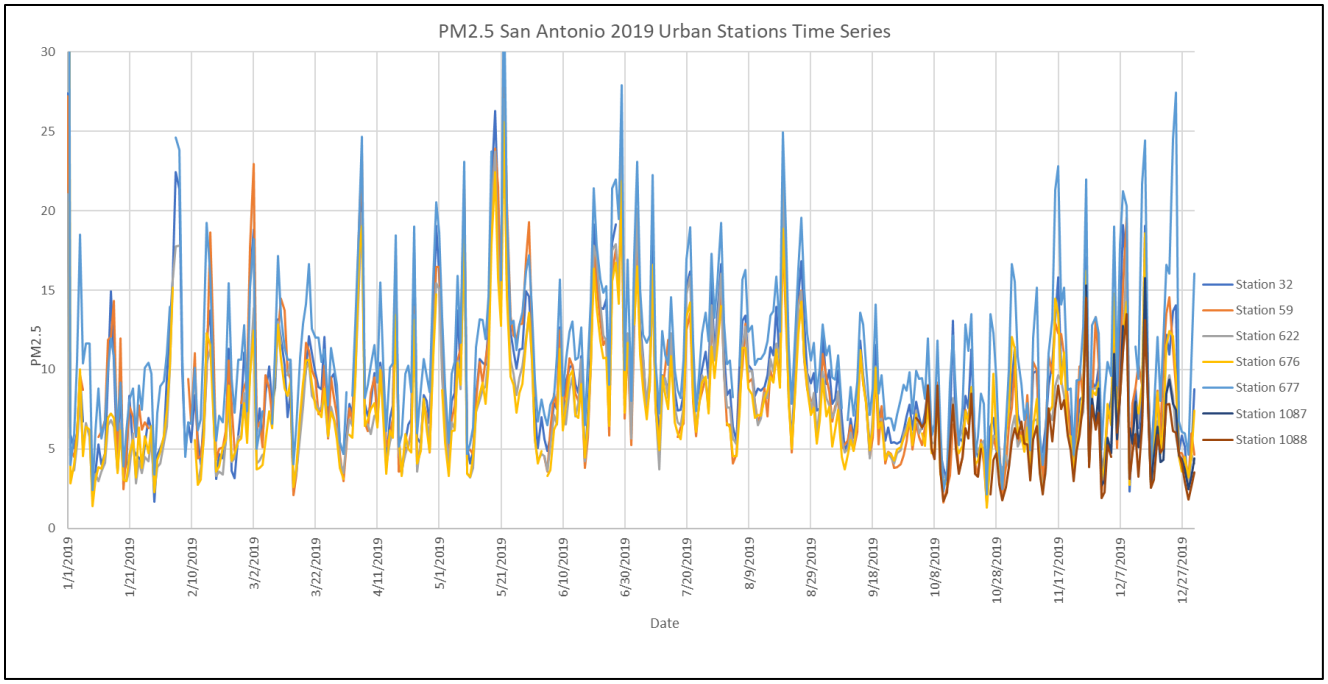
PM2.5 San Antonio 2019 Urban Stations Time Series
PM2.5
Date
Station 32
Station 59
Station 622
Station 676
Station 677
Station 1087
Station 1088

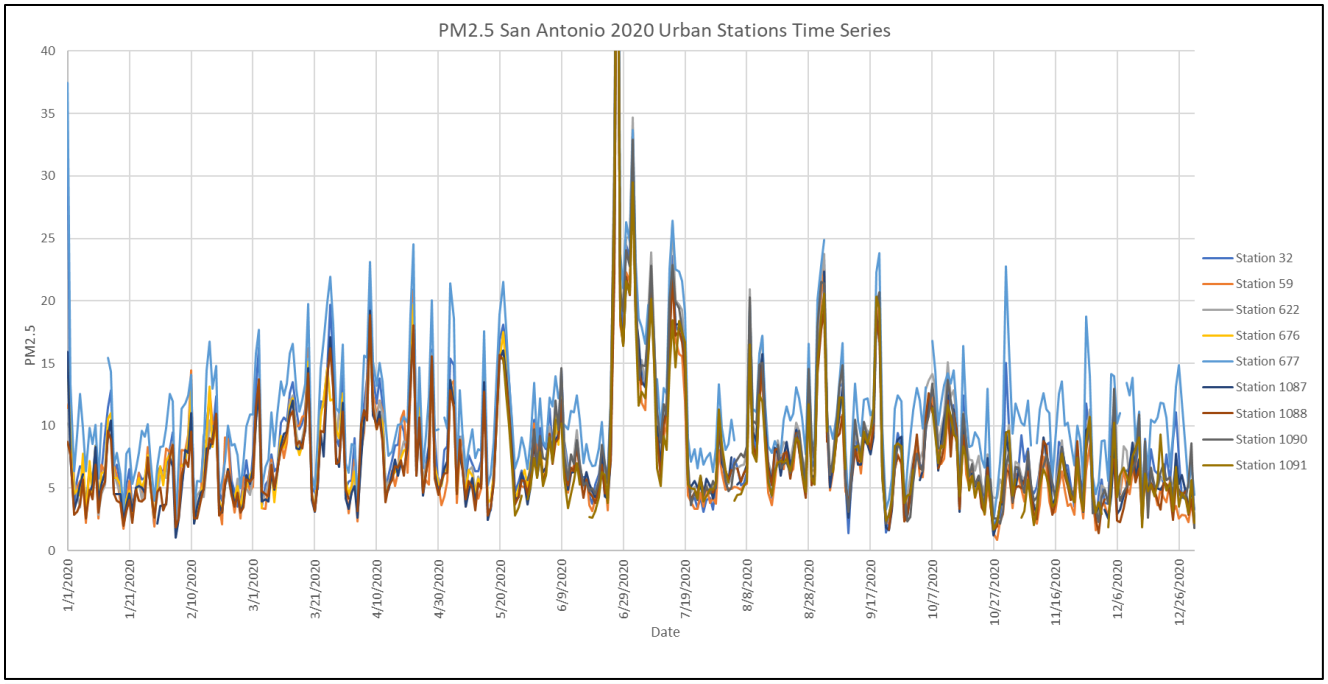
PM2.5 San Antonio 2020 Urban Stations Time Series
PM2.5
Date
Station 32
Station 59
Station 622
Station 676
Station 677
Station 1087
Station 1088
Station 1090
Station 1091

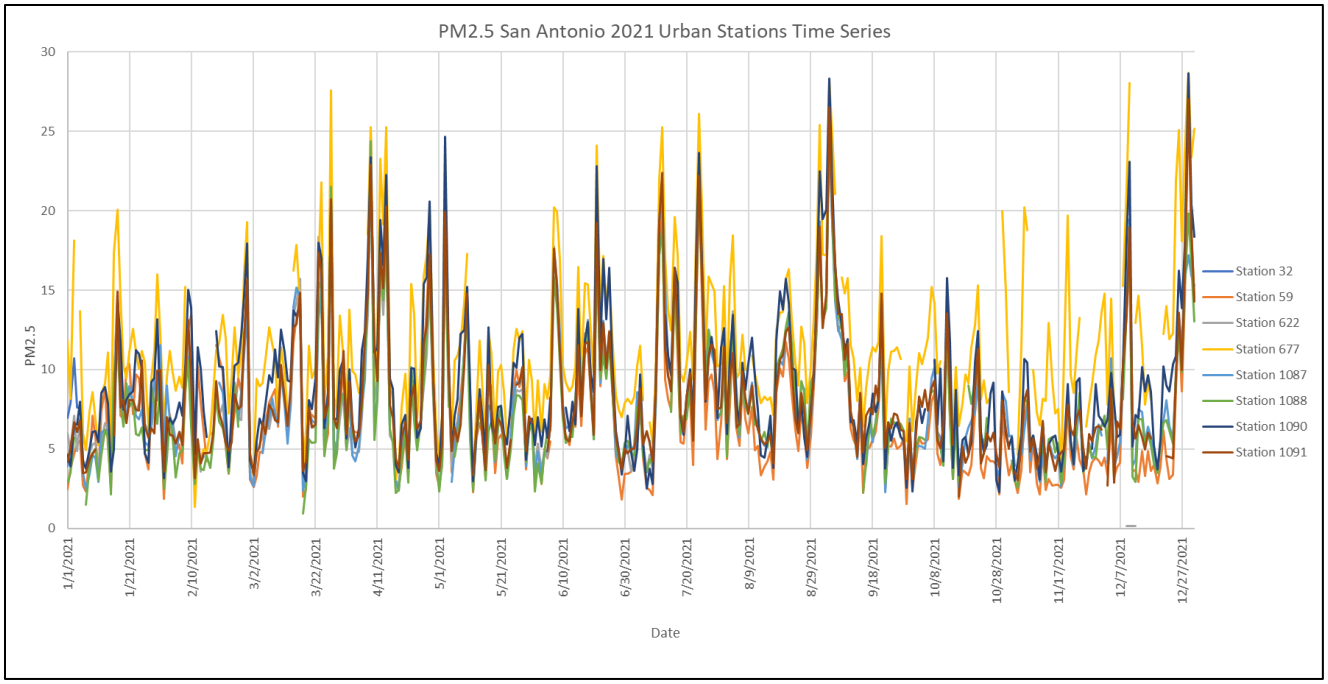
PM2.5 San Antonio 2021 Urban Stations Time Series
PM2.5
Date
Station 32
Station 59
Station 622
Station 677
Station 1087
Station 1088
Station 1090
Station 1091

HOUSTON TIME SERIES BETWEEN 2015 TO 2021

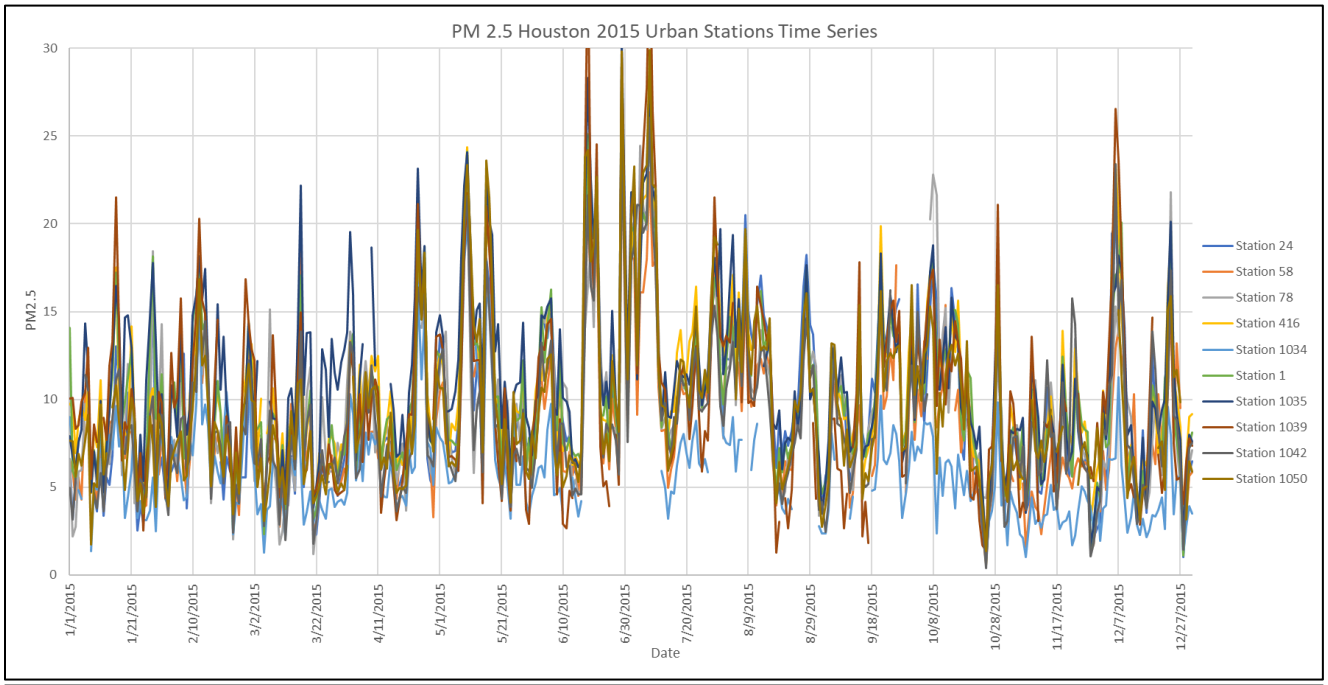

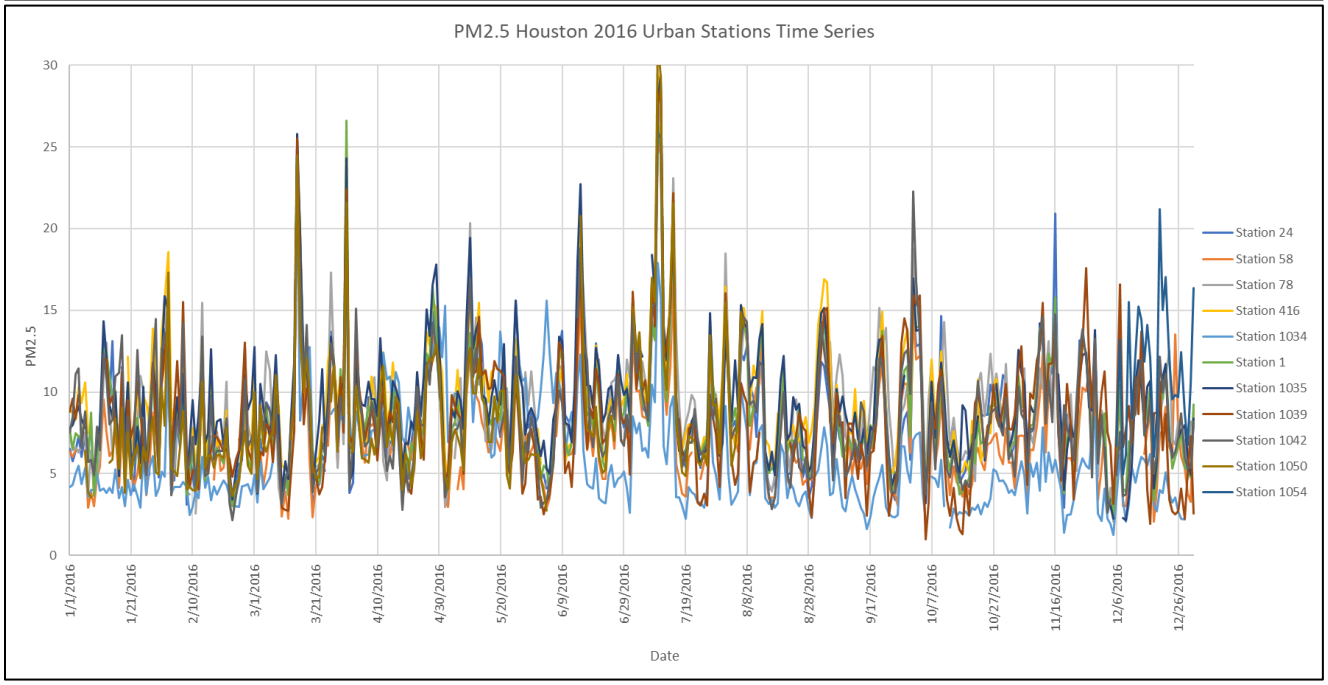

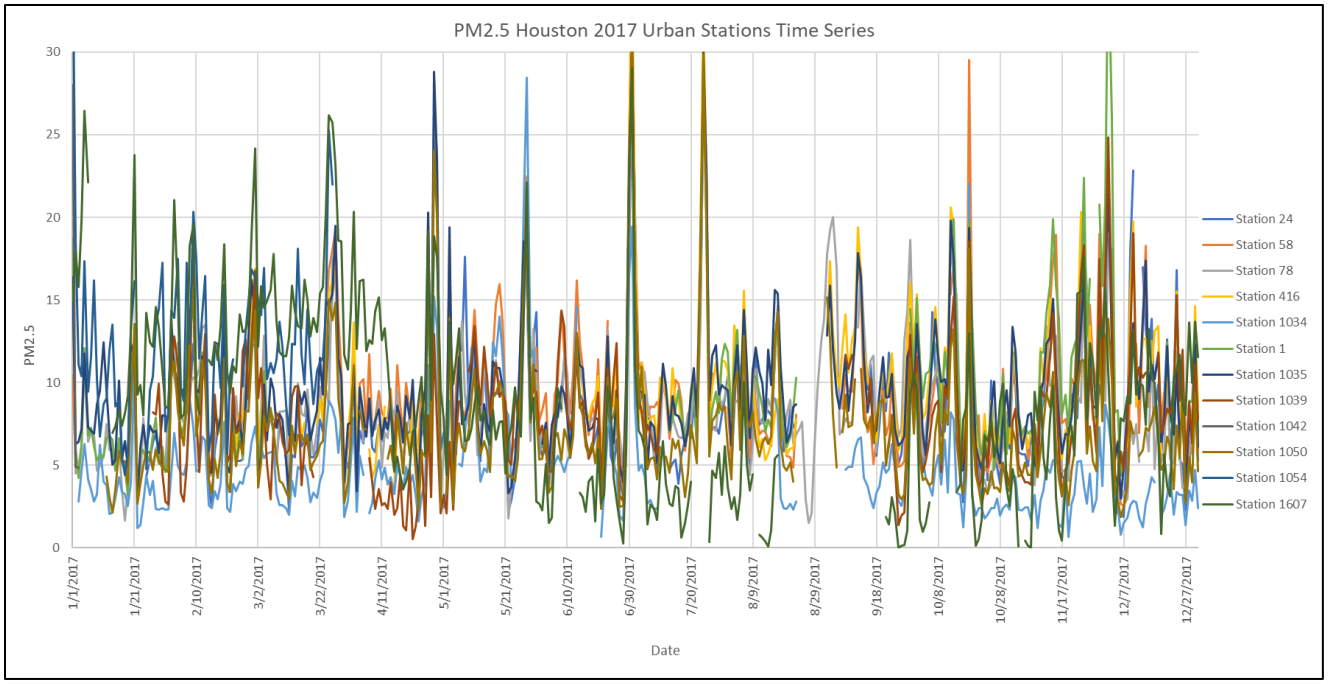
PM2.5 Houston 2017 Urban Stations Time Series
PM2.5
Date
Station 24
Station 58
Station 78
Station 416
Station 1034
Station 1
Station 1035
Station 1039
Station 1042
Station 1050
Station 1054
Station 1607

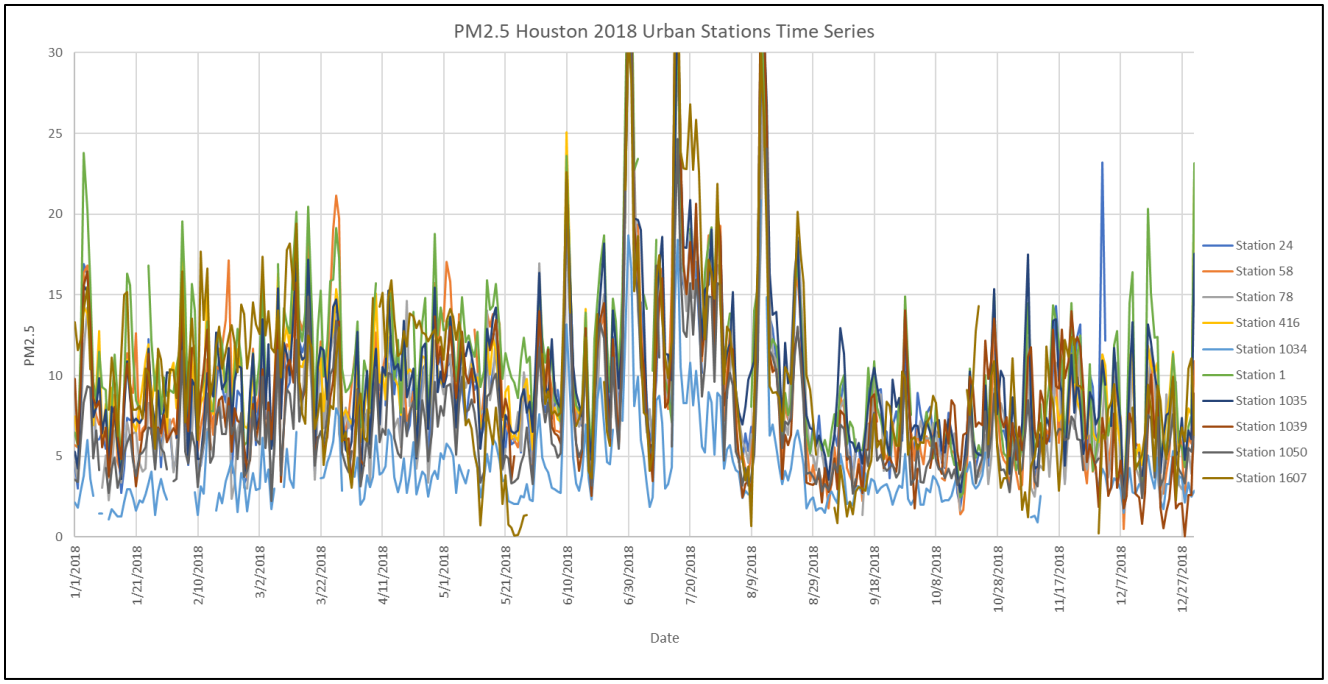
PM2.5 Houston 2018 Urban Stations Time Series
PM2.5
Date
Station 24
Station 58
Station 78
Station 416
Station 1034
Station 1
Station 1035
Station 1039
Station 1050
Station 1607

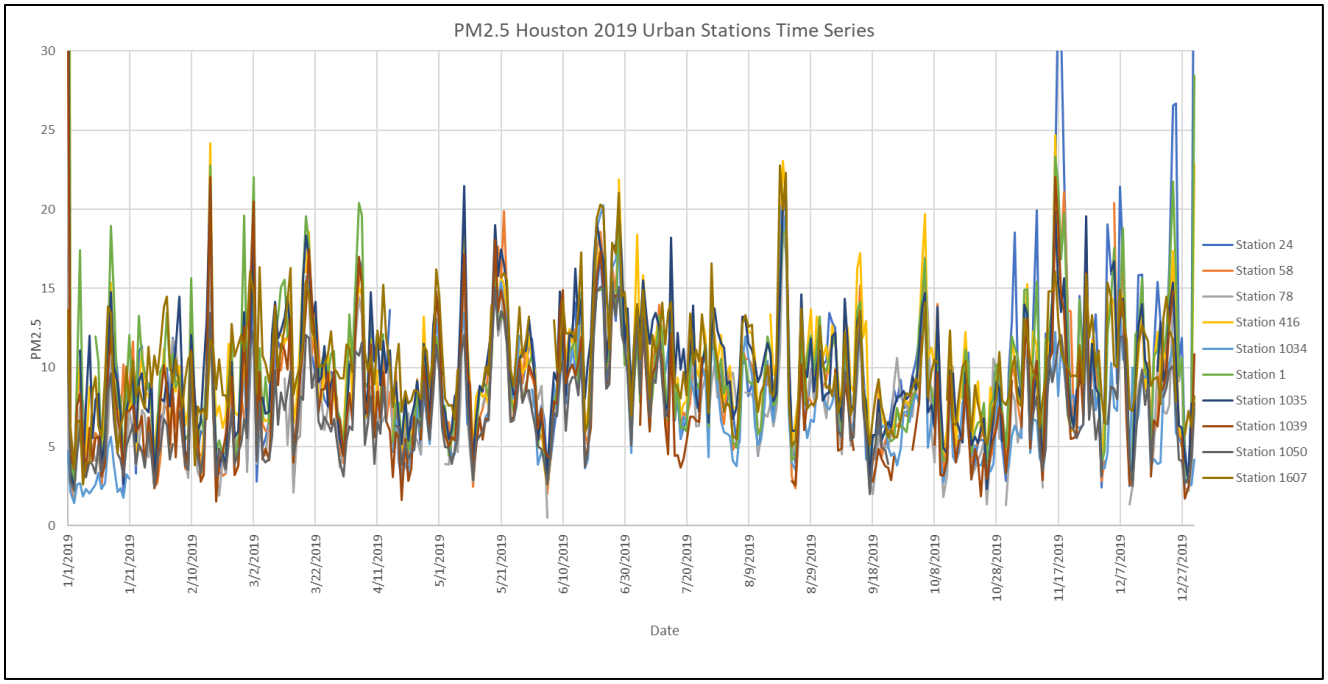
PM2.5 Houston 2019 Urban Stations Time Series
PM2.5
Date
Station 24
Station 58
Station 78
Station 416
Station 1034
Station 1
Station 1035
Station 1039
Station 1050
Station 1607

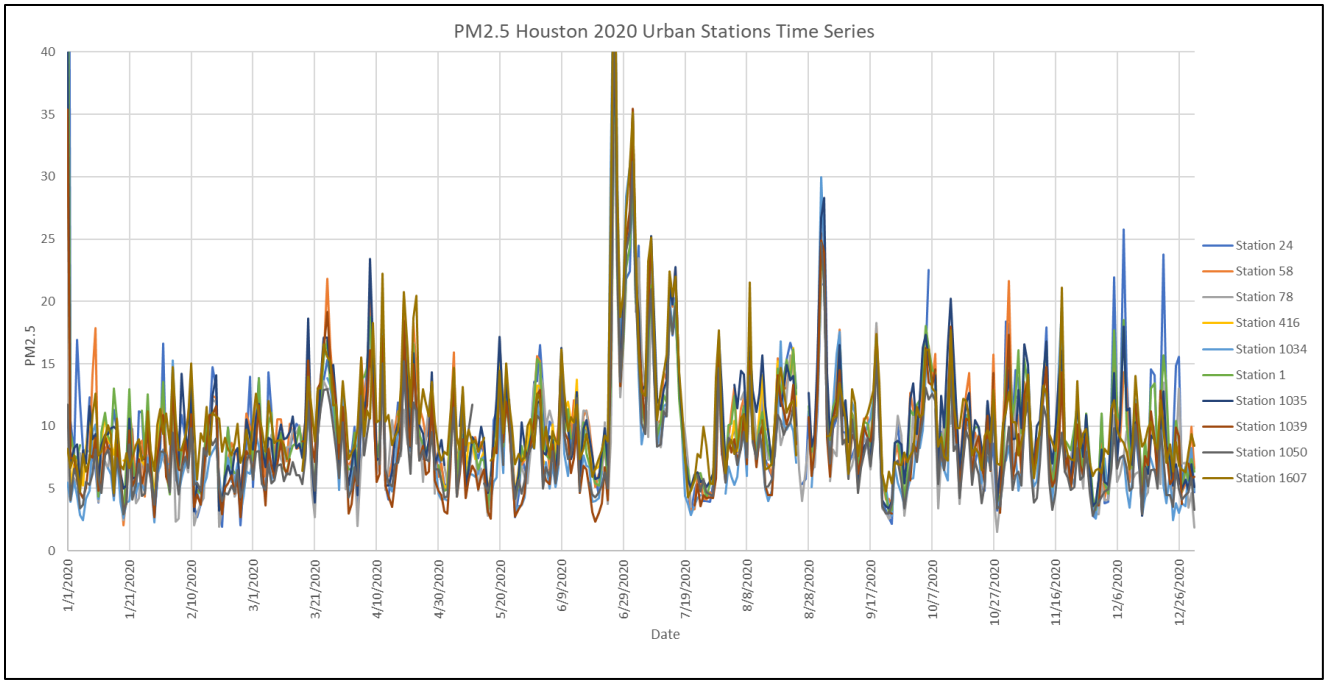
PM2.5 Houston 2020 Urban Stations Time Series
PM2.5
Date
Station 24
Station 58
Station 78
Station 416
Station 1034
Station 1
Station 1035
Station 1039
Station 1050
Station 1607

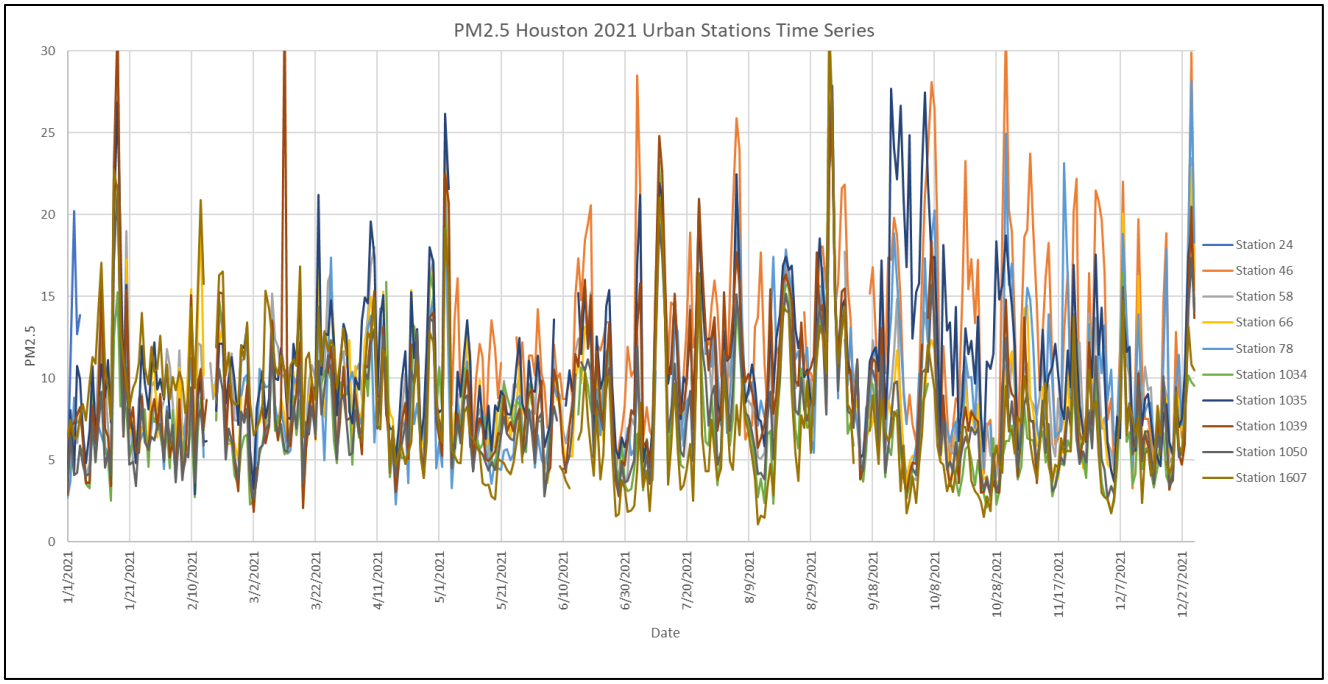

DALLAS – FORT WORTH TIME SERIES BETWEEN 2015 TO 2021

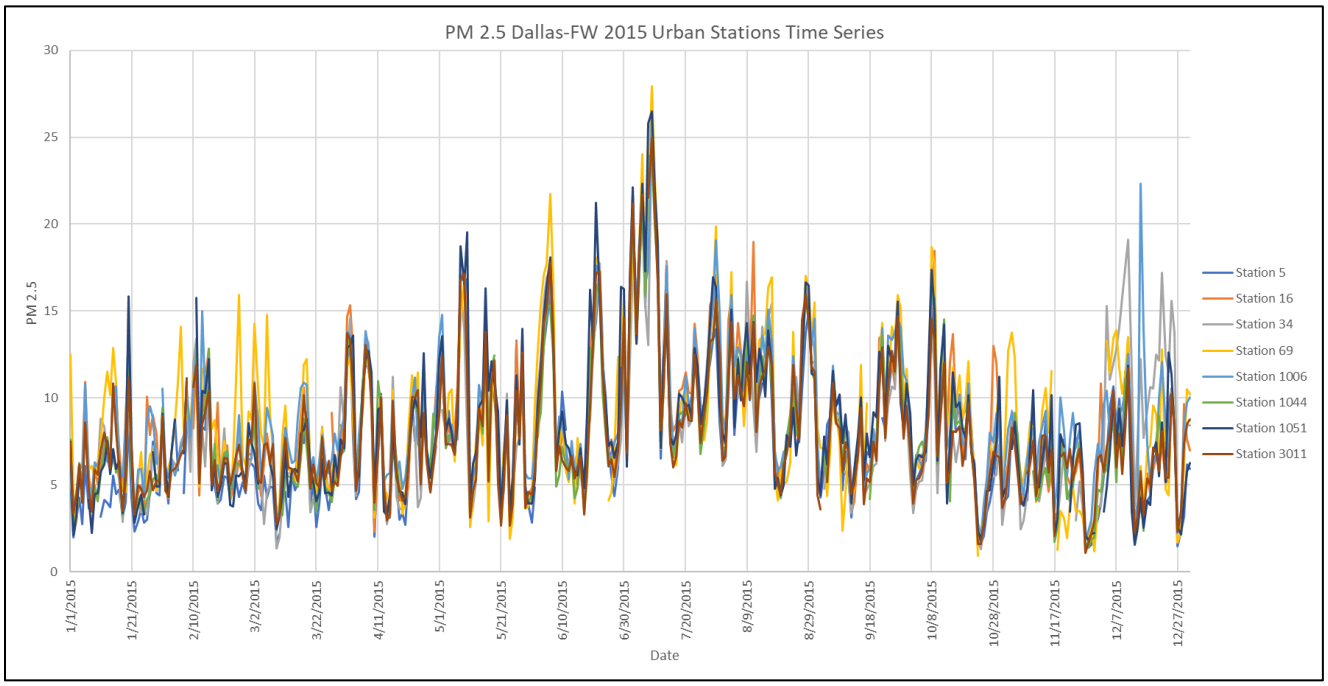

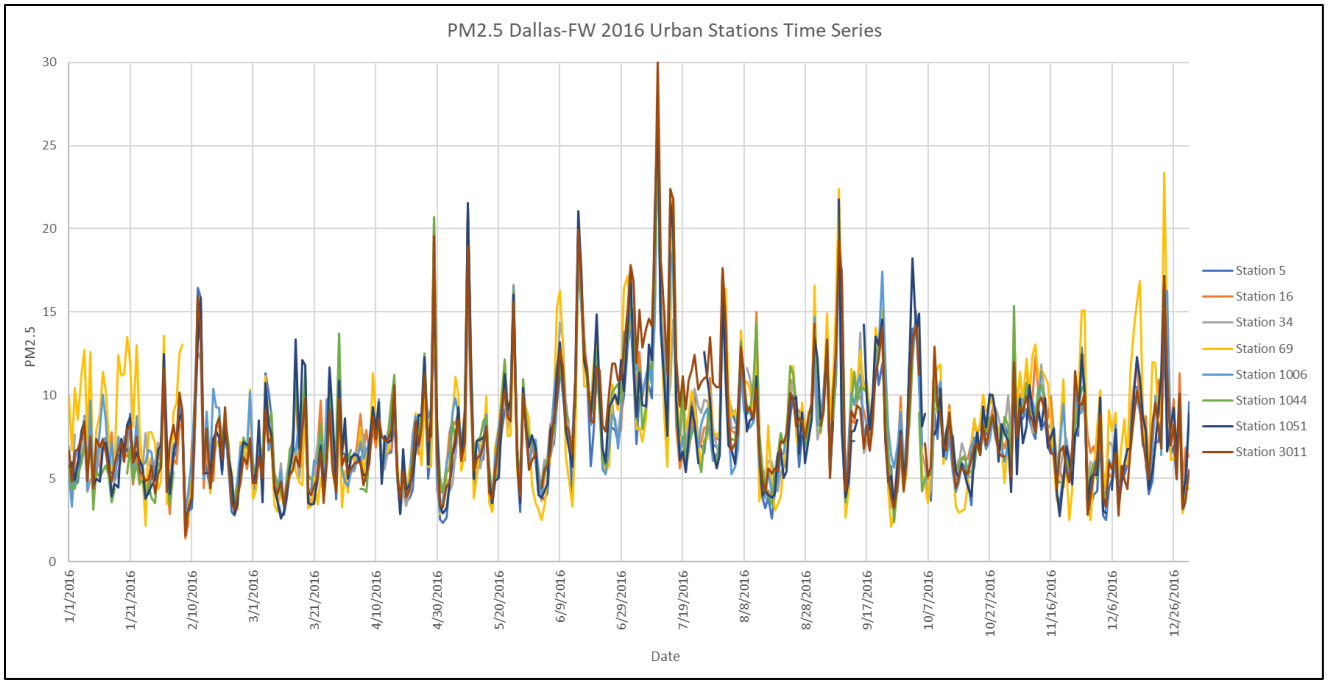
PM2.5 Dallas-FW 2016 Urban Stations Time Series
PM2.5
Date
Station 5
Station 16
Station 34
Station 69
Station 1006
Station 1044
Station 1051
Station 3011

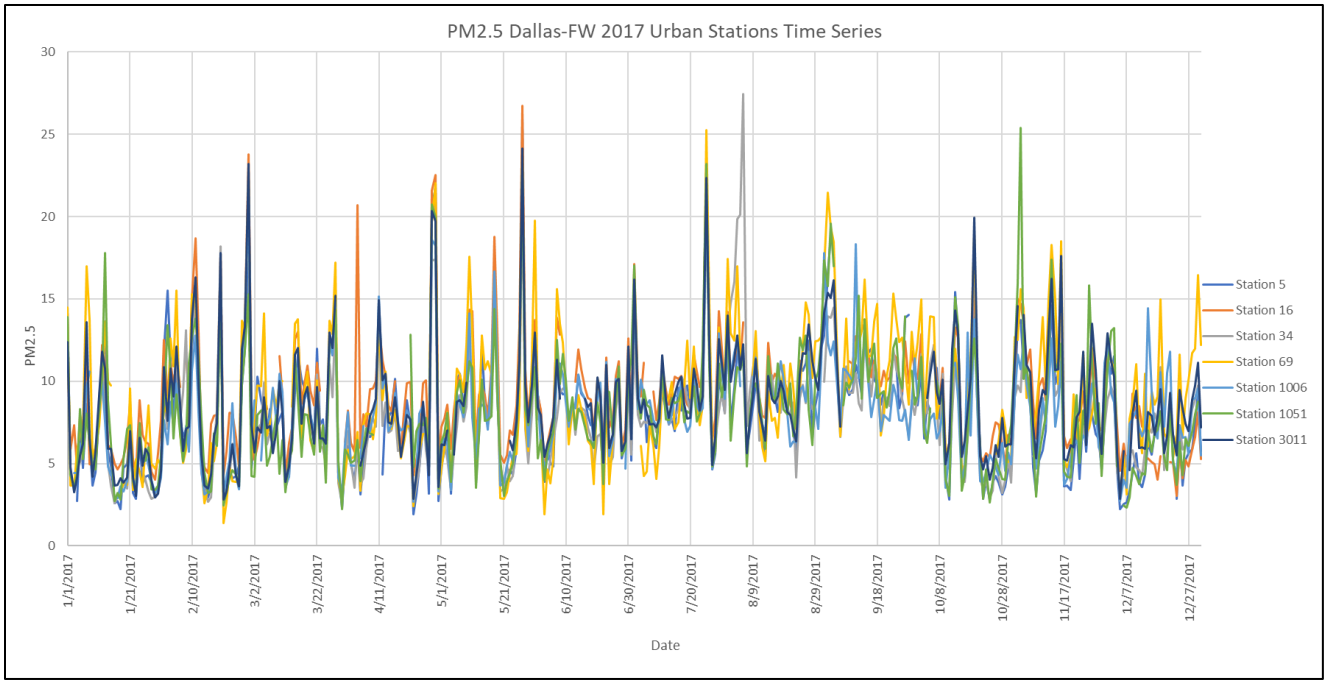
PM2.5 Dallas-FW 2017 Urban Stations Time Series
PM2.5
Date
Station 5
Station 16
Station 34
Station 69
Station 1006
Station 1051
Station 3011

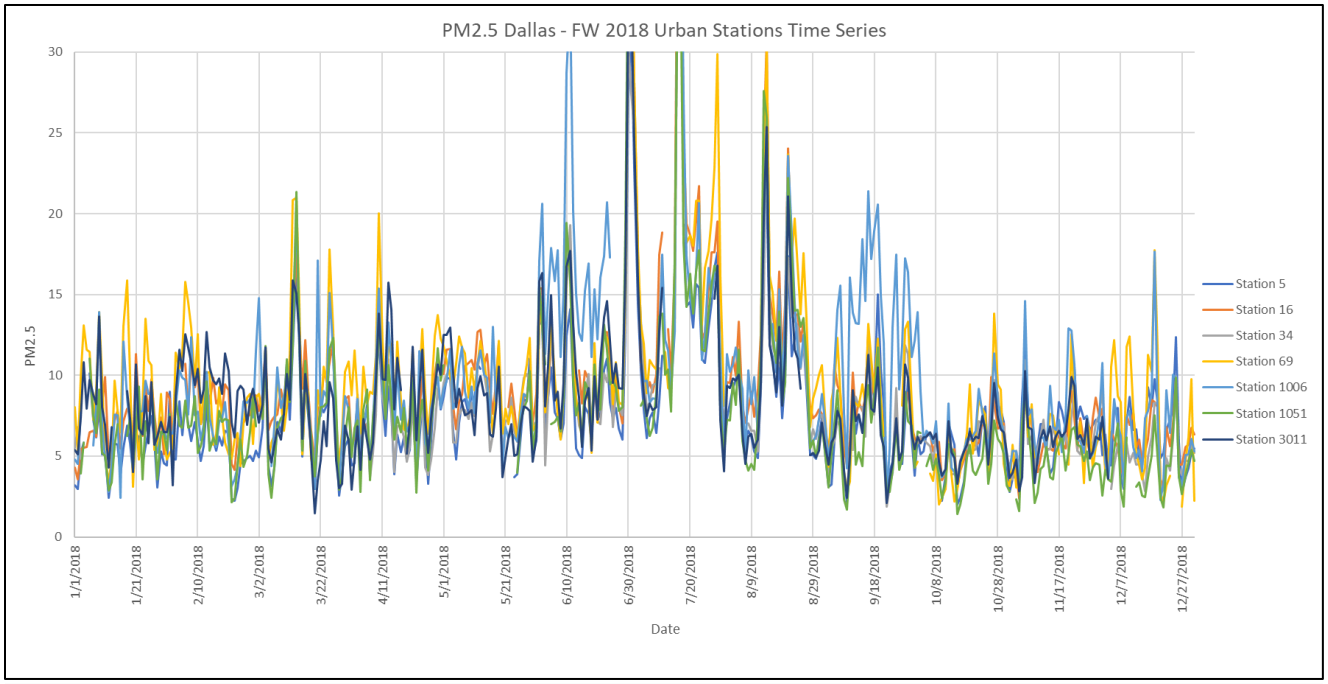
PM2.5 Dallas - FW 2018 Urban Stations Time Series
PM2.5
Date
Station 5
Station 16
Station 34
Station 69
Station 1006
Station 1051
Station 3011

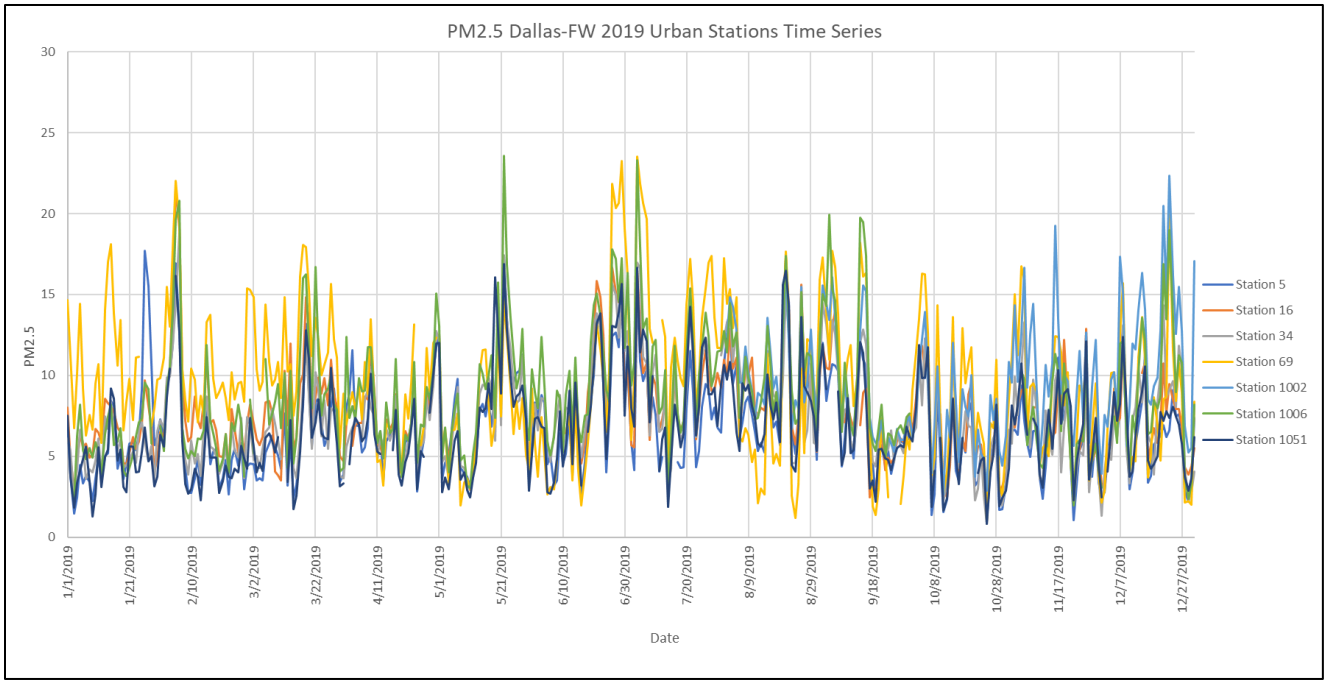
PM2.5 Dallas-FW 2019 Urban Stations Time Series
PM2.5
Date
Station 5
Station 16
Station 34
Station 69
Station 1002
Station 1006
Station 1051

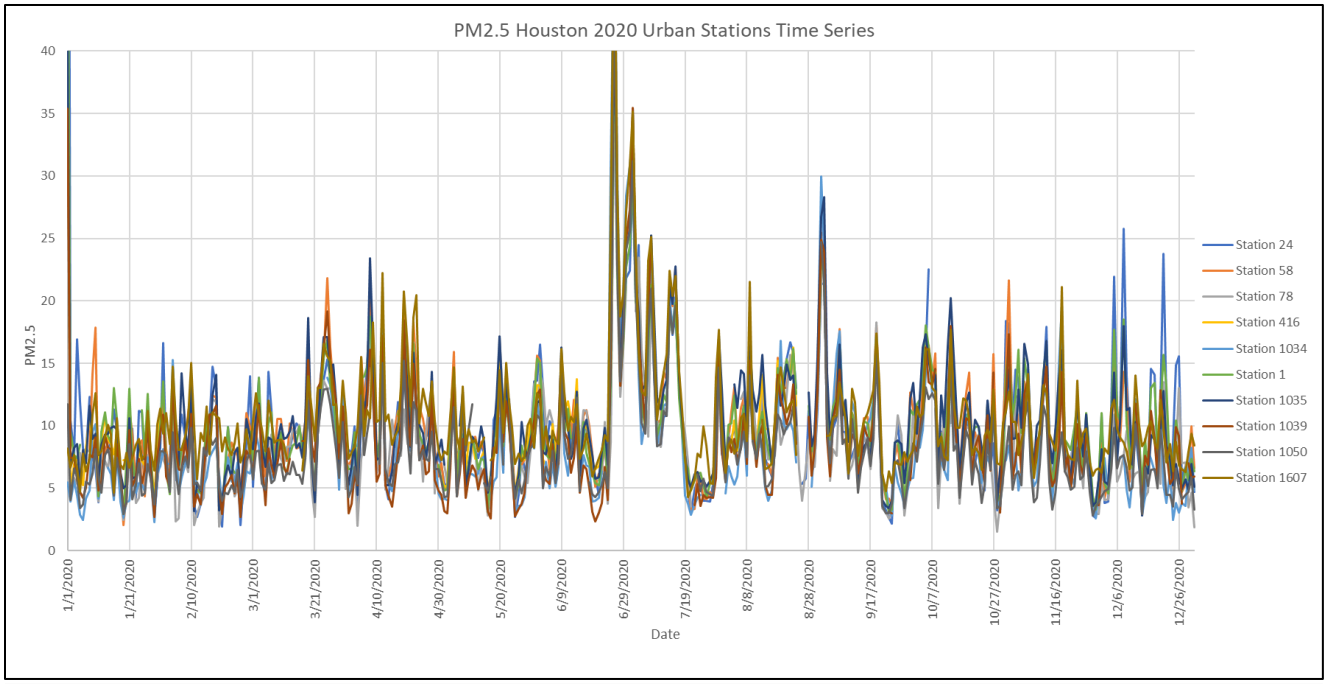
PM2.5 Houston 2020 Urban Stations Time Series
PM2.5
Date
Station 24
Station 58
Station 78
Station 416
Station 1034
Station 1
Station 1035
Station 1039
Station 1050
Station 1607

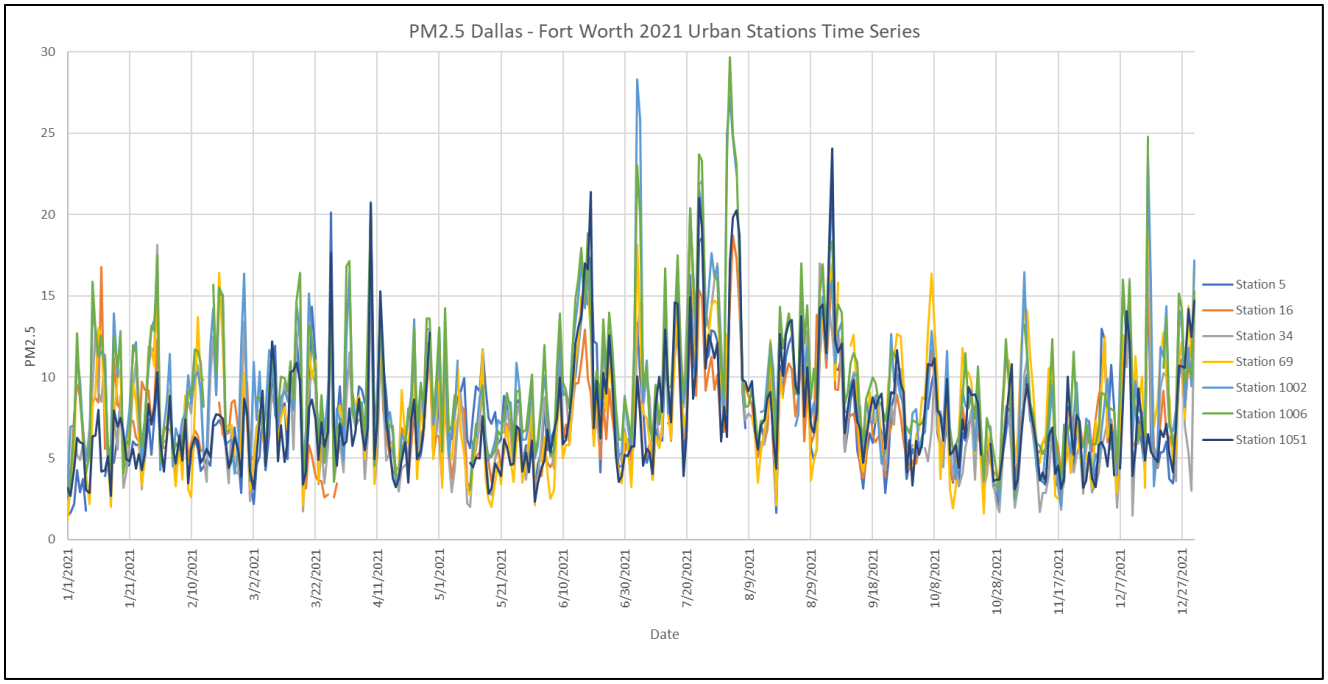
PM2.5 Dallas - Fort Worth 2021 Urban Stations Time Series
PM2.5
Date
Station 5
Station 16
Station 34
Station 69
Station 1002
Station 1006
Station 1051

Vita

Marcos A. Banda Morales graduated from high school in 2013. He completed an associate degree in Civil Engineering in 2016 and continued his education in Civil Engineering at The University of Texas at El Paso, where he received his Bachelor of Science degree in 2019 while working as a research assistant from 2018 to 2019. Upon graduating worked in construction as a field engineer. In January 2021 he began pursuing his degree of Master of Science in Environmental Engineering which was received in December 2022.